Detection Performance of Or-ing Device with Pre- and Post-Averaging: Part II – Phase-Incoherent Signal

Albert H. Nuttall
Surface Undersea Warfare Department

Naval Undersea Warfare Center Division
Newport, Rhode Island

19991122 072

PREFACE

Reviewed and Approved: 28 September 1999

Patricia J. Dean
Director, Surface Undersea Warfare

REPORT DOCUMENTATION PAGE

Public reporting burden for this collection of information is estimated to average 1 hour per response, including the time for reviewing instructions, searching existing data sources, gathering and maintaining the data needed, and completing and reviewing the collection of information. Send comments regarding this burden estimate or any other aspect of this collection of information, including suggestions for reducing this burden, to Washington Headquarters Services, Directorate for Information Operations and Reports, 1215 Jefferson Davis Highway, Suite 1204, Arlington, VA 22202-4302, and to the Office of Management and Budget, Paperwork Reduction Project (0704-0188), Washington, DC 20503.

1. AGENCY USE ONLY (Leave Blank)	2. REPORT DATE 28 September 1999	3. REPORT TYPE AND DATES COVERED Final

4. TITLE AND SUBTITLE

Detection Performance of Or-ing Device with Pre- and Post-Averaging: Part II – Phase-Incoherent Signal

5. FUNDING NUMBERS

PR B102369
PR A196009

6. AUTHOR(S)

Albert H. Nuttall

7. PERFORMING ORGANIZATION NAME(S) AND ADDRESS(ES)

Naval Undersea Warfare Center Division
1176 Howell Street
Newport, RI 02841-1708

8. PERFORMING ORGANIZATION REPORT NUMBER

TR 11,166

9. SPONSORING/MONITORING AGENCY NAME(S) AND ADDRESS(ES)

Office of Naval Research
800 North Quincy Street
Arlington, VA 22217-5160

Program Executive Office
for Undersea Warfare (ASTO D1)
2531 Jefferson Davis Highway
Arlington, VA 22242-5160

10. SPONSORING/MONITORING AGENCY REPORT NUMBER

11. SUPPLEMENTARY NOTES

12a. DISTRIBUTION/AVAILABILITY STATEMENT

Approved for public release; distribution is unlimited.

12b. DISTRIBUTION CODE

13. ABSTRACT (Maximum 200 words)

The detection performance of an or-ing device with pre-averaging and post-averaging has been determined in the form of numerous receiver operating characteristics covering a wide range of input signal-to-noise ratios. Numerical evaluation of the false alarm probability P_f and detection probability P_d has been conducted for the case of a phase-incoherent signal in the presence of additive Gaussian noise for a wide range of values of K, the amount of pre-averaging before or-ing; N, the number of channels or-ed; and M, the amount of post-averaging after or-ing. A MATLAB program that can be used to extend these results to parameter values outside the range studied here is also listed.

The tradeoffs associated with switching from post-averaging to pre-averaging, or vice-versa, have been thoroughly investigated and tabulated for a standard operating point ($P_f = 1E-3$, $P_d = 0.5$) and for a high-quality operating point ($P_f = 1E-6$, $P_d = 0.9$). The losses associated with doing too little pre-averaging can be severe, especially for large numbers, N, of or-ed channels.

14. SUBJECT TERMS

Signal Processing	Phase-Incoherent Signals	Post-averaging
Or-ing	Pre-averaging	

15. NUMBER OF PAGES 129

16. PRICE CODE

17. SECURITY CLASSIFICATION OF REPORT	18. SECURITY CLASSIFICATION OF THIS PAGE	19. SECURITY CLASSIFICATION OF ABSTRACT	20. LIMITATION OF ABSTRACT
Unclassified	Unclassified	Unclassified	SAR

TABLE OF CONTENTS

Page

TABLE OF CONTENTS (Cont'd)

LIST OF ILLUSTRATIONS

LIST OF TABLES

LIST OF ABBREVIATIONS, ACRONYMS, AND SYMBOLS

A_k, A — Signal amplitude, equations (2) and (7)

CDF — Cumulative distribution function

CF — Characteristic function

c_v — Cumulative distribution function of $v(t)$, equation (12)

c_0, c_1 — Cumulative distribution functions of $y_n(t)$, equation (12)

dB — Decibel

EDF — Exceedance distribution function

$\{e_k\}$ — Exponential random variables, equation (6)

$e_n(x)$ — Auxiliary function, equation (21)

e_w — Exceedance distribution function of $w(t)$, equations (19) and (20)

FFT — Fast Fourier transform

f_k — Characteristic function of x_k, equation (4)

f_v — Characteristic function of $v(t)$, equation (17)

f_w — Characteristic function of $w(t)$, equation (18)

f_y — Characteristic function of $y_n(t)$, equation (9)

$\{g_k\}$ — Gaussian random variables, equation (2)

$\{h_k\}$ — Gaussian random variables, equation (2)

HOP — High-quality operating point, $P_f = 1E-6$ and $P_d = 0.9$

H_0, H_1 — Signal-absent, signal-present hypotheses

K — Amount of pre-averaging, figure 1

M — Amount of post-averaging, figure 1

N — Total number of channels or-ed, figure 1

iv

LIST OF ABBREVIATIONS, ACRONYMS, AND SYMBOLS (Cont'd)

or-ing   Pass only the largest of N inputs, figure 1

p,PDF   Probability density function

P_d Detection probability

P_f False alarm probability

p_v Probability density function of $v(t)$,
              equations (13) and (14)

p_w Probability density function of $w(t)$, equation (37)

p_0, p_1 Probability density functions of $y_n(t)$, equation (13)

Q_K Q-function of order K, equation (25)

ROC   Receiver operating characteristic

RV   Random variable

SNR   Signal-to-noise ratio

SOP   Standard operating point, P_f = 1E-3 and P_d = 0.5

t   Time instant, equation (1)

T   Available time-bandwidth product (= KM), equation (10)

$v(t)$ Or-ing output, figure 1 and equation (1)

$w(t)$ System output, figure 1

$x_n(t)$ Input data in n-th channel, figure 1

$y_n(t)$ Pre-averager output in n-th channel, figure 1

Δ_ξ Sampling increment in ξ

Δ_u Sampling increment in u

θ_k Random phase, equation (2)

ρ Common input power signal-to-noise ratio, equation (8)

$\underline{\rho}$ Scaled signal-to-noise ratio, equation (25)

ρ_k	Input power signal-to-noise ratio at time k, equation (3)
ξ	Argument of characteristic functions
μ_v	Mean of $\mathbf{v}(t)$, equations (29) and (34)
boldface	Random variable
overbar	Ensemble average

DETECTION PERFORMANCE OF OR-ING DEVICE WITH PRE- AND POST-AVERAGING: PART II — PHASE-INCOHERENT SIGNAL

INTRODUCTION

BACKGROUND

The need to process and condense large amounts of data is encountered frequently in modern Navy systems that employ multiple beams, frequency bins, range cells, et cetera. One way of accomplishing this goal is by or-ing a number of inputs into a single output — that is, allowing only the largest of a set of quantities to pass on for further processing and completely rejecting the remainder. However, since this or-ing operation is highly nonlinear, destroys information, and tends to cause small-signal suppression, some pre-averaging of the inputs to the or-ing device is often employed in an effort to build up the signal-to-noise ratio (SNR) prior to the maximum comparison. Furthermore, at the or-ing output, some additional post-averaging is frequently used, this time in an effort to build up the SNR before a threshold comparison is made for the purpose of declaring a signal present or absent (hypothesis H_1 versus H_0, respectively). The pertinent block diagram is displayed in figure 1.

There are N channels of real input data available for processing, namely, $\{x_n(t)\}$ for $1 \leq n \leq N$, where time has been

1
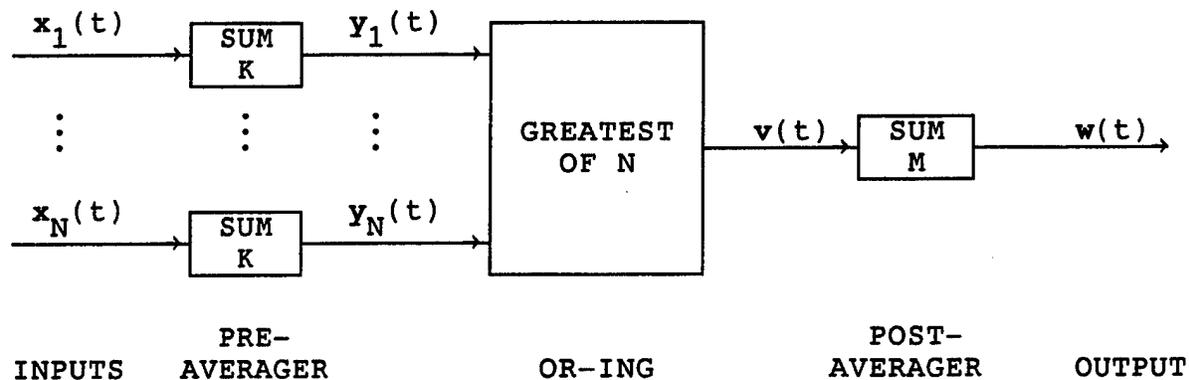
Figure 1. Or-ing with Pre- and Post-Averaging

normalized so that time sampling instant t is an integer. Under hypothesis H_0, there is Gaussian noise only in all the inputs, whereas under hypothesis H_1, a signal is also present in one (unknown) channel. The goal of the processor in figure 1 is to determine signal presence with a high detection probability P_d, while realizing a specified acceptable low false alarm probability P_f.

Each pre-averager accumulates K statistically independent consecutive time samples of its corresponding input $x_n(t)$, yielding output $y_n(t)$, which is then subjected to or-ing amongst N competitors. The or-ing output at time t is

$$v(t) = \max\{y_1(t), \cdots, y_N(t)\} \ . \tag{1}$$

Finally, the post-averager accumulates M samples of its input $v(t)$ and compares its output $w(t)$ with a fixed threshold. It is

presumed that the post-averager waits for all the K input data

samples to be summed and or-ed before an input is received; then,

another block of K input samples is summed and or-ed, leading to

the next input to the post-averager. That is, block processing

is presumed.

SCOPE

This technical report constitutes part II of a series of

three investigations of or-ing with pre- and post-averaging. In

particular, three different input signal models in additive

Gaussian noise are of interest:

(I)   Random (Gaussian) signal,

(II)   Phase-incoherent signal, and

(III) Coherent (deterministic) signal.

Results for part I, the Gaussian signal, have been documented in

reference 1; the reader must be familiar with its contents.

Specifically, the details on block and overlap processing, as

well as a scaling property and the standard of comparison for the

or-ing system in figure 1, are presented there, along with

references to related past results.

The current report addresses part II, the phase-incoherent signal in noise, and presents numerous receiver operating characteristics (ROCs) that completely quantify the performance of the or-ing system in figure 1. For all three signal models above, the optimum processors have been determined in reference 1, appendix A. Thus, the exact losses that the or-ing procedure causes can be accurately quantified.

The analytical approach utilized here can be extended to include quantizers on the inputs in figure 1, and accurate ROCs can still be obtained for decision variable $w(t)$. In fact, there can be arbitrary amounts of quantization (L levels), and the input probability density functions (PDFs) can be completely arbitrary. This procedure will be documented in part III.

For block processing in figure 1, expressions are derived that allow for accurate evaluation of the false alarm probability and the detection probability for the decision variable $w(t)$. Furthermore, this is accomplished for arbitrary amounts of pre-averaging K, arbitrary amounts of or-ing N, arbitrary amounts of post-averaging M, and arbitrary input SNRs. No approximations are involved, the analysis is not limited to mean and variance calculations, and no appeal is made to the central limit theorem. Rather, the approach employs a judicious combination of analysis with computer-aided numerical calculations. The accuracy of the end result is limited only by the accuracy of the computer. An entire ROC can be generated in minutes.

4

INPUT DATA MODELS

In this section, g_k and h_k are independent zero-mean, unit-variance Gaussian random variables (RVs), and e_k is an exponential RV with unit mean, that is, with PDF exp(-u) for u > 0.

PHASE-INCOHERENT SIGNAL IN GAUSSIAN NOISE

Here, in part II, the signal channel input at time k under H_1 is an envelope-squared variate

$$x_k = \frac{1}{2}\left[(g_k + A_k \cos\theta_k)^2 + (h_k + A_k \sin\theta_k)^2\right] , \tag{2}$$

where signal amplitude A_k is nonrandom and phase θ_k is an RV with arbitrary PDF, that is, incoherent phase. The input mean is

$$\overline{x_k} = 1 + \frac{1}{2} A_k^2 \equiv 1 + \rho_k , \tag{3}$$

regardless of the value of θ_k. Since x_k is an envelope-squared quantity, $\rho_k = A_k^2/2$ is an input (per sample) power SNR measure.

The characteristic function (CF) of x_k under H_1, conditioned on a particular value of RV θ_k, is, by use of equation (2),

$$f_k(\xi|\theta_k) = \overline{\exp(i\xi x_k)} = \frac{1}{1 - i\xi} \exp\left(\rho_k \frac{i\xi}{1 - i\xi}\right) . \tag{4}$$

But, since the right-hand side of CF (4) is independent of θ_k, it is possible to use, instead of form (2), the data value

$$x_k = \frac{1}{2}\left[(g_k + A_k)^2 + h_k^2\right] \qquad (5)$$

for the signal channel input at time k under H_1. On the other hand, for the noise channels, A_k is zero and CF (4) reduces to $1/(1 - i\xi)$, which corresponds to a unit-mean exponential RV. For the noise channel inputs, the following quantity can be used:

$$x_k = e_k \ . \qquad (6)$$

When $A_k = A$ for all k, that is, constant signal amplitudes with time, the pre-averager output for the signal channel can be expressed as

$$y = \sum_{k=1}^{K} x_k = \frac{1}{2}\sum_{k=1}^{K} (g_k^2 + h_k^2) + A \sum_{k=1}^{K} g_k + K \frac{A^2}{2} =$$

$$= y^o + A \sum_{k=1}^{K} g_k + K \frac{A^2}{2}, \qquad (7)$$

under H_1, where y^o is the corresponding noise-only pre-averager output. (However, the k-th term in the sum for y cannot be replaced by $e_k + A g_k + A^2/2$, where e_k is an independent exponential RV, because the CF of this latter combination is

$$\frac{1}{1 - i\xi} \exp[\rho \, i\xi(1 + i\xi)] \ , \qquad \rho \equiv \frac{A^2}{2}, \qquad (8)$$

which is not identical in form to equation (4). The two CFs do, however, have the same mean and variance.) The ROCs for pre-averager (7) can be parameterized by input amplitude SNR measure A or by input power SNR measure ρ.

Because of the way SNR parameters $\{\rho_k\}$ appear in equation (4), the CF of the pre-averager output can be found in the closed form

$$f_y(\xi) = (1 - i\xi)^{-K} \exp\left(\rho_K \frac{i\xi}{1 - i\xi}\right) \ , \qquad \rho_K = \sum_{k=1}^{K} \rho_k \ . \qquad (9)$$

Therefore, all the following results pertaining to the phase-incoherent signal with equal SNRs ρ and sums of squared envelopes actually hold for arbitrary SNRs $\{\rho_k\}$, if ρ is replaced by ρ_K/K. However, this observation is of limited utility unless all the M sums of $\{\rho_k\}$, one for each post-averaging interval, are identical.

OPTIMUM PROCESSING OF AVAILABLE DATA

The optimum processor for signal model (2) has been derived in appendix A of reference 1 for the case where channel occupancy identification is required, as well as for the alternative case where channel identification is irrelevant. For all situations, the optimum processor is essentially given by threshold comparison

$$\max_{1 \leq n \leq N} \left\{ \sum_{t=1}^{T} x_n(t) \right\} \underset{<}{\overset{>}{\gtrless}} v \ ; \qquad (10)$$

see equations (A-13), (A-19), and (A-26) of reference 1. This operation is equivalent to performing <u>all</u> pre-averaging and <u>no</u> post-averaging in figure 1, that is, taking K = T, the total

time-bandwidth product available, and $M = 1$. Doing so defers the nonlinearity (or-ing) until after all possible linear combining (pre-averaging) has been accomplished. This case will be thoroughly evaluated numerically and will serve as the basis of comparison for the various combinations of pre-averaging and post-averaging, that is, $K < T$ or $M > 1$.

PERFORMANCE ANALYSIS FOR BLOCK PROCESSING

Due to the pre-averaging, each RV $y_n(t)$ in figure 1 is a sum of K independent RVs with identical statistics. Also, all N channel inputs are statistically independent of each other. For or-ing to be present, $N \geq 2$ is required for the following calculations and considerations.

For a noise-only channel, let p_0 be the PDF of pre-averager output $y_n(t)$, and let c_0 be the corresponding cumulative distribution function (CDF), namely, $c_0(u) = \text{Prob}\{y_n(t) < u | H_0\}$. For a signal present in channel 1, say, let p_1 and c_1 be the corresponding PDF and CDF of $y_1(t)$, respectively.

The or-ing output $v(t)$ in figure 1 is

$$v(t) = \max\{y_1(t),\ldots,y_N(t)\} .\qquad (11)$$

Its CDF for signal present, that is, hypothesis H_1, is

$$c_{v1}(u) = c_1(u) [c_0(u)]^{N-1} ,\qquad (12)$$

which leads to the corresponding PDF of $v(t)$ under H_1 as

$$p_{v1}(u) = c'_{v1}(u) = p_1(u) [c_0(u)]^{N-1} + c_1(u) (N-1) [c_0(u)]^{N-2} p_0(u)$$

$$= [c_0(u)]^{N-2} [p_1(u) c_0(u) + (N-1) p_0(u) c_1(u)] .\qquad (13)$$

The signal-absent PDF of $v(t)$ under H_0 follows immediately as

$$p_{v0}(u) = N p_0(u) [c_0(u)]^{N-1} .\qquad (14)$$

9

The corresponding exceedance distribution functions (EDFs), namely, $e_v(u) = 1 - c_v(u)$, for or-ing output $v(t)$ can be expressed in terms of the following series expansions, which are useful for very small EDF values:

$$e_{v1}(u) = e_1(u) - c_1(u) \sum_{n=1}^{N-1} \binom{N-1}{n} [-e_0(u)]^n ,$$ (15)

$$e_{v0}(u) = - \sum_{n=1}^{N} \binom{N}{n} [-e_0(u)]^n .$$ (16)

The CF of or-ing output $v(t)$ is given by the Fourier transform

$$f_v(\xi) = \overline{\exp(i\xi v(t))} = \int du \, \exp(i\xi u) \, p_v(u) ,$$ (17)

where either relevant form, p_{v1} or p_{v0} above, is to be used. Finally, for block processing in figure 1, there is no overlap of the data used in the post-averager, meaning that the processor output $w(t)$ is the sum of M _independent_ identically distributed RVs. Therefore, the CF of the decision variable $w(t)$ in figure 1 is simply

$$f_w(\xi) = [f_v(\xi)]^M .$$ (18)

One final Fourier transform is required to manipulate CF $f_w(\xi)$ into the desired EDF of processor output $w(t)$; see reference 2. This EDF will be the false alarm probability P_f or the detection probability P_d of the or-ing processor, depending on whether PDF p_{v0} or p_{v1} is used, respectively.

10

The fundamental Fourier transform in equation (17) will generally have to be accomplished numerically by means of a fast Fourier transform (FFT). If pre-averager output statistics p_0 and c_0 can be found in closed form or readily computed form, a cascaded FFT approach will lead to exact false alarm probability results for the or-ing processor in figure 1. If pre-averager output probability functions p_1 and c_1 can also be readily evaluated, accurate detection probability results can be similarly calculated as well. Some important numerical considerations for this cascaded FFT approach are presented in appendix B of reference 1.

For the special case of $M = 1$ (no post-averaging), processor output RV $w(t) = v(t)$ in figure 1, and the corresponding EDFs follow, for any K, N, as

$$e_{w1}(u) = 1 - c_1(u) \, [c_0(u)]^{N-1} \, , \tag{19}$$

$$e_{w0}(u) = 1 - [c_0(u)]^{N} \, . \tag{20}$$

Now, return to arbitrary values of K, N, and M, and specialize the general results above to the phase-incoherent signal model of interest here, namely, equations (2) and (3).

Define $\underline{\rho} = K \rho$ and use (reference 3, equation 6.5.11)

$$e_n(x) = \sum_{k=0}^{n} \frac{x^k}{k!} \; . \tag{21}$$

For constant signal amplitudes and $u > 0$, the pertinent PDFs and CDFs of pre-averager outputs $\{y_n(t)\}$ are (using equation (9); reference 4, equation 6.631 4; and reference 5, equation (1))

$$p_0(u) = \frac{u^{K-1} \exp(-u)}{(K-1)!} \; , \qquad c_0(u) = 1 - \exp(-u) \, e_{K-1}(u) \; , \tag{22}$$

$$p_1(u) = \left(\frac{u}{\underline{\rho}}\right)^{\frac{K-1}{2}} \exp(-u-\underline{\rho}) \, I_{K-1}\left(2(\underline{\rho}u)^{\frac{1}{2}}\right) \; , \tag{23}$$

$$f_1(\xi) = (1 - i\xi)^{-K} \exp\left(\underline{\rho} \, \frac{i\xi}{1 - i\xi}\right) \; , \tag{24}$$

$$c_1(u) = 1 - Q_K\left((2\underline{\rho})^{\frac{1}{2}}, (2u)^{\frac{1}{2}}\right) \; ; \quad \underline{\rho} = K \rho \; . \tag{25}$$

The PDFs for or-ing output $v(t)$, for $u > 0$, then follow from equations (14) and (13), respectively, as

$$P_{v0}(u) = N \frac{u^{K-1} \exp(-u)}{(K-1)!} \, [1 - \exp(-u) \, e_{K-1}(u)]^{N-1} \; , \tag{26}$$

$$P_{v1}(u) = [1 - \exp(-u) \, e_{K-1}(u)]^{N-2}\left[\left(\frac{u}{\underline{\rho}}\right)^{\frac{K-1}{2}} \exp(-u-\underline{\rho}) \, I_{K-1}\left(2(\underline{\rho}u)^{\frac{1}{2}}\right) \times \right.$$

$$\left. \times \, [1 - \exp(-u) \, e_{K-1}(u)] + (N-1)\frac{u^{K-1} \exp(-u)}{(K-1)!}\left(1-Q_K\left((2\underline{\rho})^{\frac{1}{2}}, (2u)^{\frac{1}{2}}\right)\right)\right] \; . \tag{27}$$

SPECIAL CASES

In the special case of K = 1, that is, no pre-averaging, the CF of v(t) with or-ing and signal present is available in closed form by Fourier transforming $p_{v1}(u)$ to obtain (using reference 4, equation 6.631 4, and reference 5, equation (24))

$$f_{v1}(\xi) = i\xi \sum_{k=0}^{N-1} \binom{N-1}{k} \frac{(-1)^{k+1}}{(k - i\xi)(k + 1 - i\xi)} \exp\left(-\rho \frac{k - i\xi}{k + 1 - i\xi}\right) \quad (28)$$

for any $N \geq 1$. The mean of v(t) with signal present follows as

$$\mu_{v1} = 1 + \rho + \sum_{k=1}^{N-1} \binom{N-1}{k} \frac{(-1)^{k-1}}{k(k + 1)} \exp\left(-\rho \frac{k}{k + 1}\right) . \quad (29)$$

Finally, when $\rho = 0$, equation (28) reduces to the more useful form for the CF as

$$f_{v0}(\xi) = \left[\prod_{n=1}^{N}\left(1 - \frac{i\xi}{n}\right)\right]^{-1} , \qquad \mu_{v0} = \sum_{n=1}^{N} \frac{1}{n} ; \quad (30)$$

this alternative form was derived in reference 1, equation (73).

For the special case of K = 2 with no signal present, the CF of v(t) is available by Fourier transforming PDF $p_{v0}(u)$, yielding

$$f_{v0}(\xi) = N! \sum_{n=0}^{N-1} \frac{(-1)^n}{(N-1-n)!} \sum_{k=0}^{n} \frac{k+1}{(n-k)! \ (n+1-i\xi)^{k+2}} . \quad (31)$$

This result holds for arbitrary amounts of or-ing, i.e., $N \geq 1$.

For N = 2, the CF of v(t) under H_1 is available (after considerable labor) by Fourier transforming PDF $p_{v1}(u)$ to obtain

$$f_{v1}(\xi) = \frac{1}{z_1 \, z_2^{2K-1}} \exp\left(-\underline{\rho} \, \frac{z_1}{z_2}\right) \sum_{k=0}^{K-1} \binom{2K-1}{K+k} z_1^{-k} \, e_k\left(\underline{\rho} \, \frac{z_1}{z_2}\right) +$$

$$+ \frac{1}{z_1^K} \exp\left(\underline{\rho} \, \frac{i\xi}{z_1}\right) - \frac{1}{z_2^{2K-1}} \exp\left(-\underline{\rho} \, \frac{z_1}{z_2}\right) \sum_{k=0}^{K-1} \binom{2K-1}{K+k} z_1^k \, e_k\left(\frac{\underline{\rho}}{z_1 z_2}\right) \quad (32)$$

for any $K \geq 1$, where $z_1 = 1 - i\xi$ and $z_2 = 2 - i\xi$. For K = 2, the mean follows as $\mu_{v1} = 2(1 + \rho) + \exp(-\rho)\,(6 + \rho)/8$, using $\underline{\rho} = 2\rho$.

For N = 2 and signal absent, the Fourier transform of PDF $p_{v0}(u)$ yields CF

$$f_{v0}(\xi) = \frac{2}{(1 - i\xi)^K} - 2 \sum_{k=0}^{K-1} \binom{K+k-1}{k} \frac{1}{(2 - i\xi)^{K+k}} \quad (33)$$

for any K, with mean

$$\mu_{v0} = 2K\left(1 - \sum_{k=0}^{K-1} \binom{K+k}{k} \frac{1}{2^{K+k+1}}\right) . \quad (34)$$

This form for CF $f_{v0}(\xi)$ in equation (33) is not obtained by setting $\underline{\rho} = 0$ in equation (32); however, numerical investigation of both forms reveals that they are equal. For K = 2, the CF in equation (33) further specializes to

$$f_{v0}(\xi) = \frac{2}{(1 - i\xi)^2} - \frac{2}{(2 - i\xi)^2} - \frac{4}{(2 - i\xi)^3} . \quad (35)$$

14

The CF of decision variable $w(t)$ for signal present is given by

$$f_{w1}(\xi) = [f_{v1}(\xi)]^M \ . \qquad (36)$$

When CF $f_{w1}(\xi)$ is available, a Fourier transform will yield the detection (or false alarm) probabilities for any K, N, and M. When M = 1, the EDFs in equations (19) and (20) can be combined with results (22) and (25) to immediately yield closed form expressions for P_d and P_f for any K, N, and SNR ρ.

When N = 1 (no or-ing) and K and M are arbitrary, the results simplify to output PDF and EDF

$$p_{w1}(u) = \left(\frac{u}{B}\right)^{\frac{T-1}{2}} \exp(-u-B) \ I_{T-1}\left(2(Bu)^{\frac{1}{2}}\right) \quad \text{for } u > 0 \ , \qquad (37)$$

$$P_d(v) = \int_v^\infty du \ p_{w1}(u) = Q_T\left((2B)^{\frac{1}{2}},(2v)^{\frac{1}{2}}\right) \quad \text{for } v > 0 \ , \qquad (38)$$

respectively, where T = KM and B = Tρ = KMρ. Obviously, for N = 1 here, only the product KM matters; this presumes all unity weights in both the pre- and post-averagers.

NUMERICAL APPROACH

When the CF $f_v(\xi)$ of or-ing output $v(t)$ can be derived in closed form, such as in special cases (28) through (35), $f_v(\xi)$

can be used directly in equation (18) to find the CF of decision variable $w(t)$. This route is preferred because CF $f_v(\xi)$ can decay rather slowly with ξ for some values of K and N. In particular, if the properties

$$1 - \exp(-u) \ e_{K-1}(u) \propto u^K \quad \text{as} \quad u \to 0+ \ , \tag{39}$$

$$I_n(x) \propto x^n \quad \text{as} \quad x \to 0+ \ , \tag{40}$$

$$1 - Q_K(a,x) \propto x^{2K} \quad \text{as} \quad x \to 0+ \tag{41}$$

are used, it follows that both PDFs $p_{v0}(u)$ and $p_{v1}(u)$ in equations (26) and (27) are proportional to u^{KN-1} as $u \to 0+$. For small KN, this abrupt change (from the constant value 0 for $u < 0$) leads to a slow decay of $f_v(\xi)$ with ξ, namely, $1/\xi^{KN}$, with the attendant aliasing problems; see reference 1. Therefore, closed form results for CF $f_v(\xi)$, when available, can be very useful in terms of avoiding some numerical problems in the discrete Fourier transform of $p_v(u)$. When this is not possible, the closed-form results for the or-ing output PDFs given in equations (26) and (27) are used, instead, in the cascaded FFT procedure outlined in equations (17) and (18).

The very special case of $K = 1$, $M = 1$ can be solved explicitly for P_f and P_d, as shown in appendix A. Also, the required input SNRs for two typical operating points are tabulated in this appendix. For other K,M values, the alias-suppression technique of appendix B has been used to evaluate the ROCs directly from PDF equations (26) and (27).

16

QUANTITATIVE PERFORMANCE RESULTS

This section gives specific quantitative detectability results for or-ing with various amounts of pre-averaging K and post-averaging M. In particular, numerous ROCs are presented in appendixes C, D, E, and F for the cases of KM = 4, 16, 64, and 256, respectively. The particular cases run are indicated in table 1; a total of 124 ROCs are represented. For N = 1, since only the product KM matters, only one ROC need be presented (the first curve in each appendix) under the title labeled M = 1.

Table 1. Cases Run

K	M	N	
4	1	1,2,4,8,16,32	Appendix C
2	2		1 + 15 ROCs
1	4		
16	1	1,2,4,8,16,32	Appendix D
8	2		1 + 25 ROCs
4	4		
2	8		
1	16		
64	1	1,2,4,8,16,32	Appendix E
32	2		1 + 35 ROCs
16	4		
8	8		
4	16		
2	32		
1	64		
256	1	1,2,4,8,16,32	Appendix F
128	2		1 + 45 ROCs
64	4		
32	8		
16	16		
8	32		
4	64		
2	128		
1	256		

REQUIRED INPUT SIGNAL-TO-NOISE RATIOS

The numerous ROCs in appendixes C through F enable a user to easily investigate and determine the amount of system input SNR required for the or-ing device in figure 1 to achieve a specified level of detectability performance, in terms of a desired false alarm probability P_f and detection probability P_d, over a wide range of parameter values. To partially condense this voluminous information, a standard operating point (SOP) is defined here as $P_f = 1E-3$ and $P_d = 0.5$, and a high-quality operating point (HOP) is defined as $P_f = 1E-6$ and $P_d = 0.9$. The corresponding required values of the input SNR $\rho(dB) = 10 \log(\rho)$, as determined from the ROCs in appendixes C through F, are listed in tables 2 through 9. (These accurate values were interpolated from the ROCs while the false alarm and detection probability numbers, P_f and P_d, were still resident in the computer; eyeball interpolation from the plotted ROCs cannot be accomplished this accurately.)

The input SNR requirements are plotted in figures 2 through 9. As expected, the required input SNR ρ increases monotonically with the number (N) of channels or-ed if K and M are held fixed. Also, the required input SNR ρ increases monotonically with the amount (M) of post-averaging employed if N and product KM are held fixed; alternatively, the required input SNR ρ decreases with the amount (K) of pre-averaging employed if N and product KM are held fixed. The exact rates can be determined from figures 2 through 9 and the ROCs in the appendixes.

Table 2. Required Input SNR ρ(dB) for P_f = 1E-3, P_d = 0.5, KM = 4, Phase-Incoherent Signal

K	M	N = 1	N = 2	N = 4	N = 8	N = 16	N = 32
4	1	3.78	4.15	4.50	4.82	5.10	5.38
2	2	3.78	4.40	4.95	5.43	5.87	6.27
1	4	3.78	4.62	5.40	6.07	6.68	7.21

Table 3. Required Input SNR ρ(dB) for P_f = 1E-6, P_d = 0.9, KM = 4, Phase-Incoherent Signal

K	M	N = 1	N = 2	N = 4	N = 8	N = 16	N = 32
4	1	8.25	8.40	8.54	8.68	8.83	8.95
2	2	8.25	8.53	8.81	9.05	9.29	9.50
1	4	8.25	8.71	9.14	9.53	9.90	10.23

Table 4. Required Input SNR ρ(dB) for P_f = 1E-3, P_d = 0.5, KM = 16, Phase-Incoherent Signal

K	M	N = 1	N = 2	N = 4	N = 8	N = 16	N = 32
16	1	−0.08	0.25	0.55	0.83	1.08	1.32
8	2	−0.08	0.48	0.97	1.41	1.79	2.12
4	4	−0.08	0.74	1.44	2.03	2.56	3.02
2	8	−0.08	0.96	1.88	2.68	3.37	3.97
1	16	−0.08	1.11	2.25	3.26	4.14	4.92

Table 5. Required Input SNR ρ(dB) for P_f = 1E-6, P_d = 0.9, KM = 16, Phase-Incoherent Signal

K	M	N = 1	N = 2	N = 4	N = 8	N = 16	N = 32
16	1	3.84	3.97	4.09	4.22	4.34	4.45
8	2	3.84	4.09	4.33	4.54	4.75	4.94
4	4	3.84	4.28	4.66	5.02	5.34	5.63
2	8	3.84	4.48	5.07	5.59	6.04	6.45
1	16	3.84	4.69	5.48	6.18	6.80	7.36

Table 6. Required Input SNR ρ(dB) for $P_f = 1E-3$, $P_d = 0.5$, KM = 64, Phase-Incoherent Signal

K	M	N = 1	N = 2	N = 4	N = 8	N = 16	N = 32
64	1	-3.59	-3.28	-3.01	-2.75	-2.53	-2.32
32	2	-3.59	-3.06	-2.61	-2.22	-1.88	-1.57
16	4	-3.59	-2.82	-2.16	-1.61	-1.14	-0.73
8	8	-3.59	-2.57	-1.71	-1.00	-0.39	0.14
4	16	-3.59	-2.37	-1.30	-0.40	0.39	1.05
2	32	-3.59	-2.22	-0.96	0.15	1.12	1.95
1	64	-3.59	-2.14	-0.72	0.58	1.77	2.79

Table 7. Required Input SNR ρ(dB) for $P_f = 1E-6$, $P_d = 0.9$, KM = 64, Phase-Incoherent Signal

K	M	N = 1	N = 2	N = 4	N = 8	N = 16	N = 32
64	1	-0.08	0.03	0.15	0.26	0.37	0.46
32	2	-0.08	0.14	0.36	0.55	0.74	0.91
16	4	-0.08	0.33	0.68	0.99	1.28	1.53
8	8	-0.08	0.54	1.07	1.53	1.94	2.29
4	16	-0.08	0.77	1.50	2.13	2.67	3.15
2	32	-0.08	0.97	1.92	2.74	3.44	4.05
1	64	-0.08	1.11	2.26	3.28	4.17	4.96

Table 8. Required Input SNR ρ(dB) for $P_f = 1E-3$, $P_d = 0.5$, KM = 256, Phase-Incoherent Signal

K	M	N = 1	N = 2	N = 4	N = 8	N = 16	N = 32
256	1	-6.87	-6.57	-6.31	-6.08	-5.86	-5.65
128	2	-6.87	-6.36	-5.94	-5.56	-5.24	-4.96
64	4	-6.87	-6.11	-5.50	-4.99	-4.54	-4.16
32	8	-6.87	-5.87	-5.06	-4.38	-3.81	-3.33
16	16	-6.87	-5.65	-4.63	-3.78	-3.07	-2.47
8	32	-6.87	-5.48	-4.25	-3.21	-2.35	-1.61
4	64	-6.87	-5.36	-3.96	-2.72	-1.67	-0.78
2	128	-6.87	-5.29	-3.75	-2.34	-1.09	-0.02
1	256	-6.87	-5.28	-3.67	-2.10	-0.64	0.64

Table 9. Required Input SNR ρ(dB) for P_f = 1E-6, P_d = 0.9,
KM = 256, Phase-Incoherent Signal

K	M	N = 1	N = 2	N = 4	N = 8	N = 16	N = 32
256	1	-3.62	-3.51	-3.41	-3.31	-3.21	-3.12
128	2	-3.62	-3.41	-3.21	-3.04	-2.87	-2.71
64	4	-3.62	-3.25	-2.92	-2.62	-2.37	-2.13
32	8	-3.62	-3.03	-2.54	-2.11	-1.75	-1.43
16	16	-3.62	-2.81	-2.13	-1.54	-1.05	-0.63
8	32	-3.62	-2.58	-1.69	-0.96	-0.33	0.21
4	64	-3.62	-2.40	-1.31	-0.38	0.42	1.09
2	128	-3.62	-2.26	-0.99	0.14	1.11	1.96
1	256	-3.62	-2.19	-0.78	0.54	1.73	2.76

The actual numerical procedure used to generate the ROCs in appendixes C through F is based upon appendix B and, in particular, on smoother function b_1(u) and equation (B-14). However, an alternative approach, presented in appendix G, for evaluation of a CF directly from samples of a CDF utilizes a model CDF function that mimics the general behavior of the CDF of interest. Proper control of aliasing and efficient use of an FFT are demonstrated in appendix G, along with an example of the application of the alternative procedure to a Gaussian CF. The inadequacy of simply using CDF differences as estimates of the PDF is also illustrated by example there.

TRADEOFF BETWEEN PRE- AND POST-AVERAGING

For a fixed amount of total time-bandwidth product, that is, KM constant, it is possible to shift some of the pre-averaging to post-averaging, or vice-versa. For example, if KM = 16, this could be accomplished by taking K = 16, M = 1, which corresponds to no post-averaging, and switching to K = 1, M = 16, which corresponds to no pre-averaging. Alternatively, intermediate values such as K = 4, M = 4, could be used, still keeping KM = 16.

In all cases, increasing M at the sake of K requires larger input SNRs to maintain the same operating point; see figures 2 through 9. This is related to the fact that the optimum processor conducts all pre-averaging before any nonlinear operations; see appendix A. For example, to maintain the SOP when KM = 16, table 4 indicates that increases of 0.86 dB, 1.70 dB, 2.43 dB, 3.06 dB, and 3.60 dB are required for N = 2, 4, 8, 16, and 32, respectively, if the switch is made from all pre-averaging to all post-averaging. Alternatively, for the HOP, the corresponding differences in table 5 are smaller (0.72 dB, 1.39 dB, 1.96 dB, 2.46 dB, and 2.91 dB for N = 2, 4, 8, 16, and 32, respectively).

For a HOP such as P_f = 1E-6 and P_d = 0.9, larger input SNRs are naturally required to achieve the higher level of performance. At these larger input SNRs, the or-ing process

is more frequently dominated by the signal-bearing channel. Therefore, as the number (N) of channels or-ed increases, the required increases in SNR are less severe than for a lower-quality operating point, such as P_f = 1E-3 and P_d = 0.5. For example, for K = 16 and M = 1, increasing N from 2 to 32 requires a 1.07-dB SNR increase to maintain the SOP, whereas only an additional 0.48 dB is needed at the HOP.

A related observation is that, for a given configuration (fixed K and M), the increase in SNR required to maintain the SOP, as the amount of or-ing increases, is more severe for the larger M values. Thus, for KM = 16, as N increases from 2 to 32, a 1.07-dB SNR increase (1.32 - 0.25) suffices to maintain the SOP for M = 1, whereas a 3.81-dB increase (4.92 - 1.11) is required for M = 16. The corresponding increases at the HOP are 0.48 dB (4.45 - 3.97) for M = 1 versus 2.67 dB (7.36 - 4.69) for M = 16, as N increases from 2 to 32. The behaviors are similar for the other values of KM, although the required input SNR ρ values are smaller as KM increases, due to the additional observation times allowed.
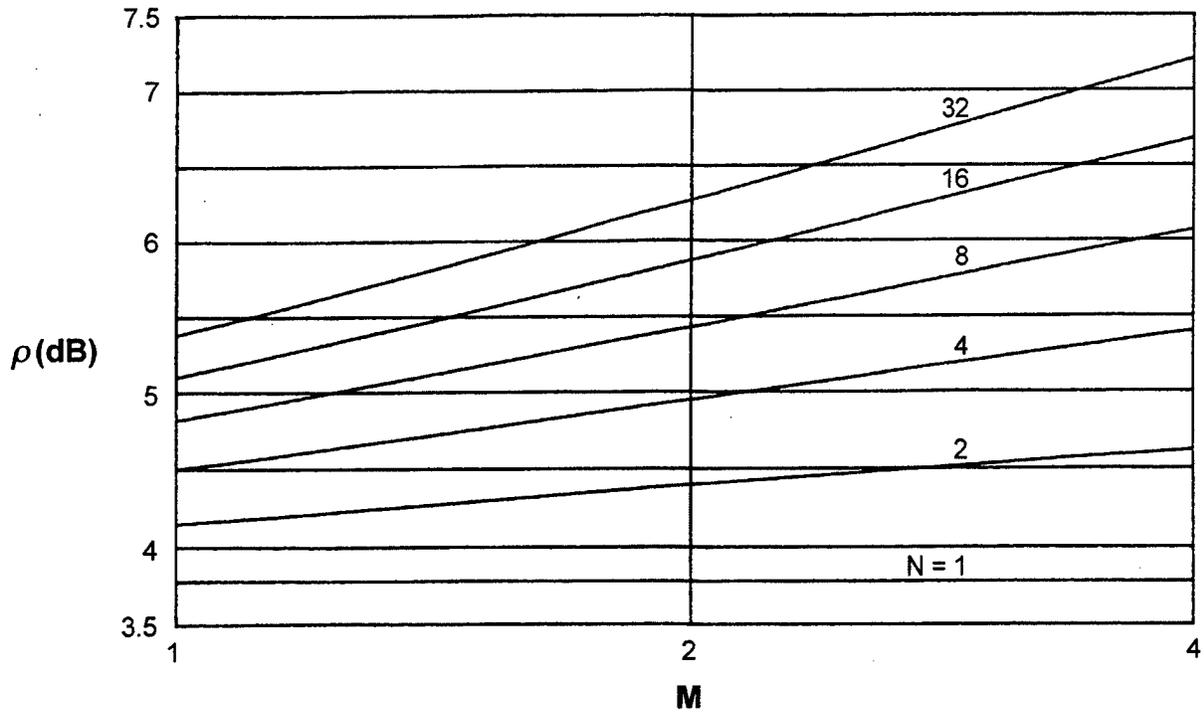
Figure 2. Required Input SNR for $P_f = 1E-3$, $P_d = 0.5$, KM = 4, Phase-Incoherent Signal
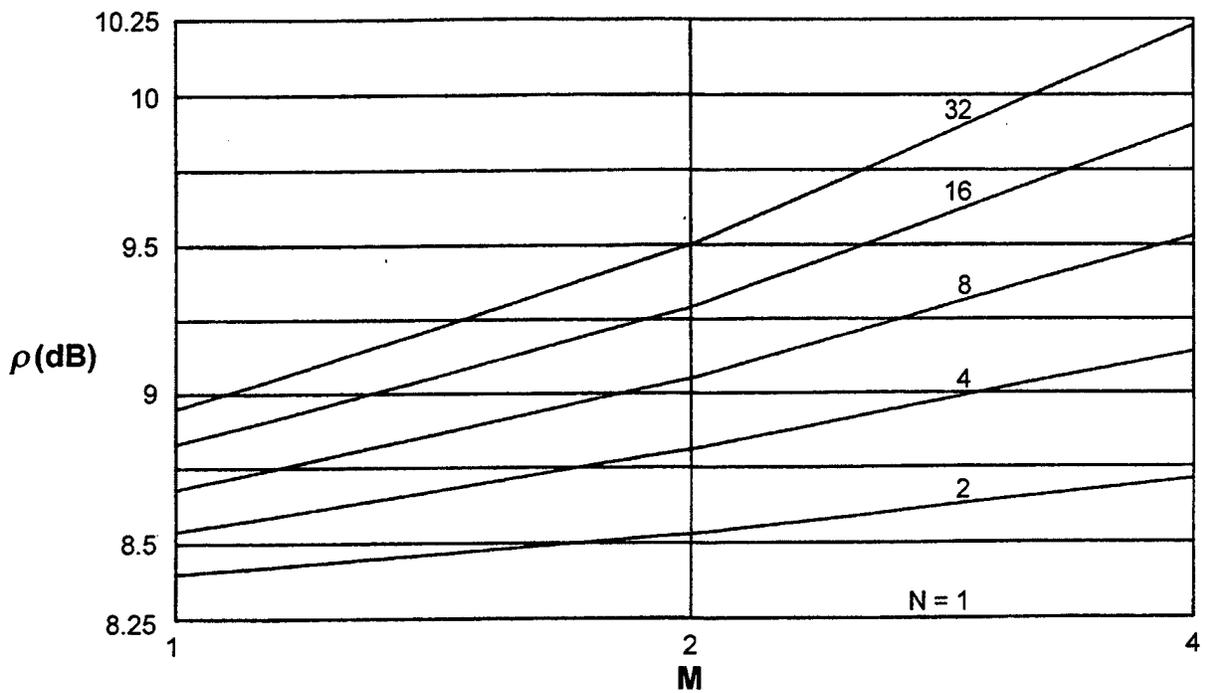
Figure 3. Required Input SNR for $P_f = 1E-6$, $P_d = 0.9$, KM = 4, Phase-Incoherent Signal
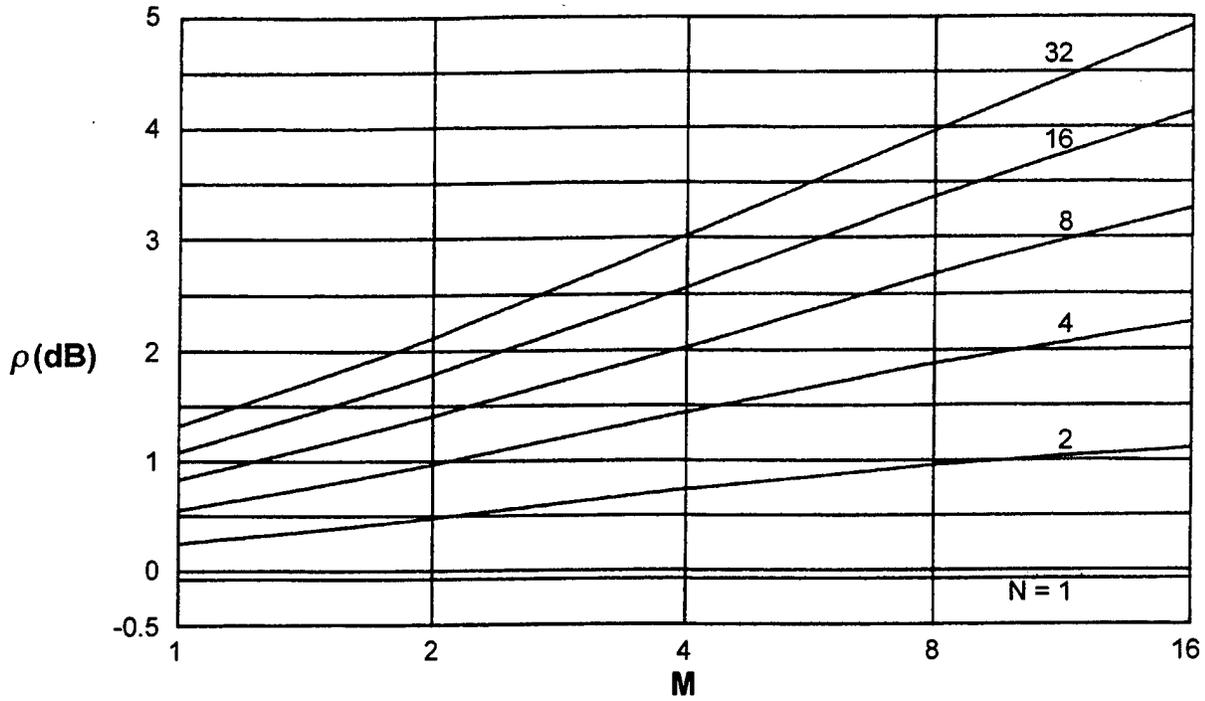
Figure 4.   Required Input SNR for P_f = 1E-3, P_d = 0.5, KM = 16,
Phase-Incoherent Signal
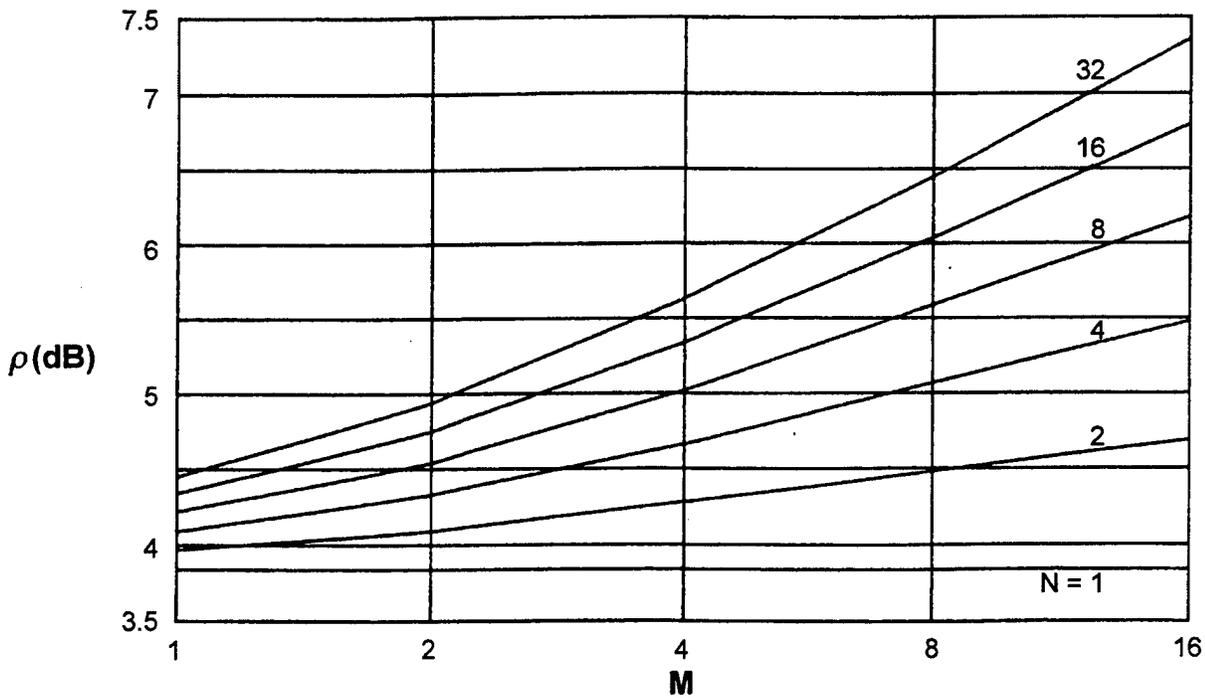
Figure 5.   Required Input SNR for P_f = 1E-6, P_d = 0.9, KM = 16,
Phase-Incoherent Signal
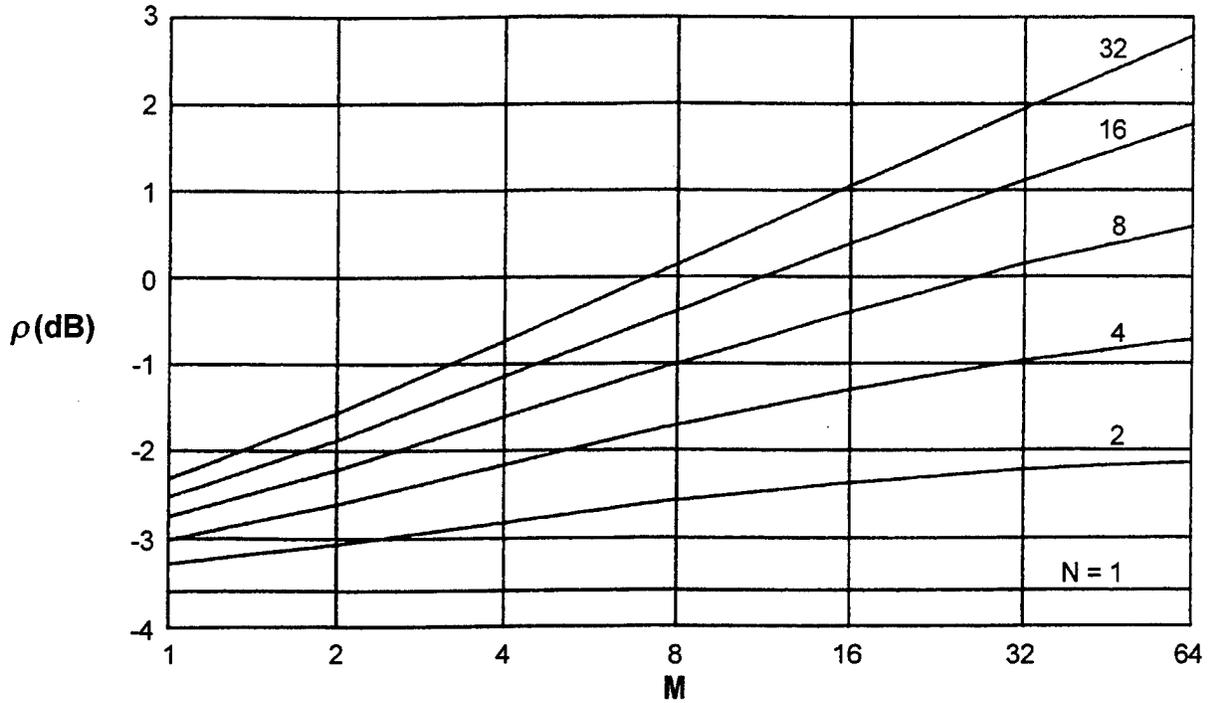
Figure 6. Required Input SNR for P_f = 1E-3, P_d = 0.5, KM = 64, Phase-Incoherent Signal
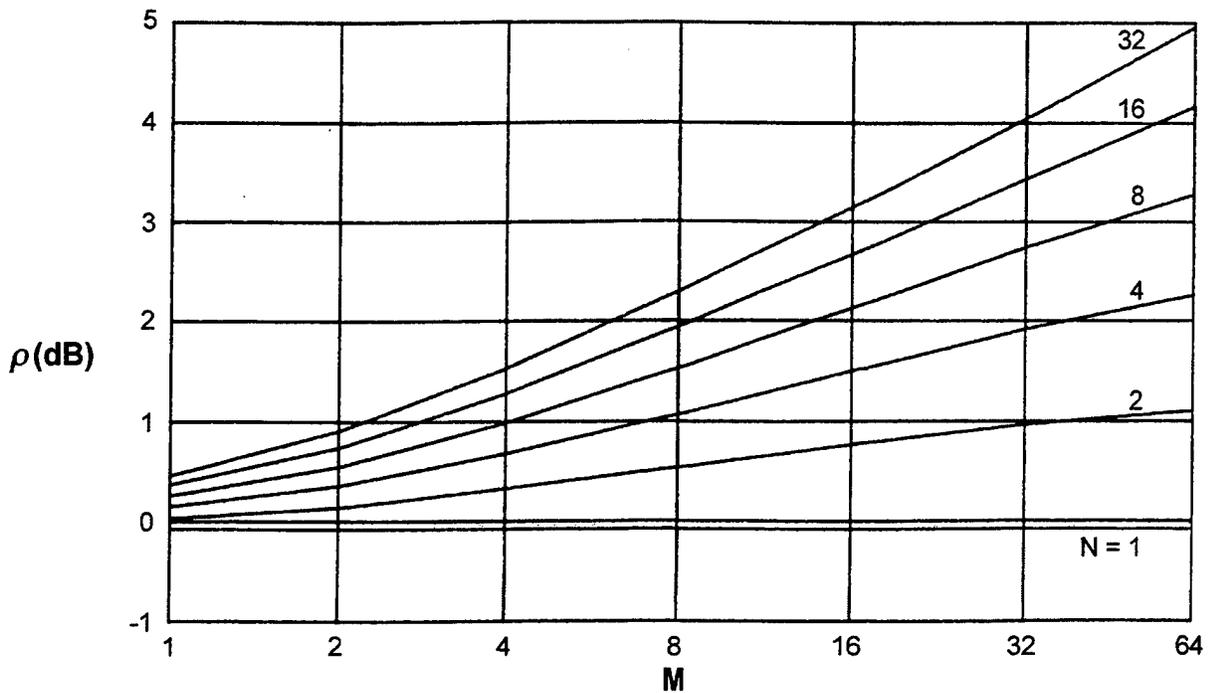
Figure 7. Required Input SNR for P_f = 1E-6, P_d = 0.9, KM = 64, Phase-Incoherent Signal
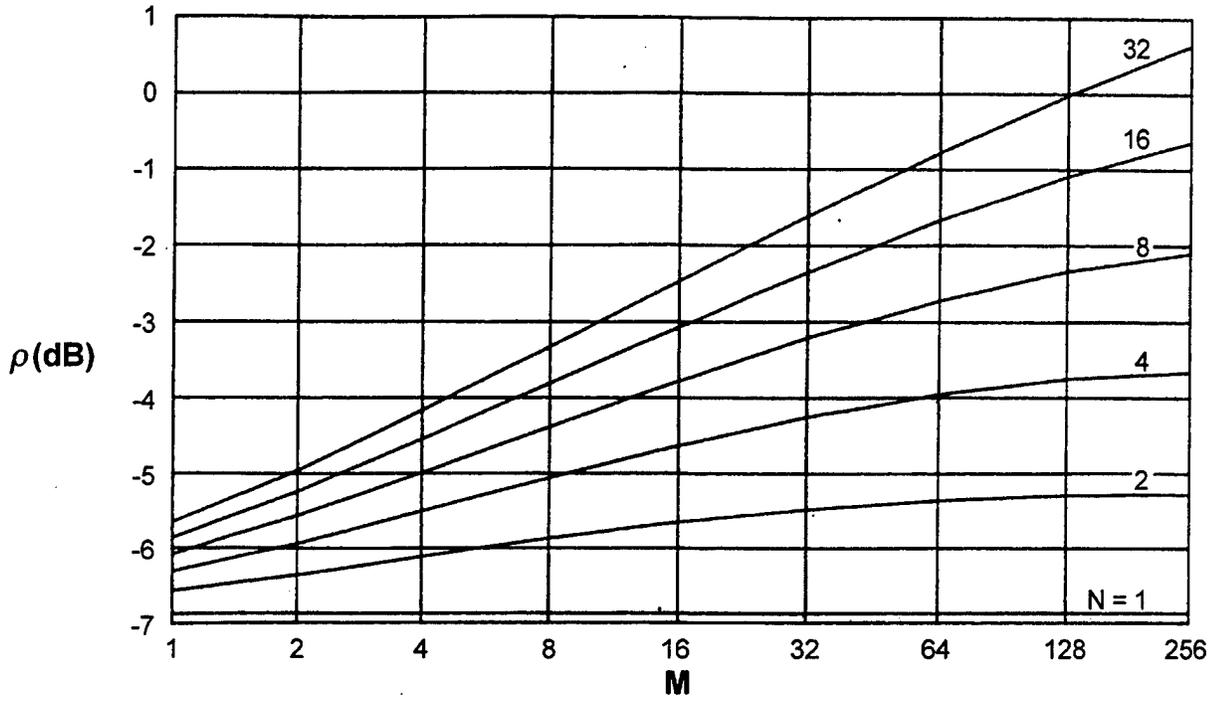
Figure 8. Required Input SNR for P_f = 1E-3, P_d = 0.5, KM = 256, Phase-Incoherent Signal
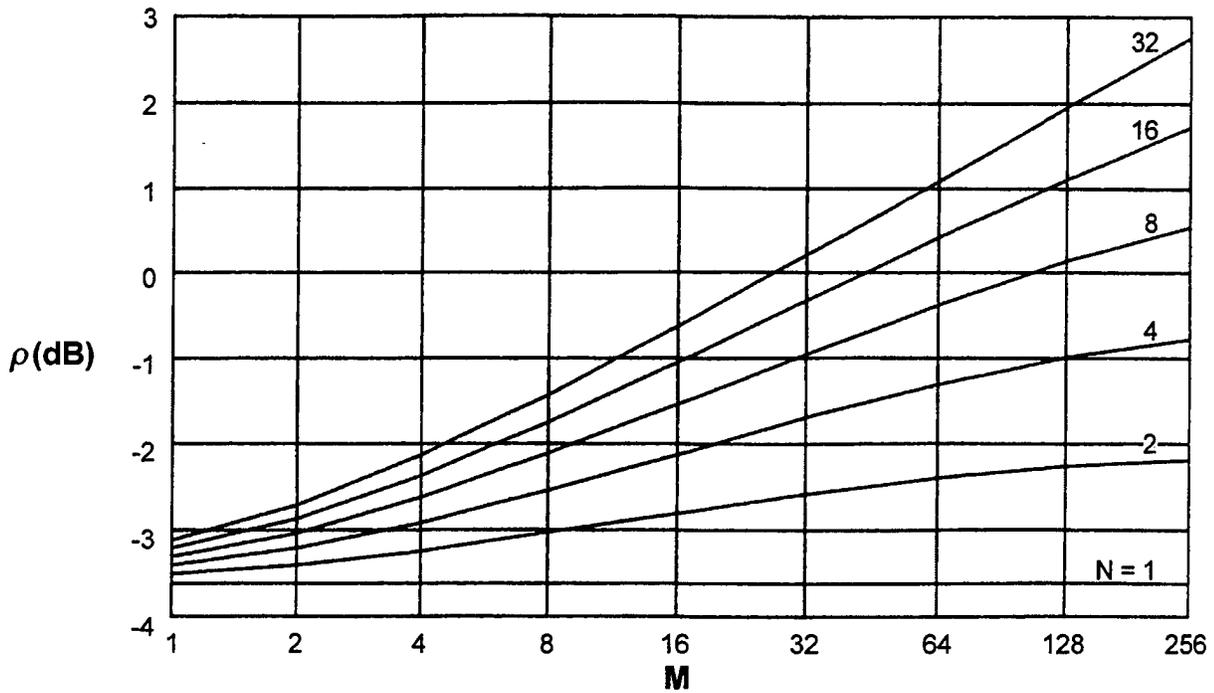
Figure 9. Required Input SNR for P_f = 1E-6, P_d = 0.9, KM = 256, Phase-Incoherent Signal

SUMMARY

For a phase-incoherent signal in Gaussian noise, closed forms have been derived for the PDFs at the output of a pre-averager followed by an or-ing operation. These forms have been numerically doubly Fourier-transformed to yield accurate results for the EDFs at the output of a post-averager, under both hypotheses H_0 and H_1, for numerous values of the parameters of the complete processor (figure 1). Such results enable investigation of the or-ing processor for false alarm probabilities P_f in the range of 1E-6 and smaller; there is no need to resort to lengthy simulations.

Numerous ROCs have been generated, which enable a user or system designer to quickly assess the losses to be expected from employing or-ing in the processor. Also, quantitative evaluation of the tradeoffs between pre-averaging and post-averaging has been conducted. Finally, since the enclosed tabulations will undoubtedly not cover all cases of practical interest, a MATLAB program for evaluation of additional ROCs is presented in appendix H.

The last case of a deterministic signal in additive Gaussian noise is currently under investigation. Tabulation of the ROCs for part III and tradeoffs between pre- and post-averaging will be conducted in a similar manner and for the same parameter values as accomplished here and in reference 1.

APPENDIX A — REQUIRED INPUT SNR FOR K = 1, M = 1

The cases of KM = 4, 16, 64, and 256 for the phase–incoherent signal have been investigated elsewhere in this report. In this appendix, to complete the sequence, results for KM = 1 are presented. Also, complete analytic results are attainable in this very special case, allowing for direct calculation of the required input SNRs to realize a specified level of performance (P_f and P_d) at the output of the or–ing processor in figure 1.

Use of equations (19) and (20) with M = 1 and any K results in

$$P_d = 1 - c_1(u) \, [c_0(u)]^{N-1} \,, \tag{A-1}$$

$$P_f = 1 - [c_0(u)]^N \,. \tag{A-2}$$

Then, in particular, for the phase–incoherent signal and K = 1, equations (22) and (25) yield, for any N and u > 0,

$$c_0(u) = 1 - \exp(-u) \,, \quad c_1(u) = 1 - Q\!\left((2\rho)^{\frac{1}{2}}, (2u)^{\frac{1}{2}}\right) \,, \tag{A-3}$$

$$P_d = 1 - \left[1 - Q\!\left((2\rho)^{\frac{1}{2}}, (2u)^{\frac{1}{2}}\right)\right] [1 - \exp(-u)]^{N-1} \,, \tag{A-4}$$

$$P_f = 1 - [1 - \exp(-u)]^N \,. \tag{A-5}$$

The ROCs for the phase–incoherent signal for K = 1, M = 1, and any N and ρ could be generated directly from these last two relations, if desired.

Define the auxiliary parameters

$$\alpha = (1 - P_f)^{1/N} \ , \qquad \beta = \frac{1 - P_d}{1 - P_f} \ , \qquad\qquad \text{(A-6)}$$

which can be computed once the desired P_f and P_d are specified. Then, the threshold u required to realize a specified P_f follows from equations (A-5) and (A-6) as

$$u = -\ln(1 - \alpha) \ . \qquad\qquad \text{(A-7)}$$

In a similar vein, the required input SNR ρ follows from equation (A-4), using the threshold u given by equation (A-7), as the solution of the transcendental equation

$$Q\left((2\rho)^{\frac{1}{2}}, (-2 \ \ln(1 - \alpha))^{\frac{1}{2}} \right) = 1 - \beta \ \alpha \ . \qquad\qquad \text{(A-8)}$$

Results for the SOP and HOP are shown in tables A-1 and A-2.

Table A-1.   Required Input SNR ρ(dB) for P_f = 1E-3, P_d = 0.5, K = 1, M = 1, Phase-Incoherent Signal

N	1	2	4	8	16	32
ρ(dB)	8.06	8.51	8.91	9.28	9.62	9.94

Table A-2.   Required Input SNR ρ(dB) for P_f = 1E-6, P_d = 0.9, K = 1, M = 1, Phase-Incoherent Signal

N	1	2	4	8	16	32
ρ(dB)	13.18	13.36	13.53	13.69	13.84	13.99

APPENDIX B — SUPPRESSION OF ALIASING EFFECTS NEAR ORIGIN

In this appendix, it is assumed that the PDF $p(u)$ and the CDF $c(u)$ of an RV are given and that it is desired to evaluate an accurate version of the corresponding CF $f(\xi)$, especially near the origin $\xi = 0$. This is very important when relations (18) and (36) are used for large M, where the near-origin behavior of CF $f_v(\xi)$ is the most critical feature.

To this end, define a unit-area localized function $b(u)$, centered at $u = 0$. Several examples are displayed in figure B-1.
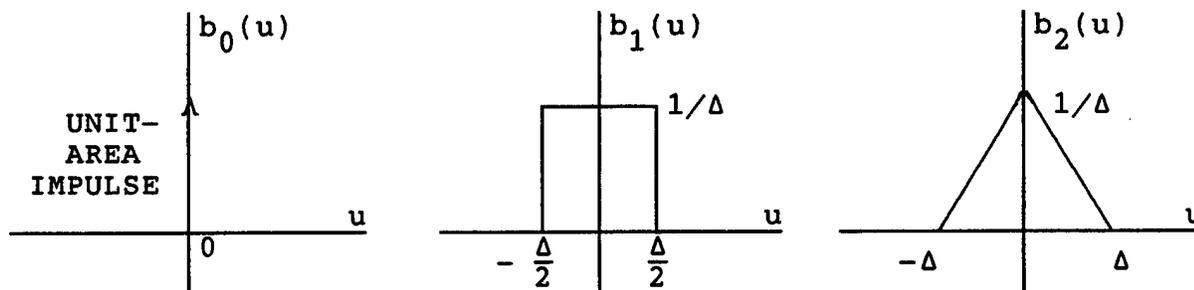
Figure B-1. Possible Localized Functions

Also, define convolution

$$s(u) = p(u) \oplus b(u) = \int dt \; p(t) \; b(u-t) = \int dt \; c(t) \; b'(u-t) \; . \quad \text{(B-1)}$$

Then, for the $b_0(u)$ function, there follows convolution $s_0(u) = p(u)$; for the $b_1(u)$ function, the convolution is

$$s_1(u) = \frac{1}{\Delta} \int_{u-\Delta/2}^{u+\Delta/2} dt \; p(t) = \frac{1}{\Delta}\left[c\left(u + \frac{\Delta}{2}\right) - c\left(u - \frac{\Delta}{2}\right)\right] \; ; \quad \text{(B-2)}$$

and for the $b_2(u)$ function, the convolution is

$$s_2(u) = \frac{1}{\Delta} \int_{u-\Delta}^{u+\Delta} dt \; p(t) \left(1 - \frac{|u-t|}{\Delta}\right) = \frac{1}{\Delta^2} \int_0^{\Delta} dt \; [c(u+t) - c(u-t)]. \quad (B-3)$$

Finally, define an impulsive approximation to PDF $p(u)$ as

$$\tilde{p}(u) \equiv \sum_n a_n \; \delta(u - n\Delta) \; , \quad\quad\quad (B-4)$$

where impulse area a_n, defined as

$$a_n \equiv \Delta \; s(n\Delta) = \Delta \int dt \; p(t) \; b(n\Delta - t) \; , \quad\quad\quad (B-5)$$

is a localized average of the PDF $p(u)$, centered at $n\Delta$. For the $b_1(u)$ example, the area is

$$a_{1n} = \Delta \; s_1(n\Delta) = c[(n + \tfrac{1}{2})\Delta] - c[(n - \tfrac{1}{2})\Delta] \; , \quad\quad\quad (B-6)$$

and for $b_0(u)$, the area is $a_{0n} = \Delta \; s_0(n\Delta) = \Delta \; p(n\Delta)$.

The impulsive PDF in equation (B-4) is expressible as

$$\tilde{p}(u) = \sum_n \Delta \; s(n\Delta) \; \delta(u - n\Delta) = \Delta \; s(u) \sum_n \delta(u - n\Delta) \equiv s(u) \; \Delta\delta_\Delta(u) \; , \quad\quad\quad (B-7)$$

where $\delta_\Delta(u)$ is an infinite impulse train of spacing Δ in u. The corresponding CF is

$$\tilde{f}(\xi) \equiv \int du \; \exp(i\xi u) \; \tilde{p}(u) = \sum_n a_n \; \exp(i\xi n\Delta) =$$

$$= \int du \; \exp(i\xi u) \; s(u) \; \Delta\delta_\Delta(u) =$$

$$= \frac{1}{2\pi} S(\xi) \oplus \left[2\pi \; \delta_{2\pi/\Delta}(\xi) \right] = \sum_n S\left(\xi - n\frac{2\pi}{\Delta} \right) , \qquad \text{(B-8)}$$

where function

$$S(\xi) \equiv \int du \; \exp(i\xi u) \; s(u) = \int du \; \exp(i\xi u) \; [p(u) \oplus b(u)] =$$

$$= f(\xi) \; B(\xi) , \qquad \text{(B-9)}$$

with definition

$$B(\xi) \equiv \int du \; \exp(i\xi u) \; b(u) . \qquad \text{(B-10)}$$

Therefore, the impulsive-approximation CF is given by

$$\tilde{f}(\xi) = \sum_n f\left(\xi - n\frac{2\pi}{\Delta} \right) B\left(\xi - n\frac{2\pi}{\Delta} \right) =$$

$$= f(\xi) \; B(\xi) + \sum_{n \neq 0} f\left(\xi - n\frac{2\pi}{\Delta} \right) B\left(\xi - n\frac{2\pi}{\Delta} \right) . \qquad \text{(B-11)}$$

The three earlier examples of $b(u)$ in figure B-1 can be Fourier transformed according to equation (B-10), yielding

$$B_0(\xi) = 1 , \qquad B_1(\xi) = \frac{\sin(\Delta\xi/2)}{\Delta\xi/2} , \qquad B_2(\xi) = \left[\frac{\sin(\Delta\xi/2)}{\Delta\xi/2} \right]^2 . \quad \text{(B-12)}$$

Thus, for no smoothing $b_0(u)$, the standard result is

$$\tilde{f}_0(\xi) = \sum_n a_{0n} \exp(i\xi n\Delta) = \Delta \sum_n p(n\Delta) \exp(i\xi n\Delta) =$$

$$= f(\xi) + \sum_{n \neq 0} f\left(\xi - n\frac{2\pi}{\Delta} \right) , \qquad \text{(B-13)}$$

where the last term represents the sum of all the undesired aliasing lobes in the ξ domain. If PDF $p(u)$ is sufficiently

smooth for _all_ u, such that CF $f(\xi)$ decays very rapidly with ξ, then sampling increment Δ in equation (B-4) can easily be chosen small enough that an essentially alias-free region near the origin $\xi = 0$ can be found where CF approximation $\tilde{f}_0(\xi)$ is essentially equal to the desired CF $f(\xi)$.

However, if PDF $p(u)$ is not sufficiently smooth (for example, $u \exp(-u)$ for $u > 0$), then CF $f(\xi)$ decays slowly, causing significant aliasing effects, due to the last term in equation (B-13). These effects can be suppressed by using first-order smoothing $b_1(u)$, giving an alternative approximate CF that utilizes CDF samples, namely,

$$\tilde{f}_1(\xi) = \sum_n a_{1n} \exp(i\xi n\Delta) = \sum_n [c(n\Delta + \tfrac{1}{2}\Delta) - c(n\Delta - \tfrac{1}{2}\Delta)] \exp(i\xi n\Delta) =$$

$$= f(\xi) B_1(\xi) + \sum_{n \neq 0} f\left(\xi - n\frac{2\pi}{\Delta}\right) B_1\left(\xi - n\frac{2\pi}{\Delta}\right) . \qquad \text{(B-14)}$$

But, from equation (B-12), since

$$B_1(n2\pi/\Delta) = \sin(n\pi)/(n\pi) = 0 \quad \text{for} \quad n \neq 0 , \qquad \text{(B-15)}$$

all the aliasing lobe contributions (real and imaginary) are zero at $\xi = 0$, the center of the desired lobe of equation (B-14). In fact, the real part of the aliasing components of $\tilde{f}_1(\xi)$ also has zero slope at $\xi = 0$; however, the imaginary part has a nonzero slope at $\xi = 0$. These effects result in a small aliasing contribution in the immediate neighborhood of $\xi = 0$, leading to the approximation

$$\tilde{f}_1(\xi) \cong f(\xi) \, B_1(\xi) \quad \text{for } \xi \text{ near } 0 \, . \tag{B-16}$$

Finally, since $B_1(\xi)$ is a known function, the desired CF $f(\xi)$ can be obtained approximately as

$$f(\xi) \cong \frac{\tilde{f}_1(\xi)}{B_1(\xi)} \quad \text{for } \xi \text{ near } 0 \, . \tag{B-17}$$

If CF $f(\xi)$ must be raised to a power, as in the averaging of several RVs, each with PDF $p(u)$, this approach is particularly attractive for circumventing aliasing effects; the larger the power, the more useful is this alternative. Notice that the division by $B_1(\xi)$ in equation (B-17) must be done before raising the CF to the power of interest.

For the smoother $b_2(u)$ in figure B-1, there follows, from equation (B-12),

$$B_2(n2\pi/\Delta) = 0 \quad \text{and} \quad B_2'(n2\pi/\Delta) = 0 \quad \text{for } n \neq 0 \, . \tag{B-18}$$

Thus, the total aliasing component of $\tilde{f}_2(\xi)$ and its slope (real and imaginary) are zero at $\xi = 0$. This leads to the approximation for the desired CF as

$$f(\xi) \cong \frac{\tilde{f}_2(\xi)}{B_2(\xi)} \quad \text{for } \xi \text{ near } 0 \, . \tag{B-19}$$

The utility of equation (B-19) depends on the ability to evaluate $s_2(n\Delta)$ in equation (B-3) simply.

Equations (B-6) and (B-14) presume that samples of the CDF $c(u)$ are available at in-between points $u = (n+\frac{1}{2})\Delta$. If the CDF samples are only available at the points $u = n\Delta$, a modified smoothing function $b_3(u)$ can be employed. The pertinent equations are

$$b_3(u) = \begin{Bmatrix} 1/(2\Delta) & \text{for } |u| < \Delta \\ 0 & \text{otherwise} \end{Bmatrix} , \qquad B_3(\xi) = \frac{\sin(\Delta\xi)}{\Delta\xi} , \qquad \text{(B-20)}$$

$$s_3(u) = \int_{u-\Delta}^{u+\Delta} dt\, p(t)\, \frac{1}{2\Delta} = \frac{1}{2\Delta}[c(u+\Delta) - c(u-\Delta)] , \qquad \text{(B-21)}$$

$$a_{3n} = \Delta\, s_3(n\Delta) = \frac{1}{2}[c(n\Delta+\Delta) - c(n\Delta-\Delta)] , \qquad \text{(B-22)}$$

$$\tilde{f}_3(\xi) = \sum_n a_{3n} \exp(i\xi n\Delta) = \frac{1}{2}\sum_n [c(n\Delta+\Delta) - c(n\Delta-\Delta)] \exp(i\xi n\Delta) =$$

$$= f(\xi)\, B_3(\xi) + \sum_{n\neq 0} f\left(\xi - n\frac{2\pi}{\Delta}\right) B_3\left(\xi - n\frac{2\pi}{\Delta}\right) , \qquad \text{(B-23)}$$

$$f(\xi) \cong \frac{\tilde{f}_3(\xi)}{B_3(\xi)} \quad \text{for } \xi \text{ near } 0 . \qquad \text{(B-24)}$$

Since $B_3(\xi)$ in equation (B-20) is zero at $|\xi| = \pi/\Delta$, it is necessary to keep $|\xi| < \pi/\Delta$ when equation (B-24) is used; this limit is twice as restrictive as the one for the use of $B_1(\xi)$ in equations (B-12) and (B-17). Relations (B-23) and (B-24) afford an alternative method of proceeding directly from samples of the CDF $c(u)$ to the CF $f(\xi)$. The quantity on the right-hand side of equation (B-21) can be interpreted as an estimate of the slope of the CDF $c(u)$ at u, that is, an estimate of the PDF $p(u)$ at u.

APPENDIX C — ROCs FOR KM = 4, PHASE-INCOHERENT SIGNAL

This appendix contains the ROCs for or-ing with pre- and post-averaging when the time-bandwidth product KM is fixed at 4; the possible combinations (from table 1) are repeated here:

K	M	N
4	1	1,2,4,8,16,32
2	2	
1	4	

For N = 1, only the product KM matters; the first plot in this appendix covers this special case, under the labeling K = 4, N = 1, M = 1. The other 5 values of N, along with the 3 possible combinations of K and M, yield 15 additional ROCs, for a total of 16 ROCs in this appendix.
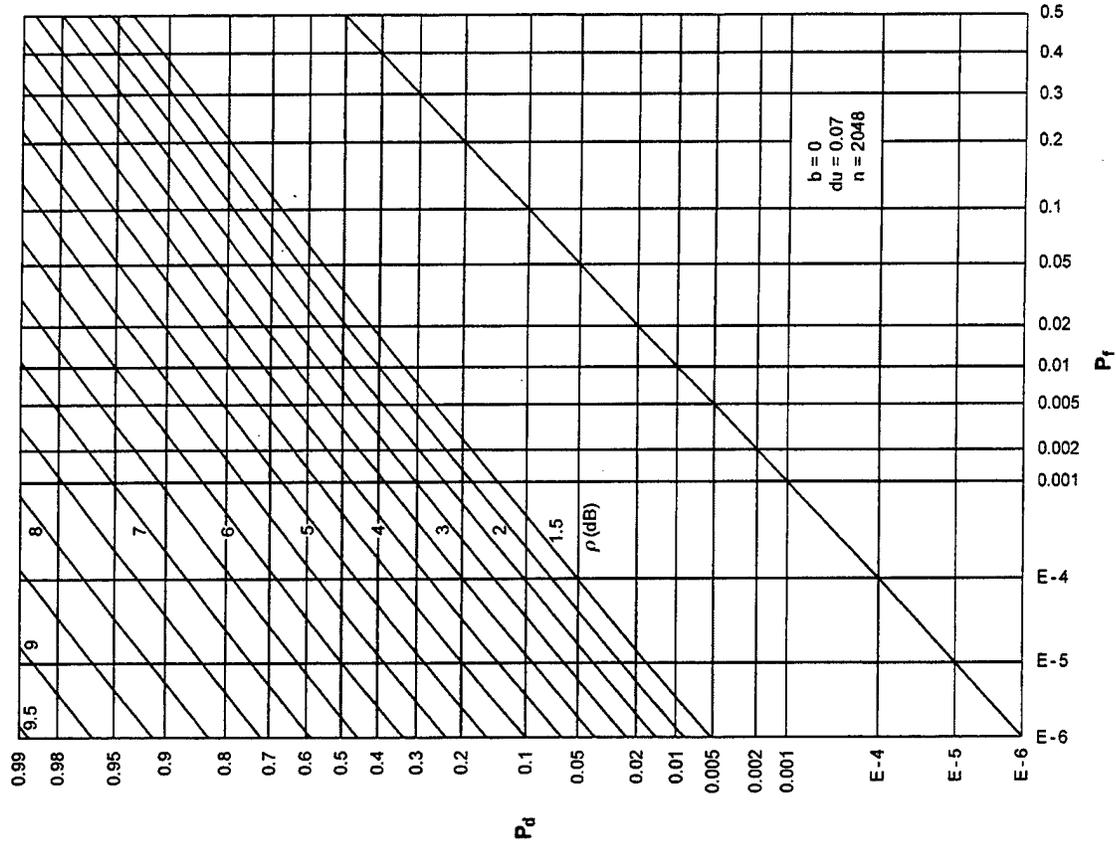
Figure C-2. ROCs for K = 4, N = 2, M = 1
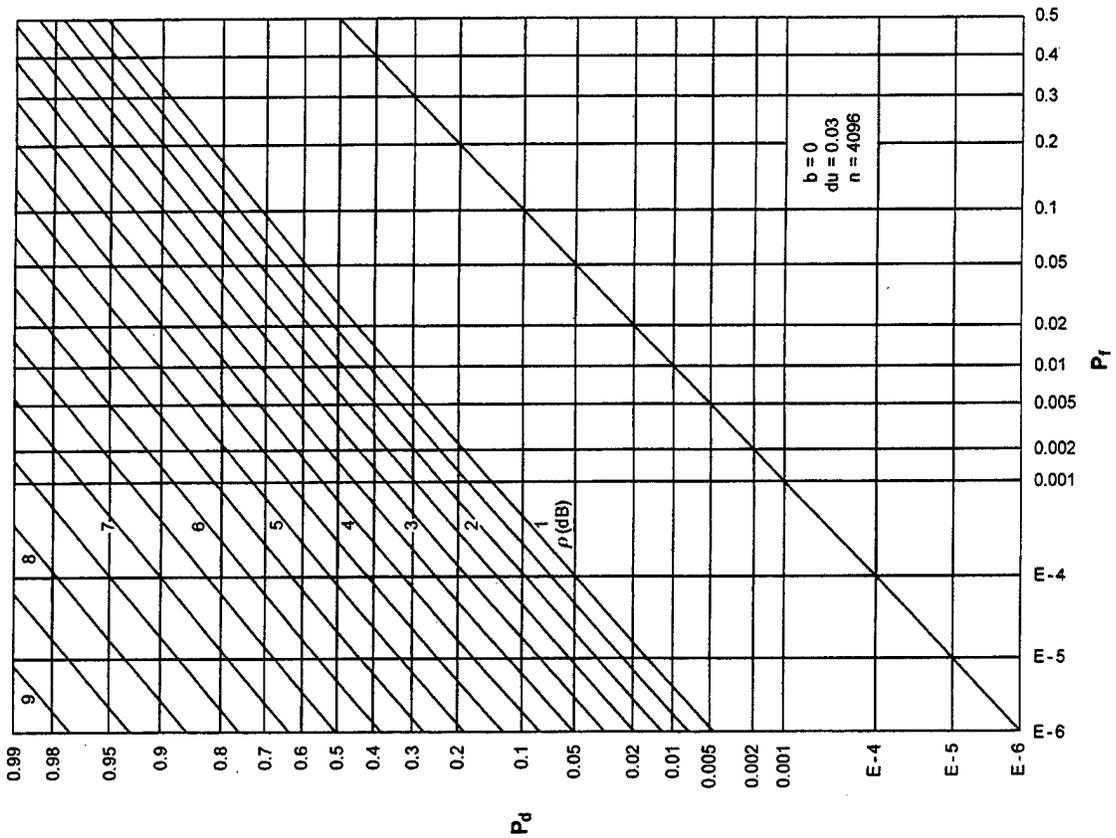
Figure C-1. ROCs for K = 4, N = 1, M = 1

C-2
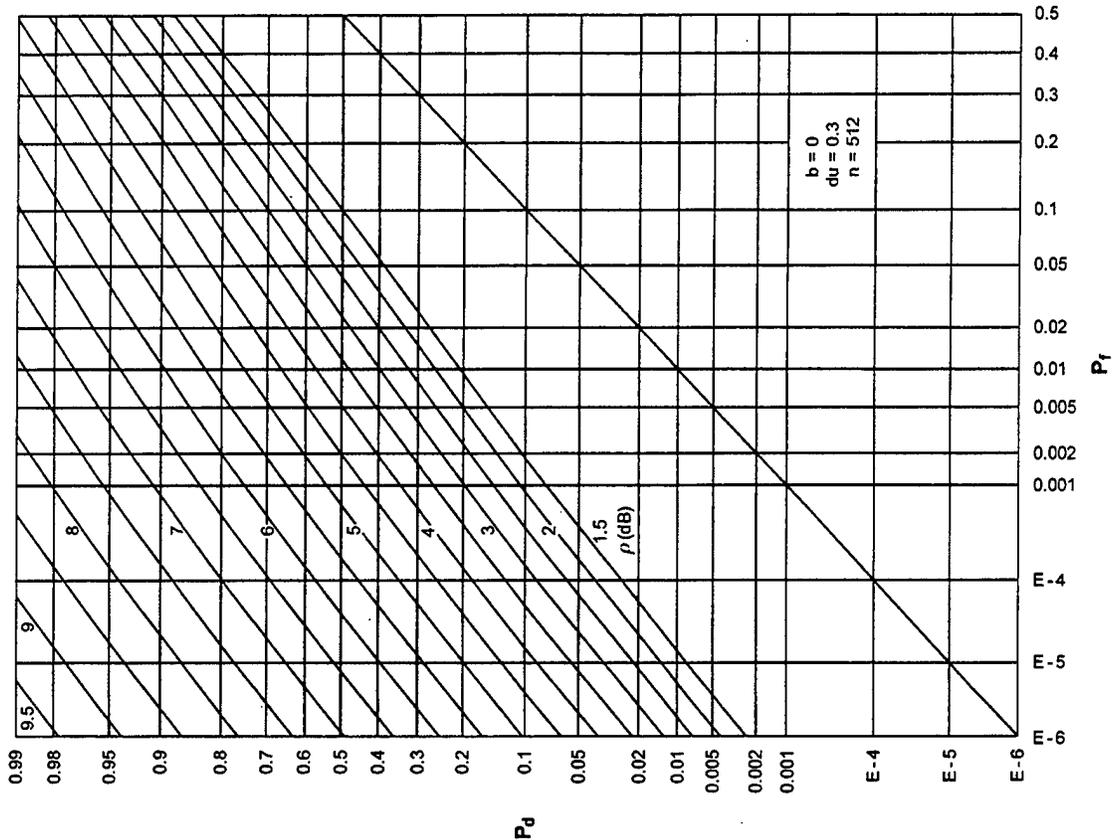
Figure C-4. ROCs for K = 4, N = 8, M = 1
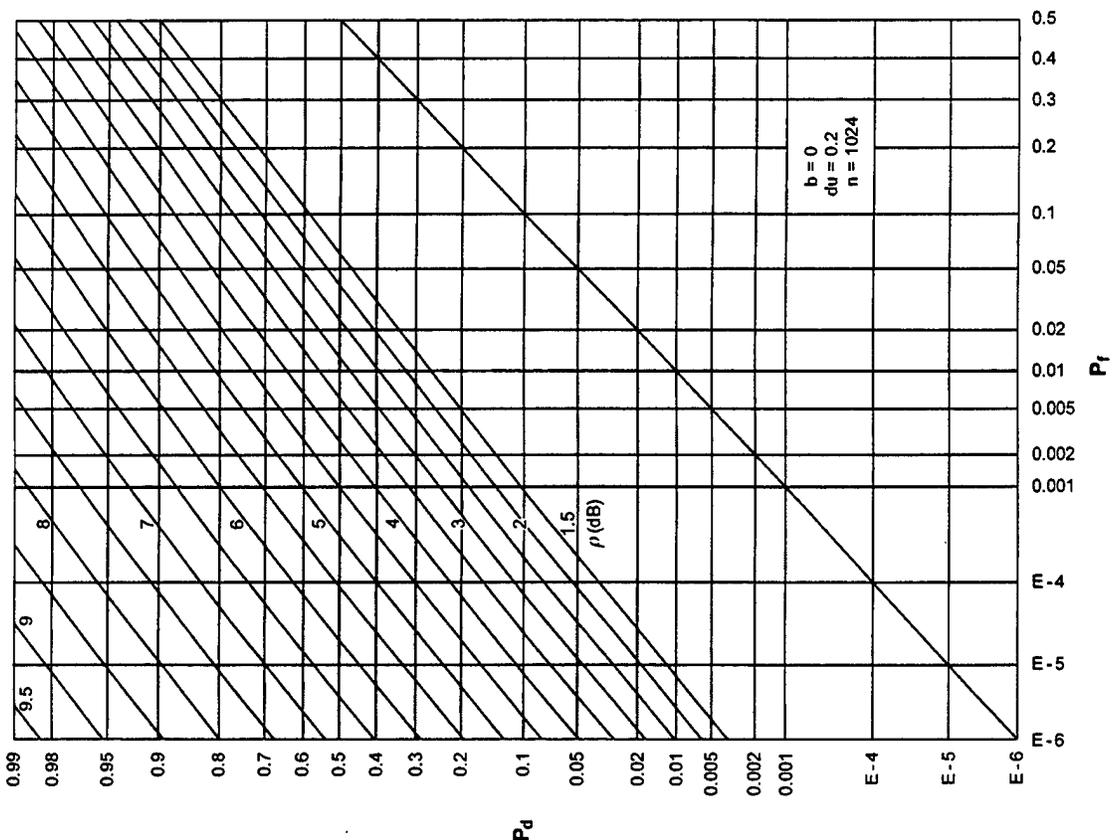
Figure C-3. ROCs for K = 4, N = 4, M = 1

C-3
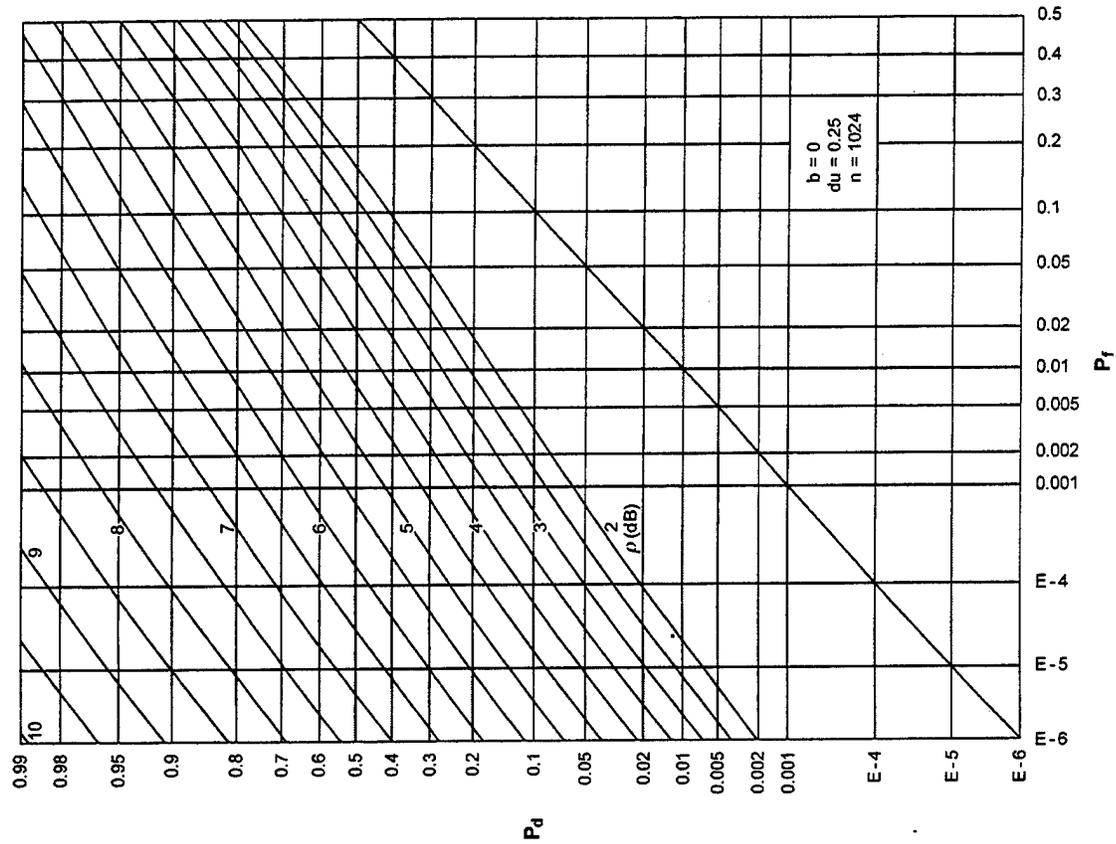
Figure C-6. ROCs for K = 4, N = 32, M = 1
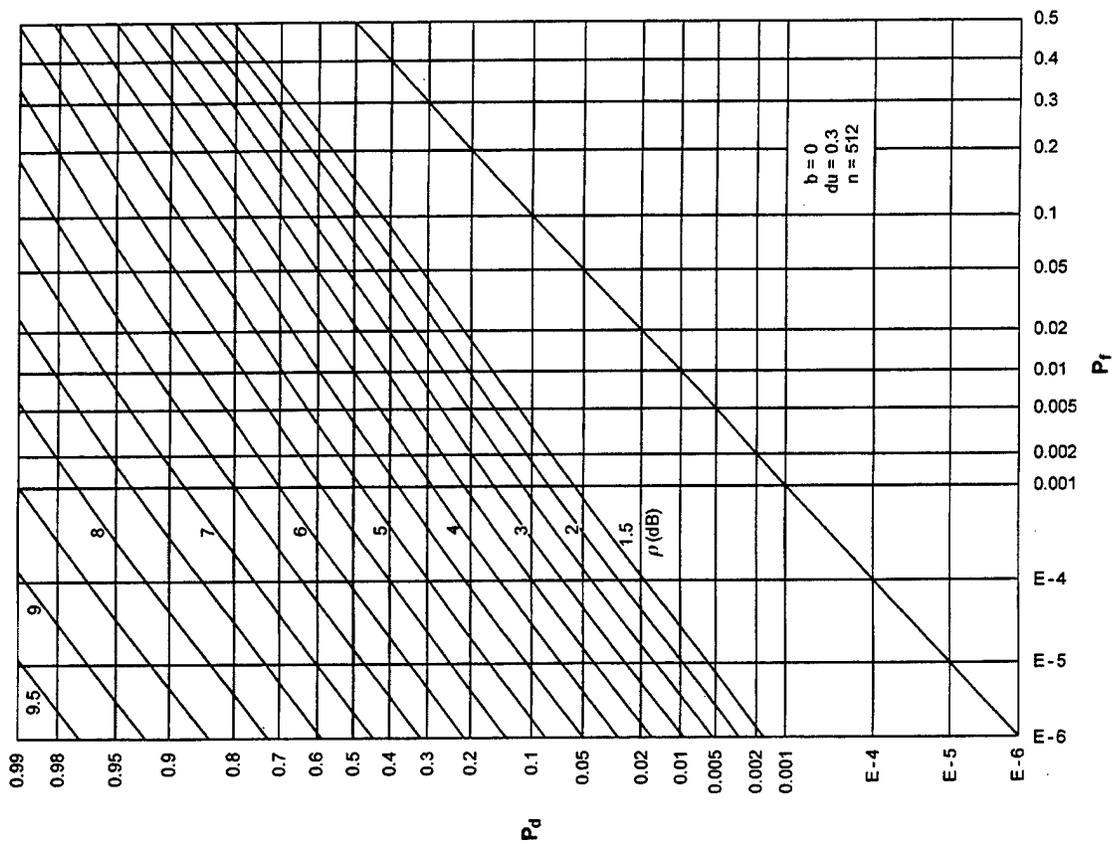
Figure C-5. ROCs for K = 4, N = 16, M = 1

C-4

Figure C-8. (top chart)

b = 0
du = 0.07
n = 2048

P_f axis values: 0.5, 0.4, 0.3, 0.2, 0.1, 0.05, 0.02, 0.01, 0.005, 0.002, 0.001, E-4, E-5, E-6

P_d axis values: 0.99, 0.98, 0.95, 0.9, 0.8, 0.7, 0.6, 0.5, 0.4, 0.3, 0.2, 0.1, 0.05, 0.02, 0.01, 0.005, 0.002, 0.001, E-4, E-5, E-6

ρ (dB) curves: 9.5, 9, 8, 7, 6, 5, 4, 3, 2, 1.5
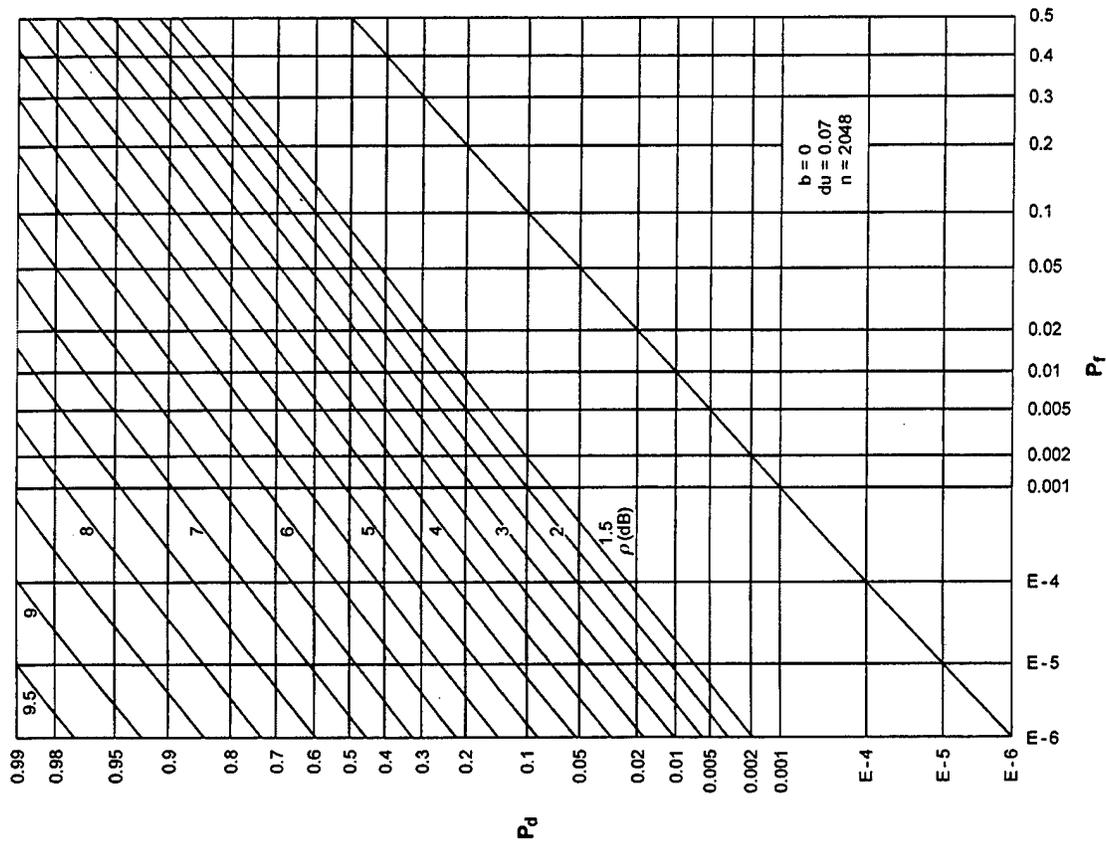
Figure C-8. ROCs for K = 2, N = 4, M = 2

Figure C-7. (bottom chart)

b = 0
du = 0.04
n = 4096

P_f axis values: 0.5, 0.4, 0.3, 0.2, 0.1, 0.05, 0.02, 0.01, 0.005, 0.002, 0.001, E-4, E-5, E-6

P_d axis values: 0.99, 0.98, 0.95, 0.9, 0.8, 0.7, 0.6, 0.5, 0.4, 0.3, 0.2, 0.1, 0.05, 0.02, 0.01, 0.005, 0.002, 0.001, E-4, E-5, E-6

ρ (dB) curves: 9.5, 9, 8, 7, 6, 5, 4, 3, 2, 1.5
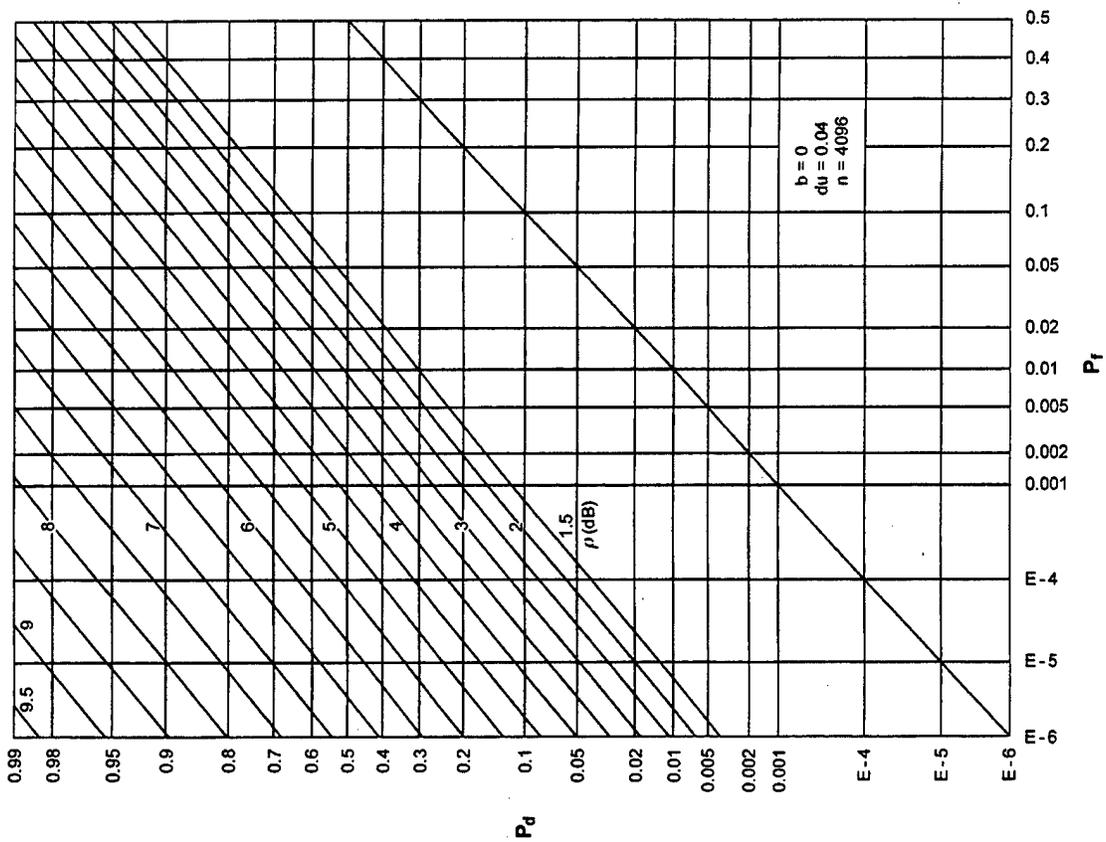
Figure C-7. ROCs for K = 2, N = 2, M = 2

Figure C-10. ROCs for K = 2, N = 16, M = 2

Figure C-9. ROCs for K = 2, N = 8, M = 2

C-6
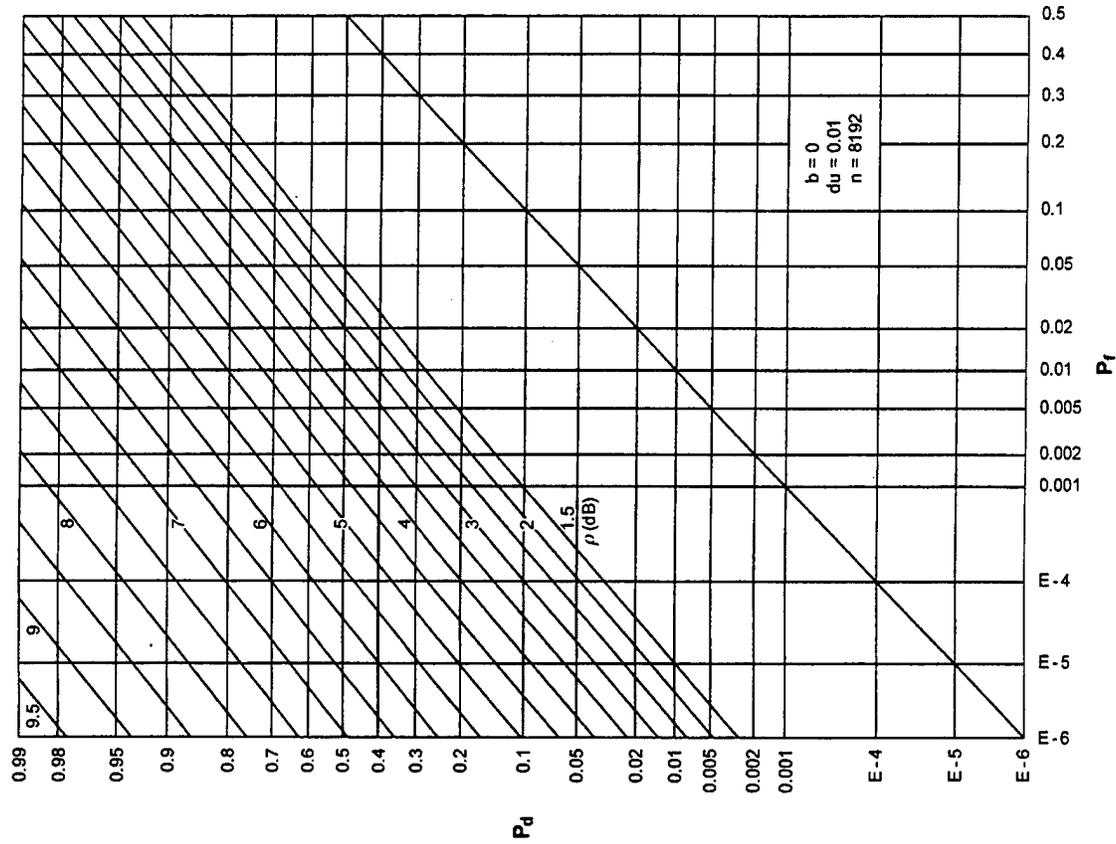
**Figure C-12. ROCs for K = 1, N = 2, M = 4**
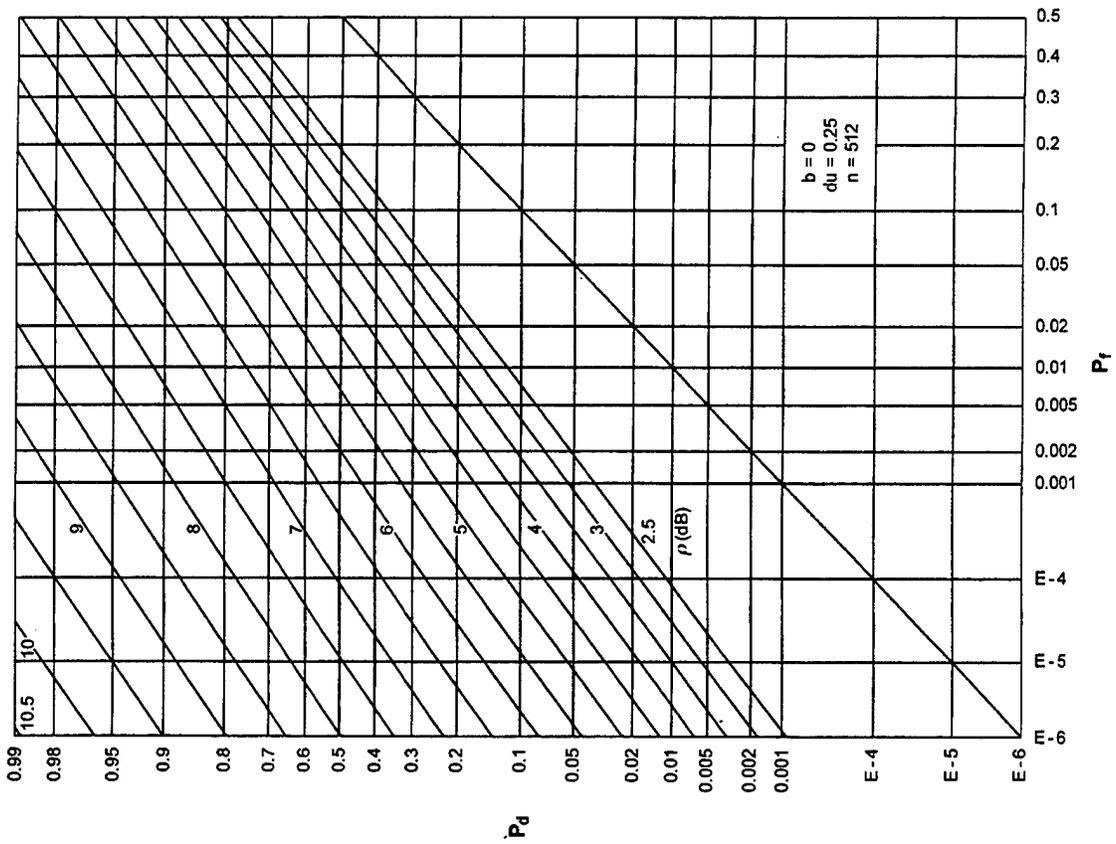
Figure C-11. ROCs for K = 2, N = 32, M = 2
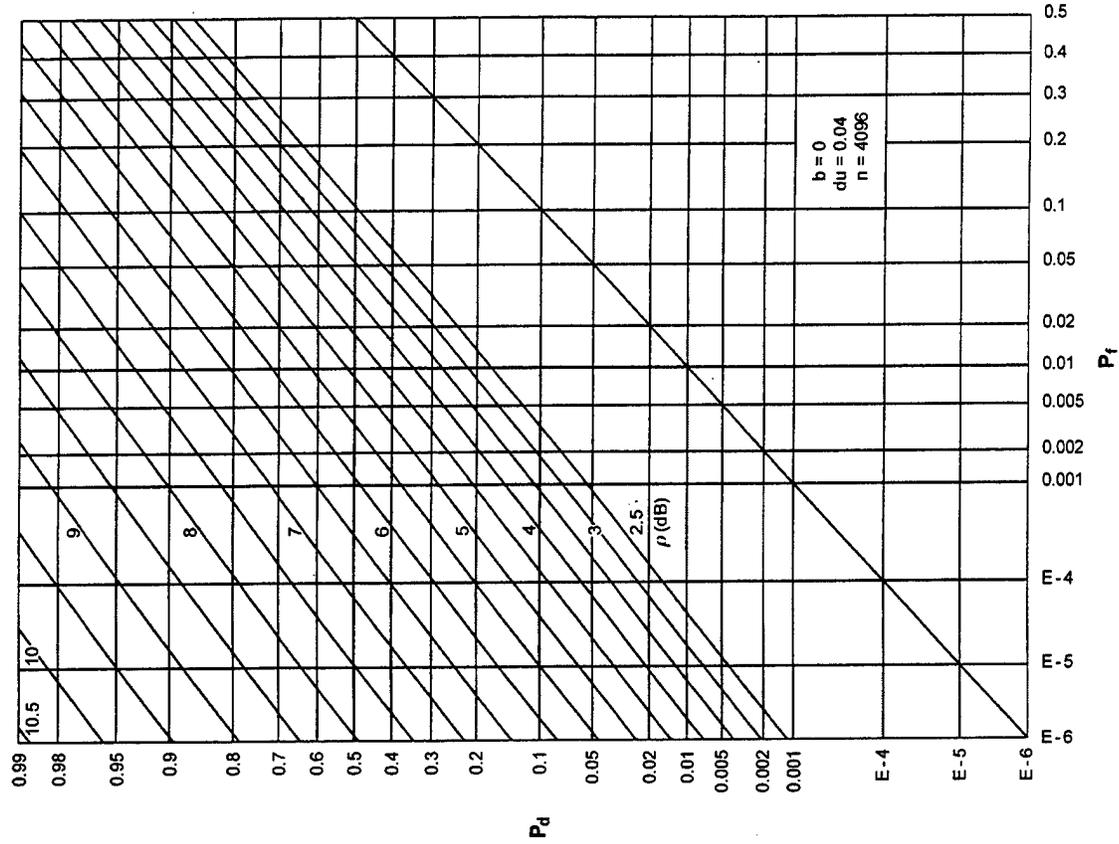
Figure C-14. ROCs for K = 1, N = 8, M = 4
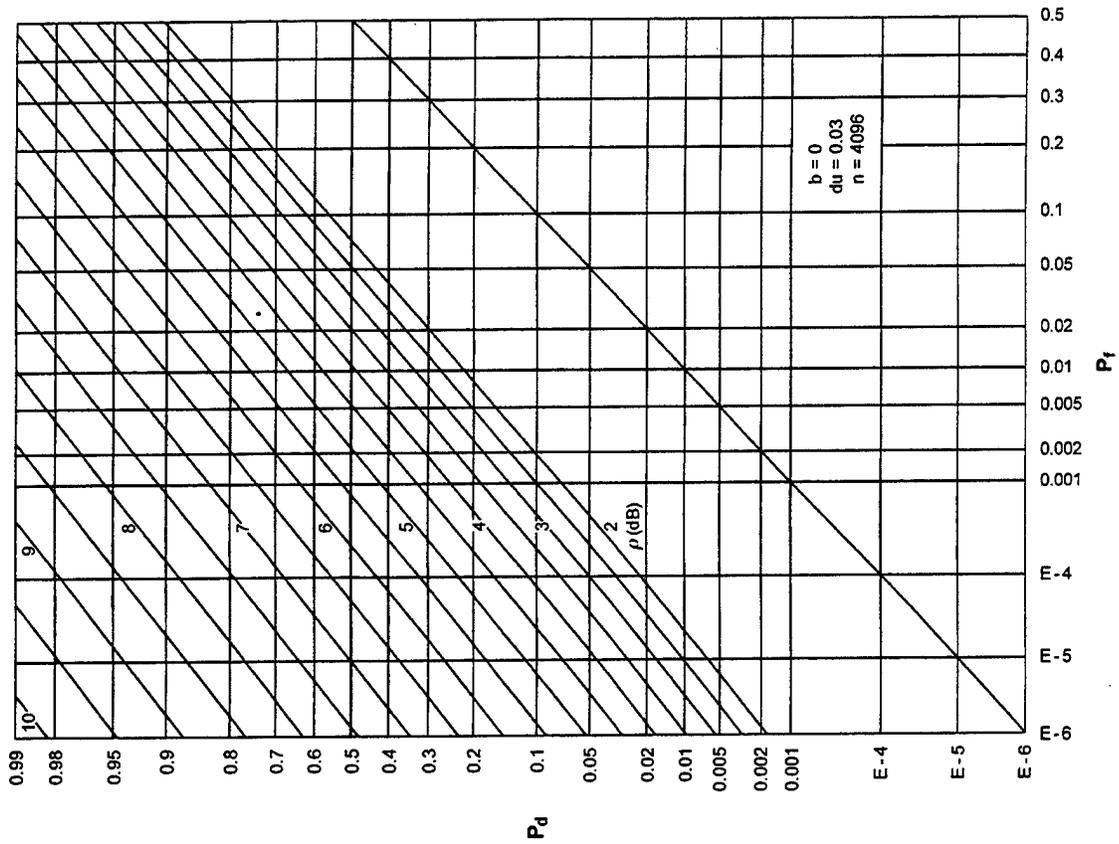
Figure C-13. ROCs for K = 1, N = 4, M = 4

C-8
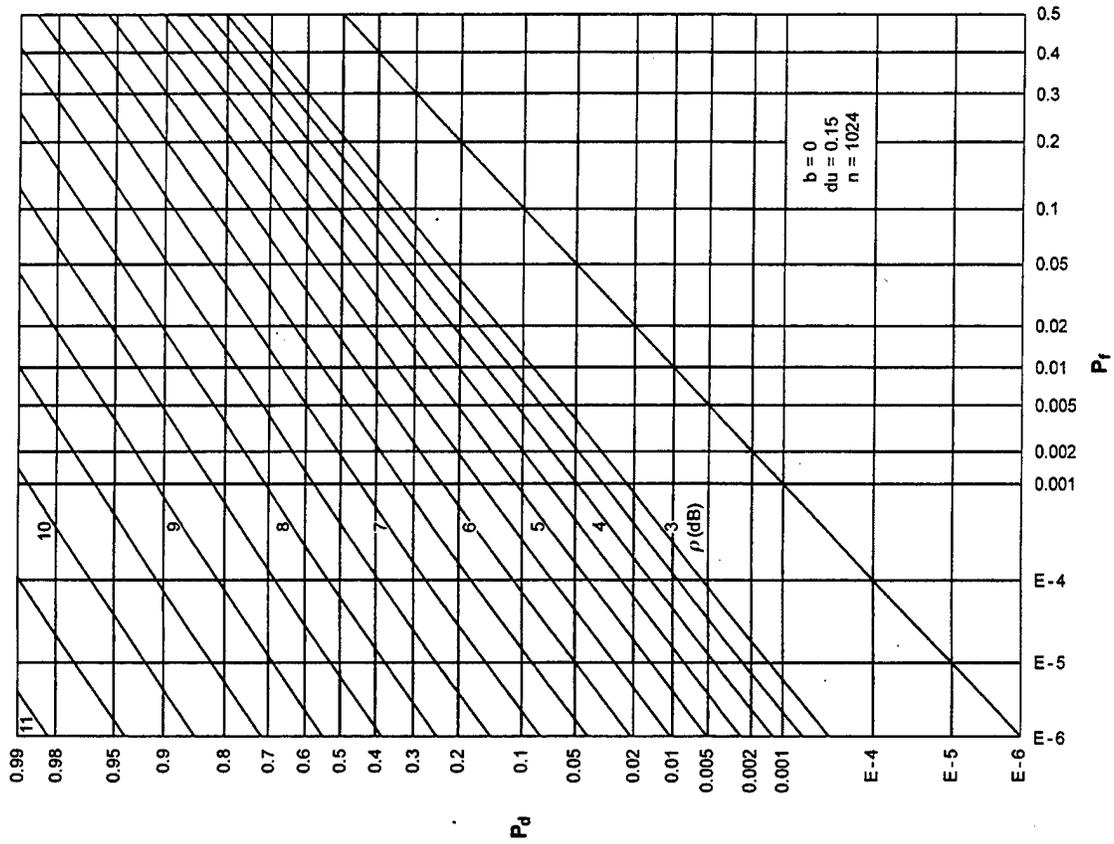
Figure C-16. ROCs for K = 1, N = 32, M = 4
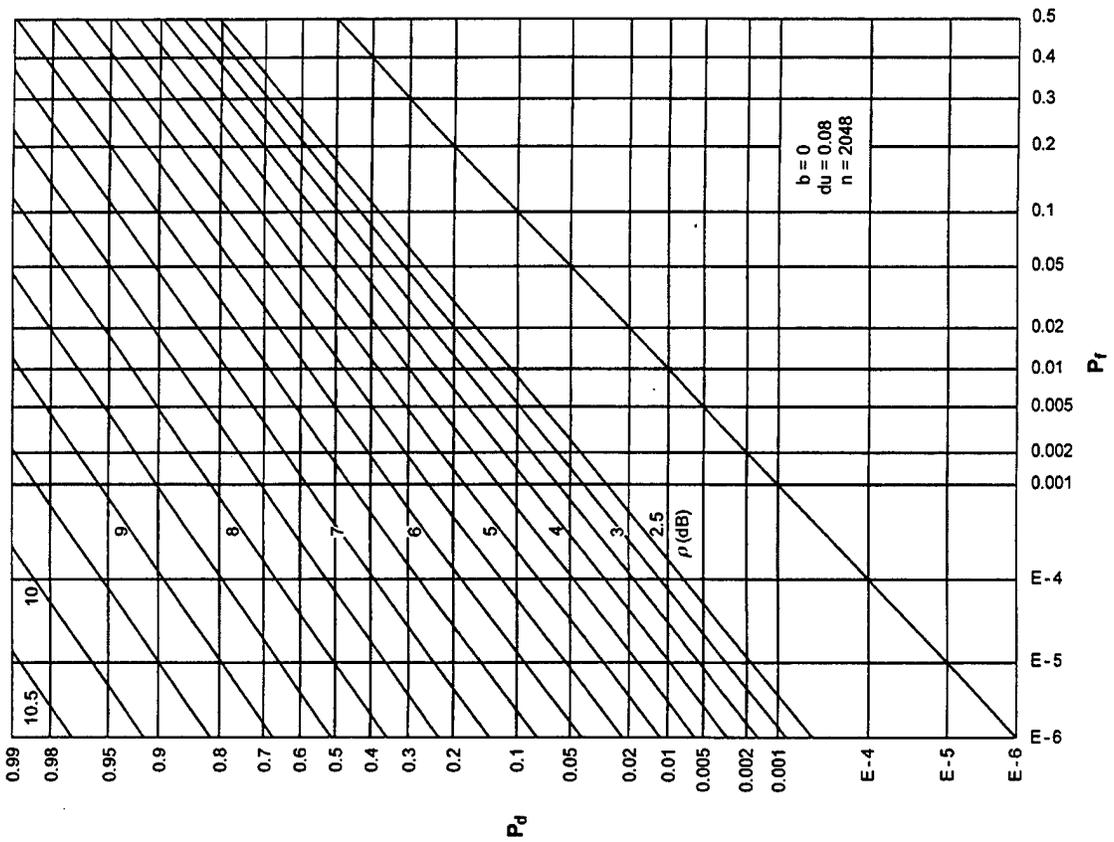
Figure C-15. ROCs for K = 1, N = 16, M = 4

APPENDIX D — ROCs FOR KM = 16, PHASE-INCOHERENT SIGNAL

This appendix contains the ROCs for or-ing with pre- and post-averaging when the time-bandwidth product KM is fixed at 16; the possible combinations (from table 1) are repeated here:

K	M	N
16	1	1,2,4,8,16,32
8	2	
4	4	
2	8	
1	16	

For N = 1, only the product KM matters; the first plot in this appendix covers this special case, under the labeling K = 16, N = 1, M = 1. The other 5 values of N, along with the 5 possible combinations of K and M, yield 25 additional ROCs, for a total of 26 ROCs in this appendix.
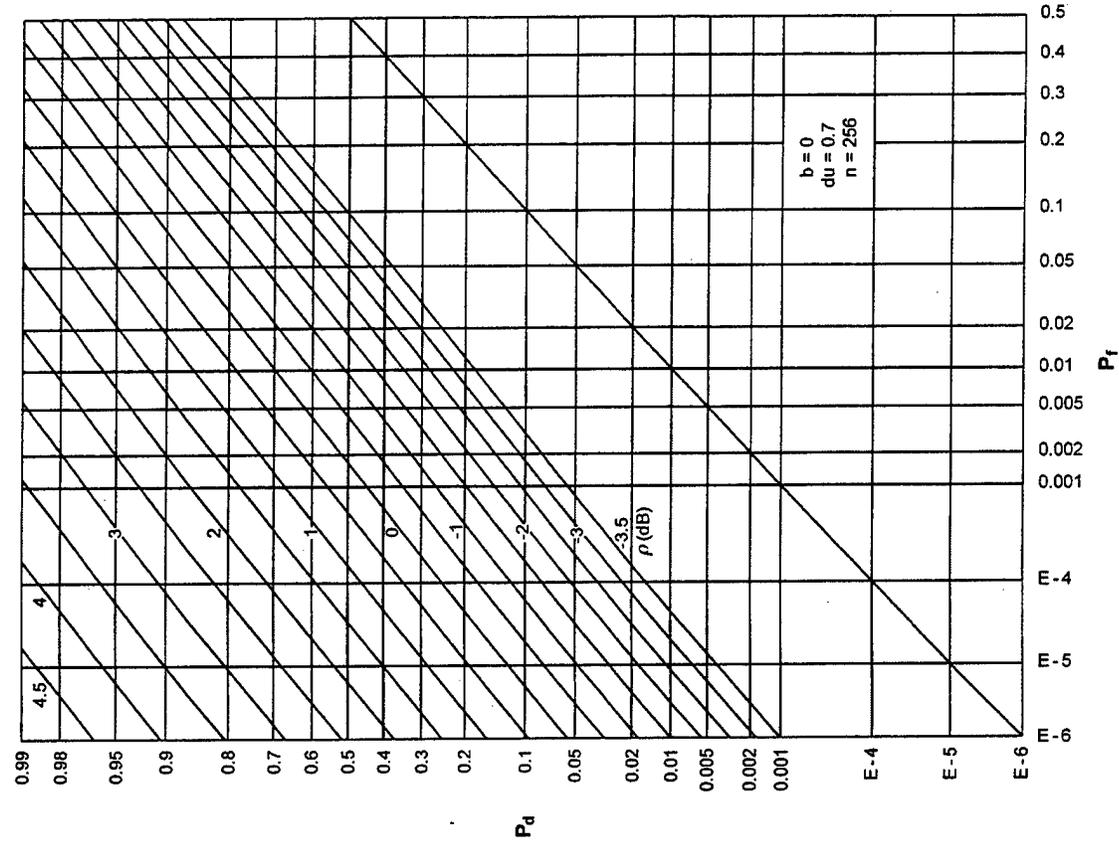
Figure D-2. ROCs for K = 16, N = 2, M = 1

$b = 0$
$du = 0.7$
$n = 256$

P_f

P_d

ρ (dB)
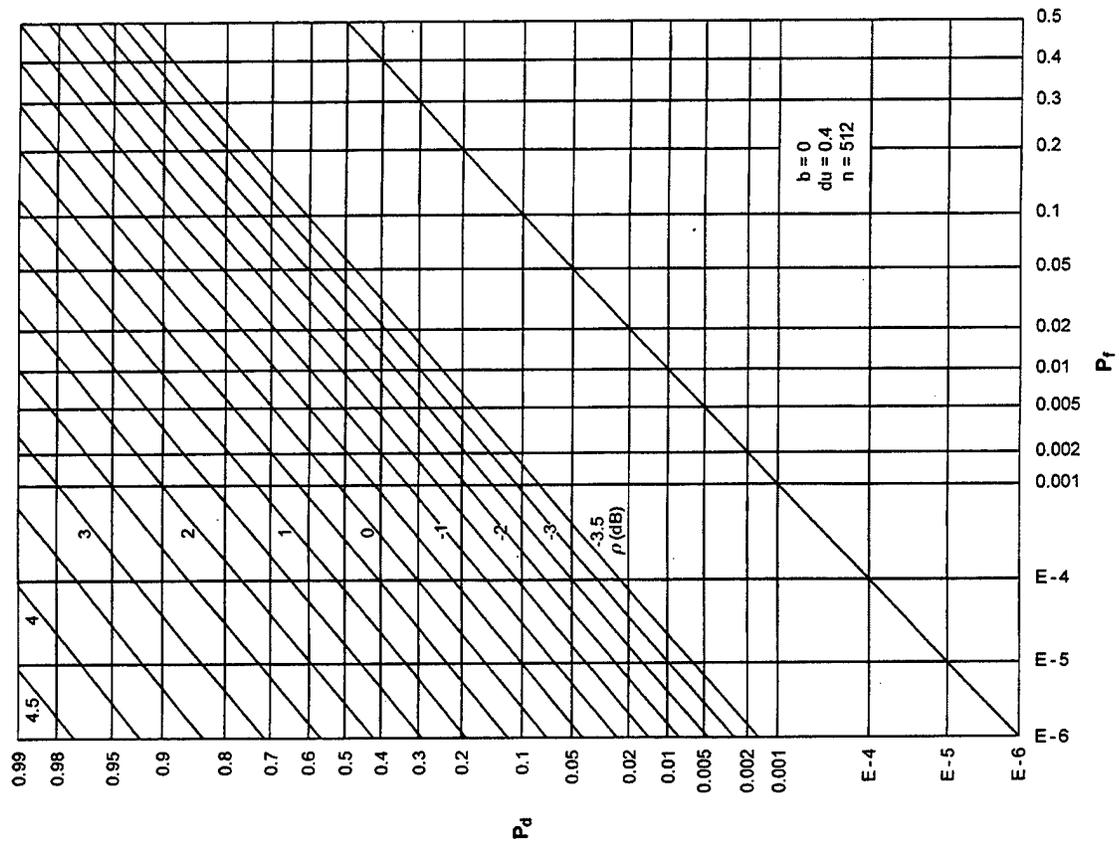
Figure D-1. ROCs for K = 16, N = 1, M = 1

$b = 0$
$du = 0.4$
$n = 512$

P_f

P_d

ρ (dB)
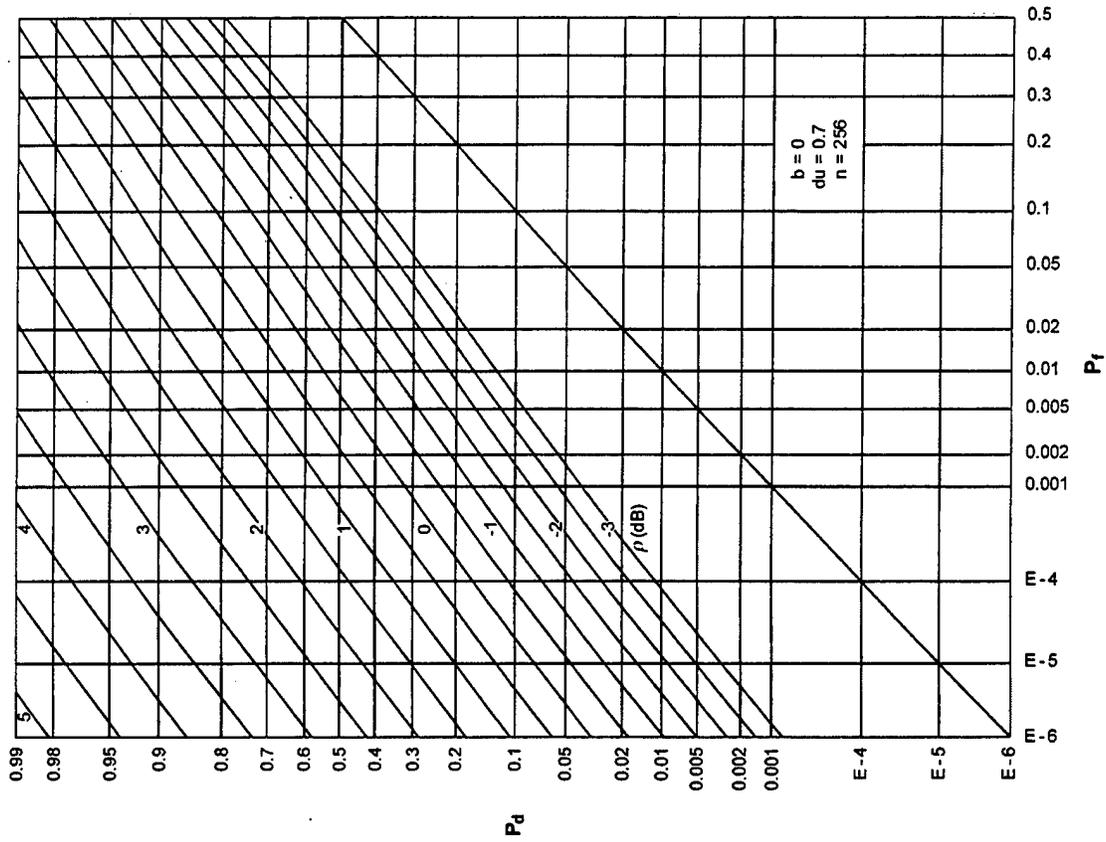
**Figure D-4. ROCs for K = 16, N = 8, M = 1**
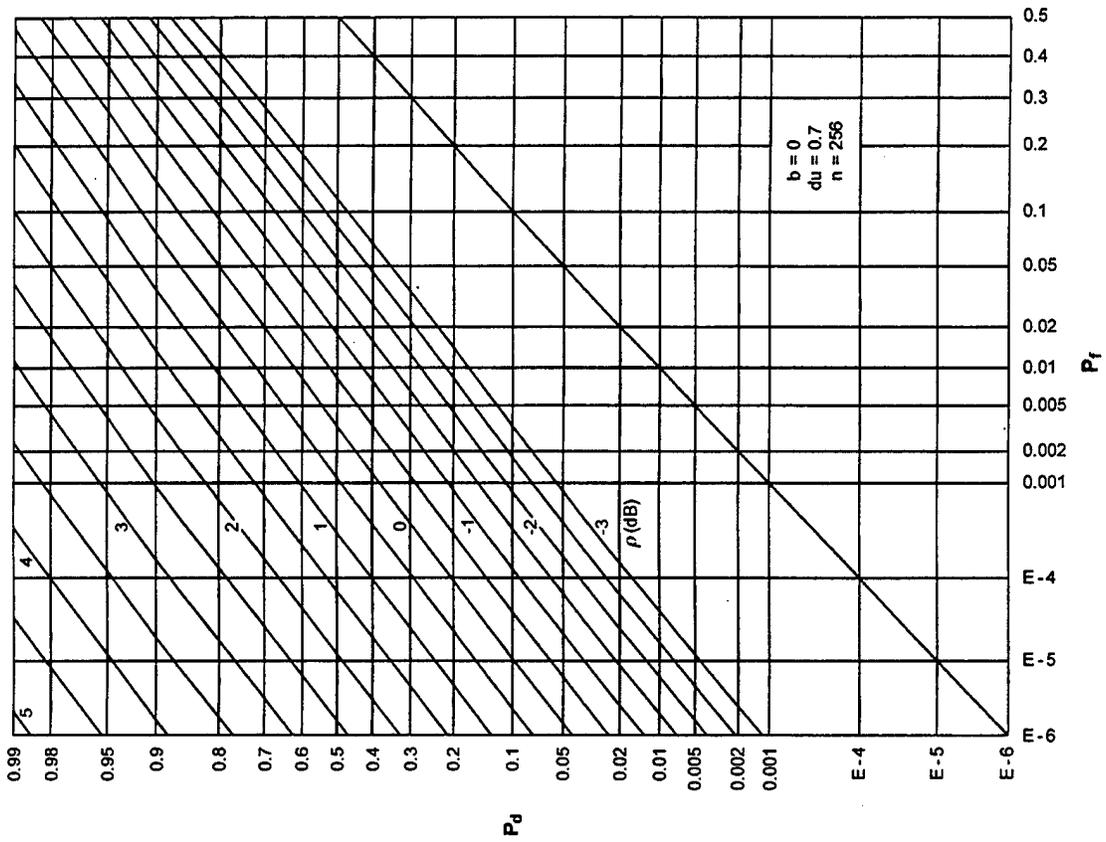
Figure D-3. ROCs for K = 16, N = 4, M = 1
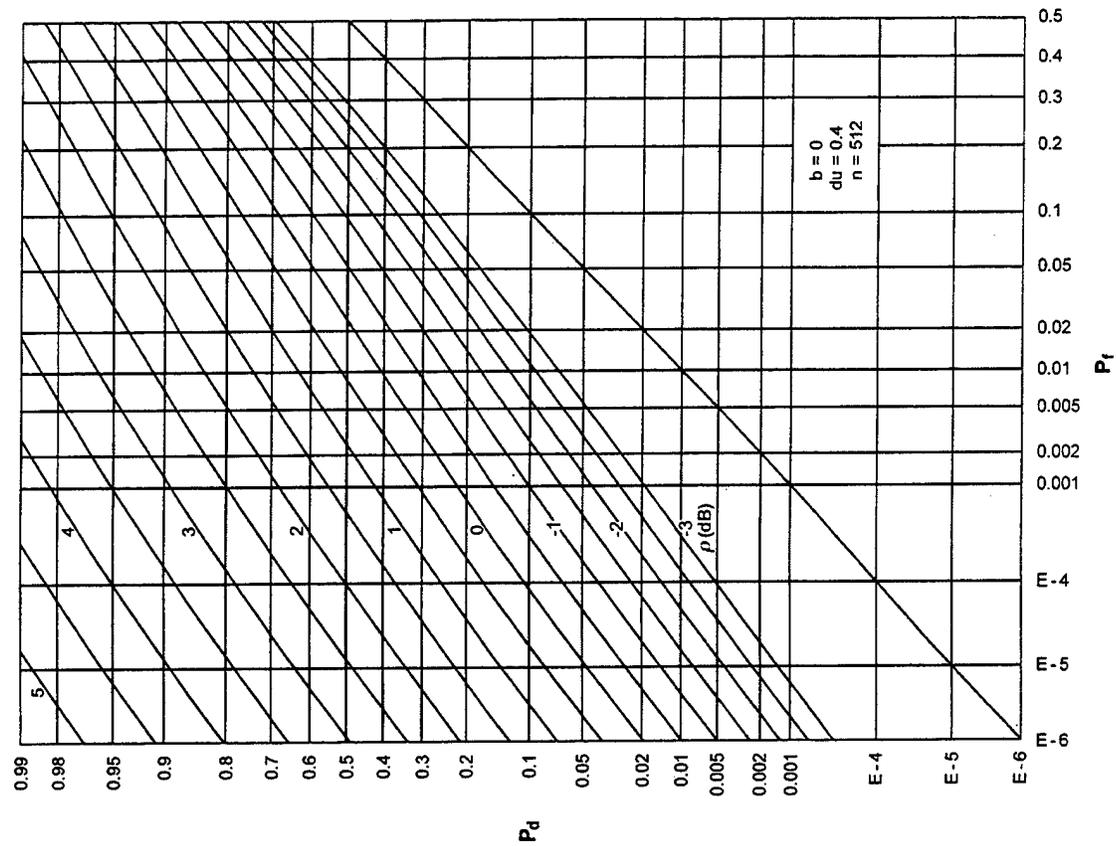
Figure D-6.   ROCs for K = 16, N = 32, M = 1

b = 0
du = 0.4
n = 512

ρ(dB)

P_f

P_d
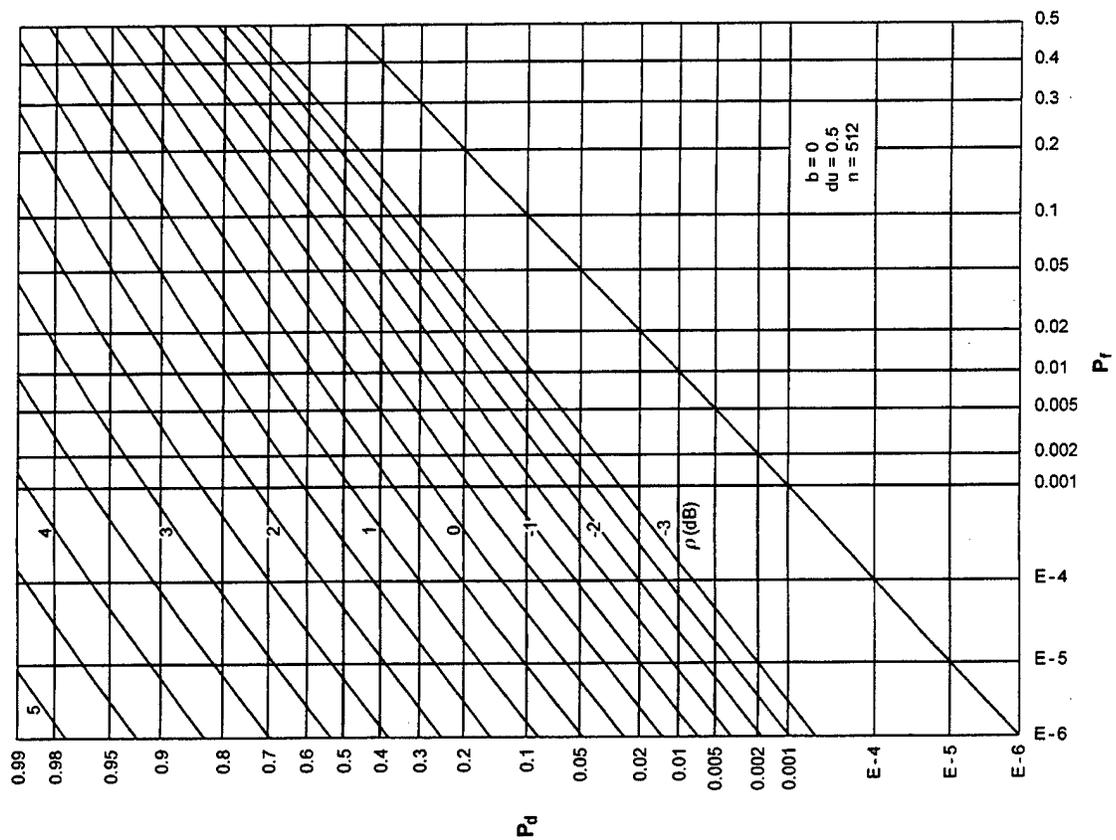
Figure D-5.   ROCs for K = 16, N = 16, M = 1

b = 0
du = 0.5
n = 512

ρ(dB)

P_f

P_d
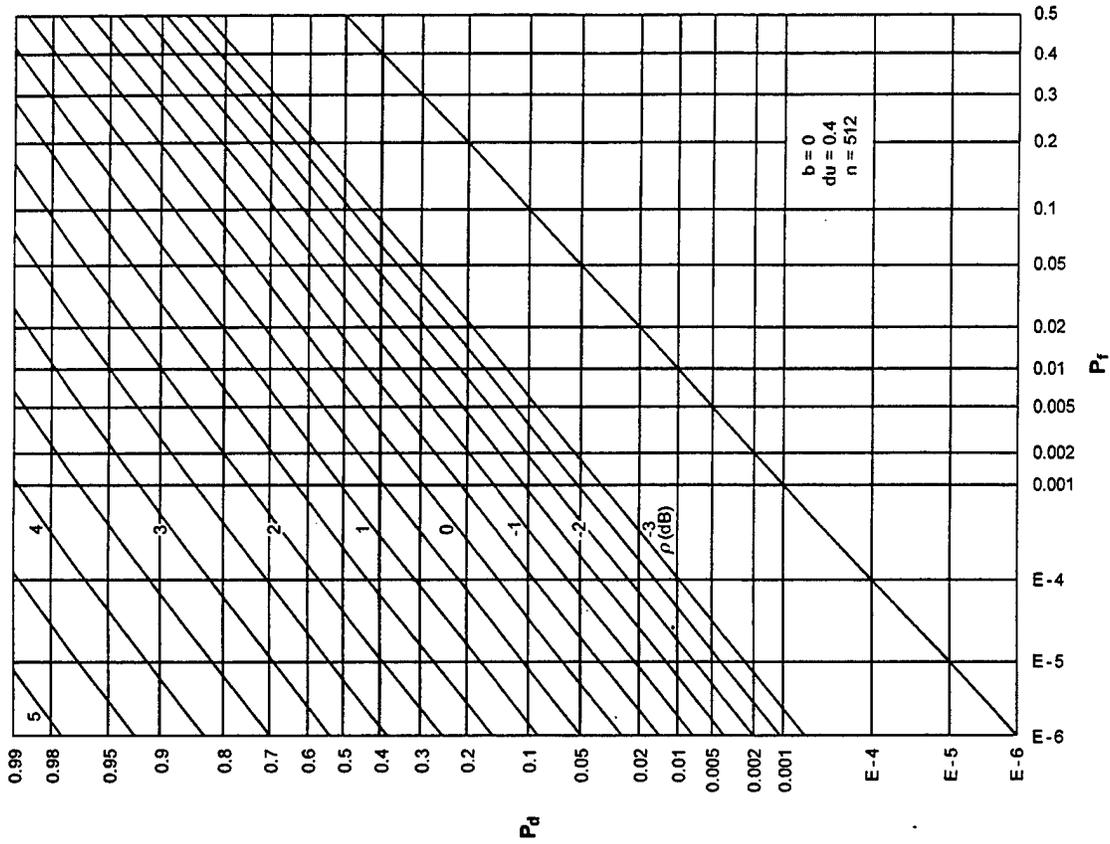
Figure D-8. ROCs for K = 8, N = 4, M = 2
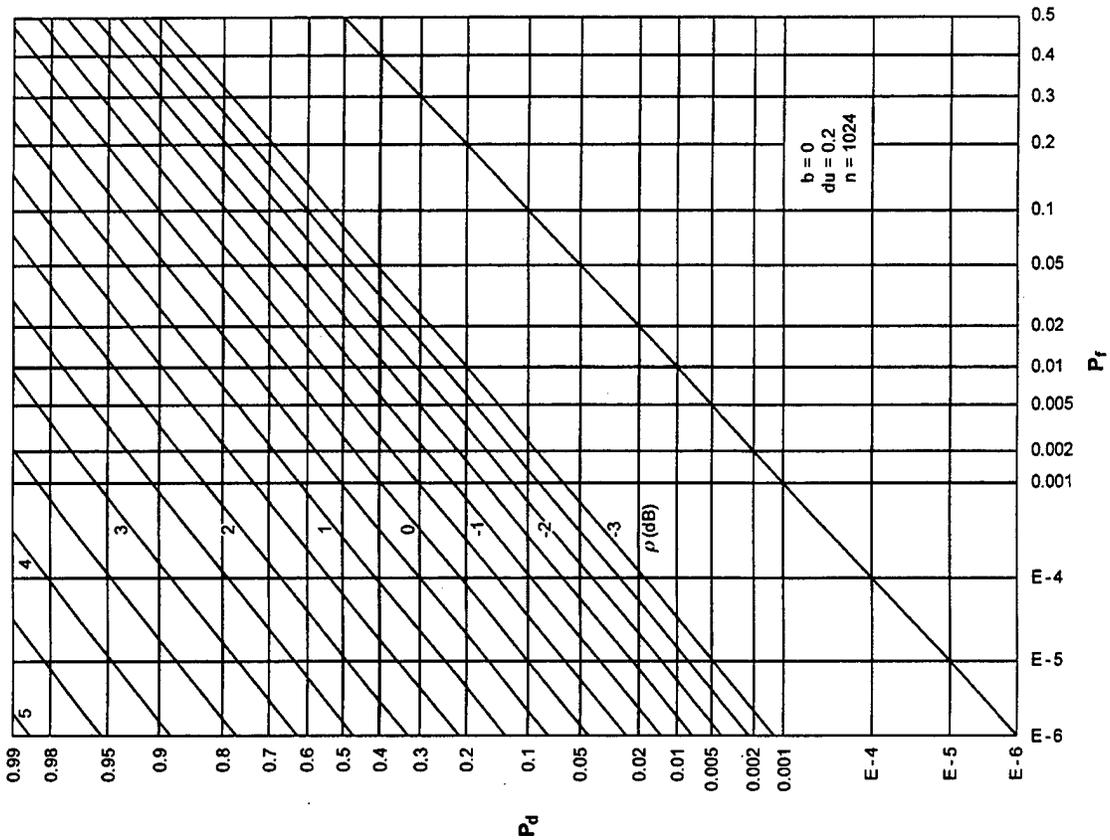
Figure D-7. ROCs for K = 8, N = 2, M = 2

Figure D-10. ROCs for K = 8, N = 16, M = 2

Figure D-9. ROCs for K = 8, N = 8, M = 2

D-6
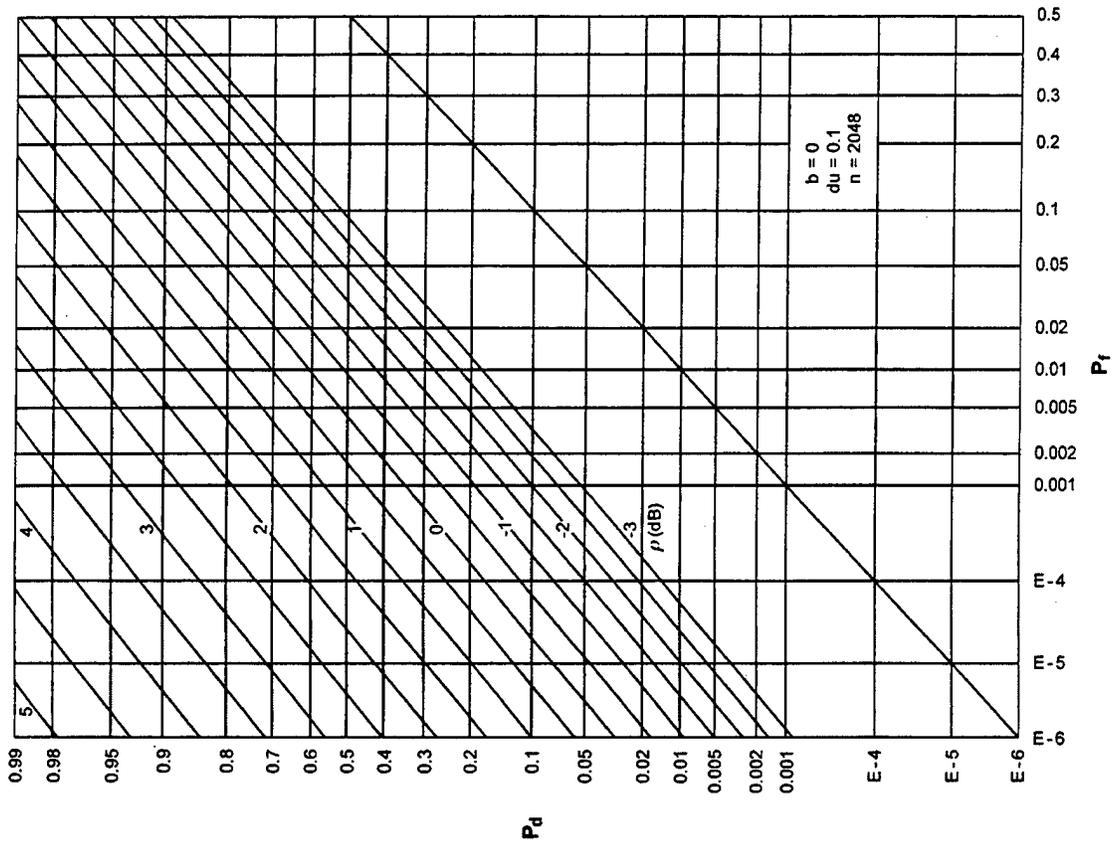
Figure D-12. ROCs for K = 4, N = 2, M = 4
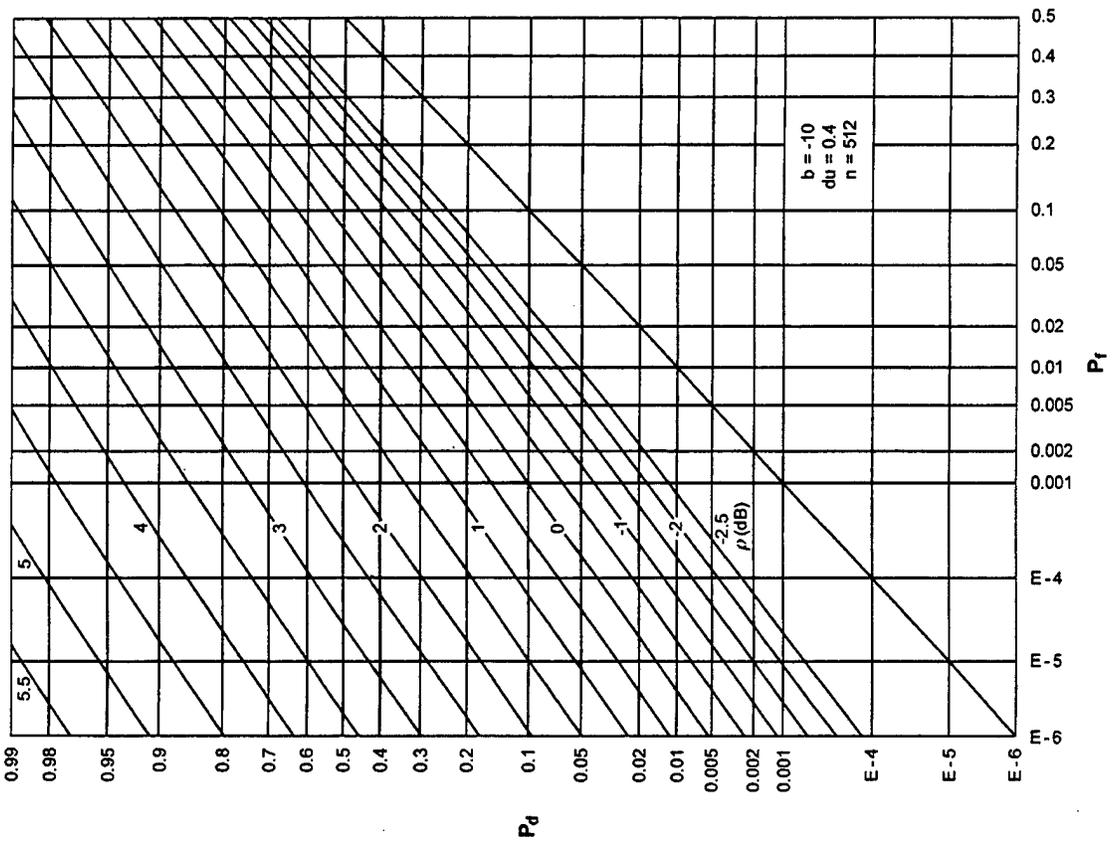
Figure D-11. ROCs for K = 8, N = 32, M = 2

D-7
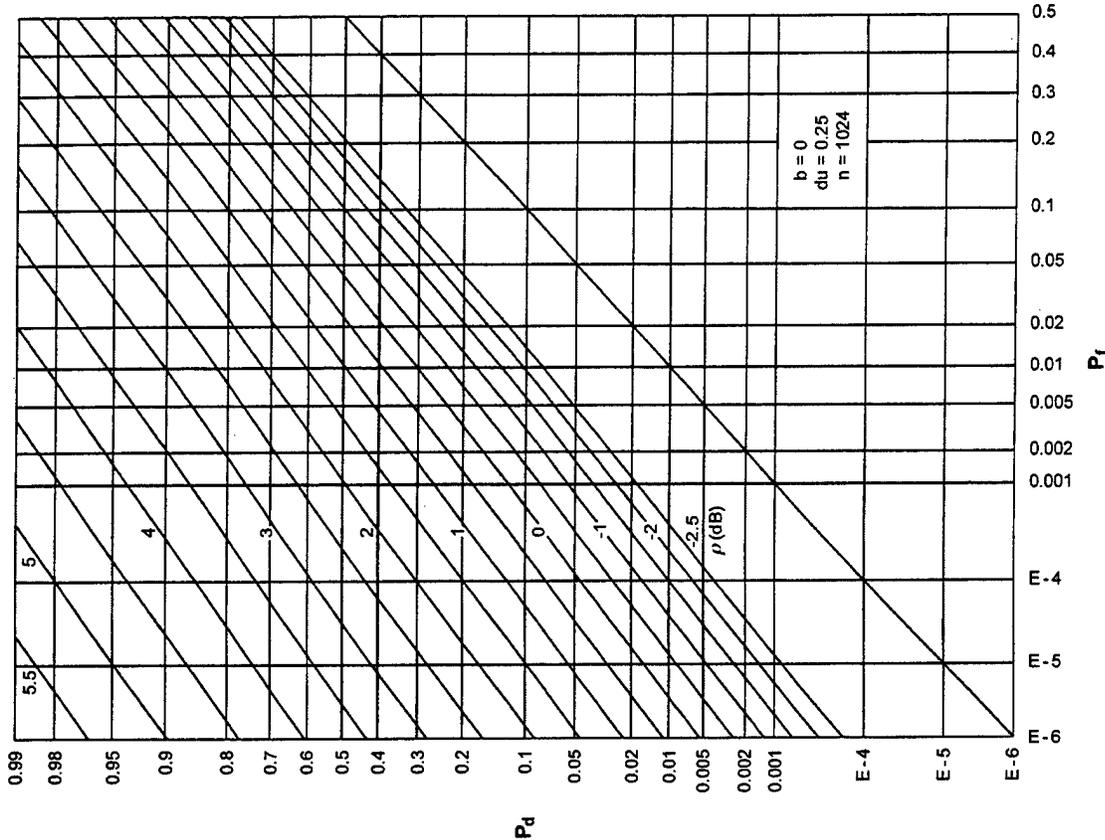
Figure D-14. ROCs for K = 4, N = 8, M = 4

b = 0
du = 0.25
n = 1024
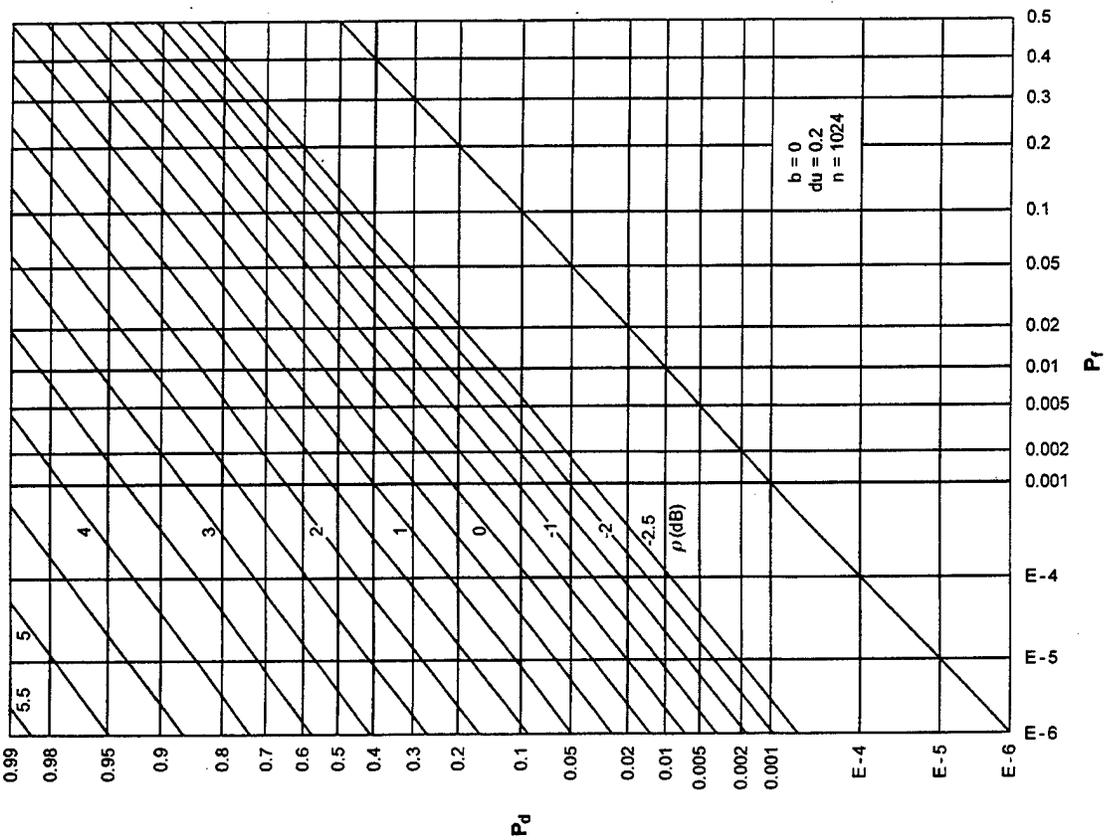
Figure D-13. ROCs for K = 4, N = 4, M = 4

b = 0
du = 0.2
n = 1024

D-8
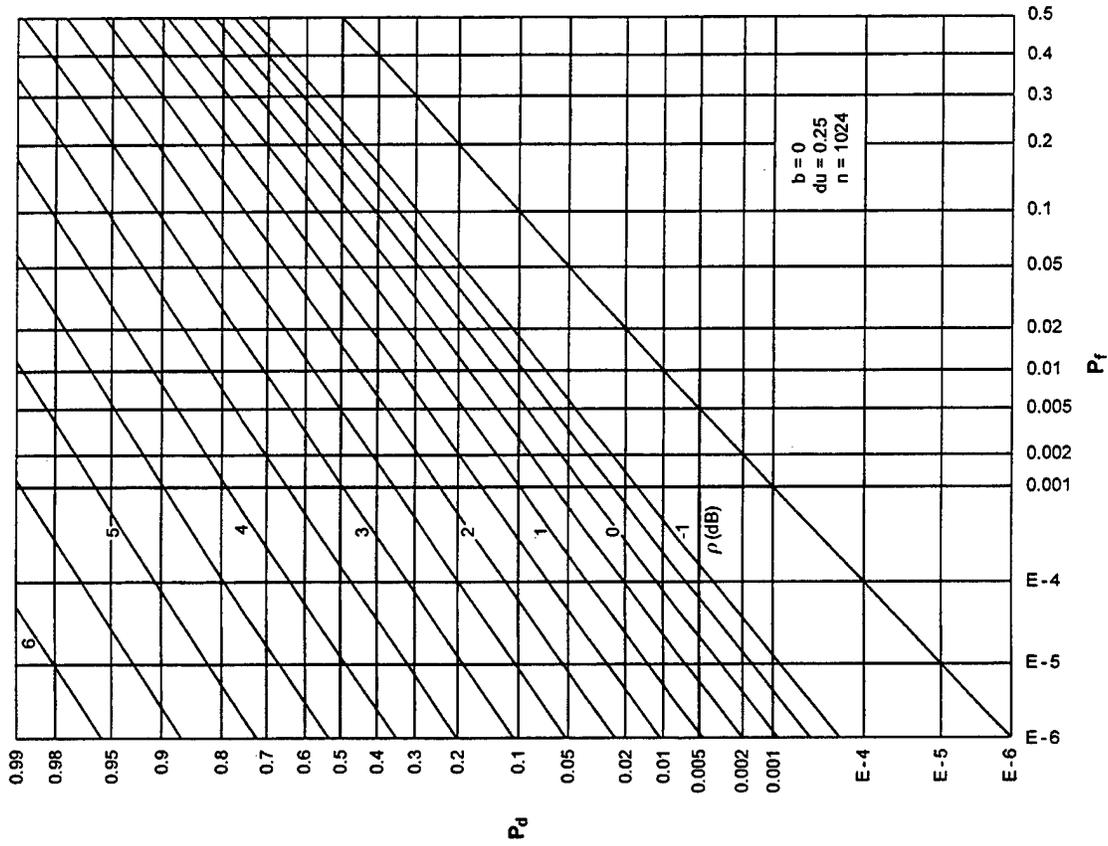
Figure D-16. ROCs for K = 4, N = 32, M = 4
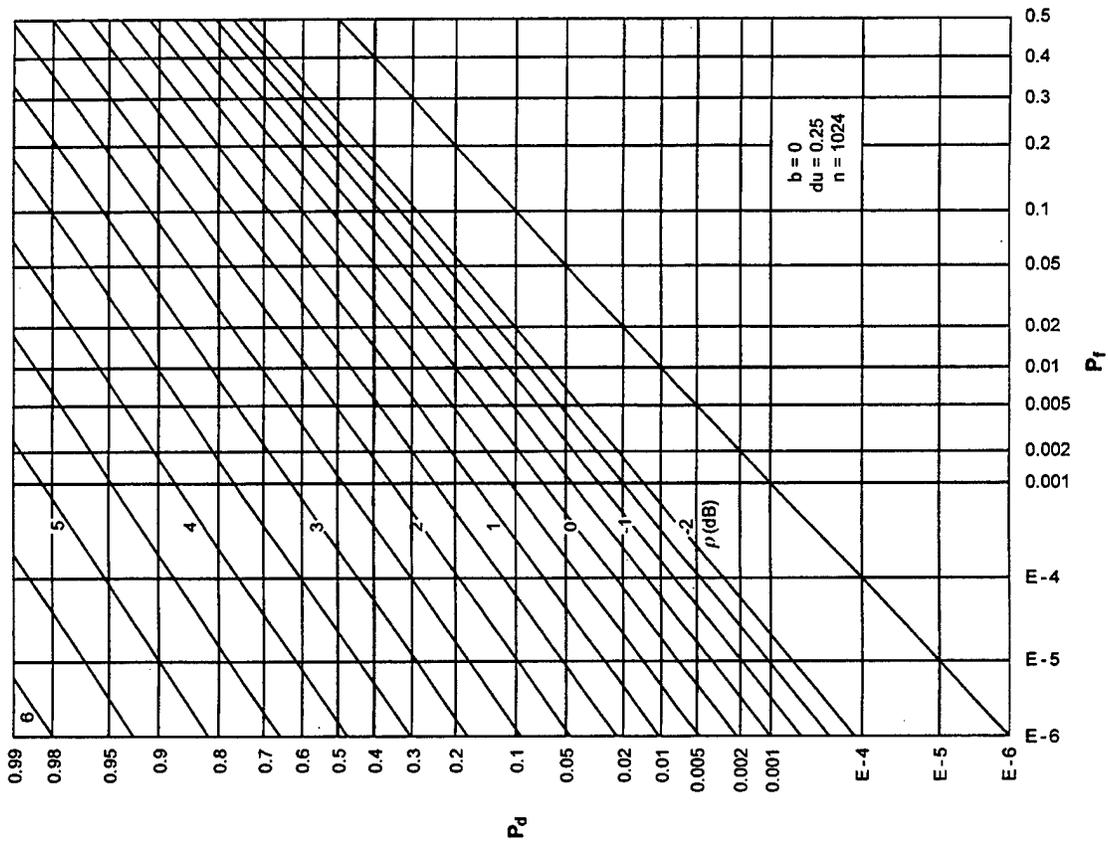
Figure D-15. ROCs for K = 4, N = 16, M = 4

D-9
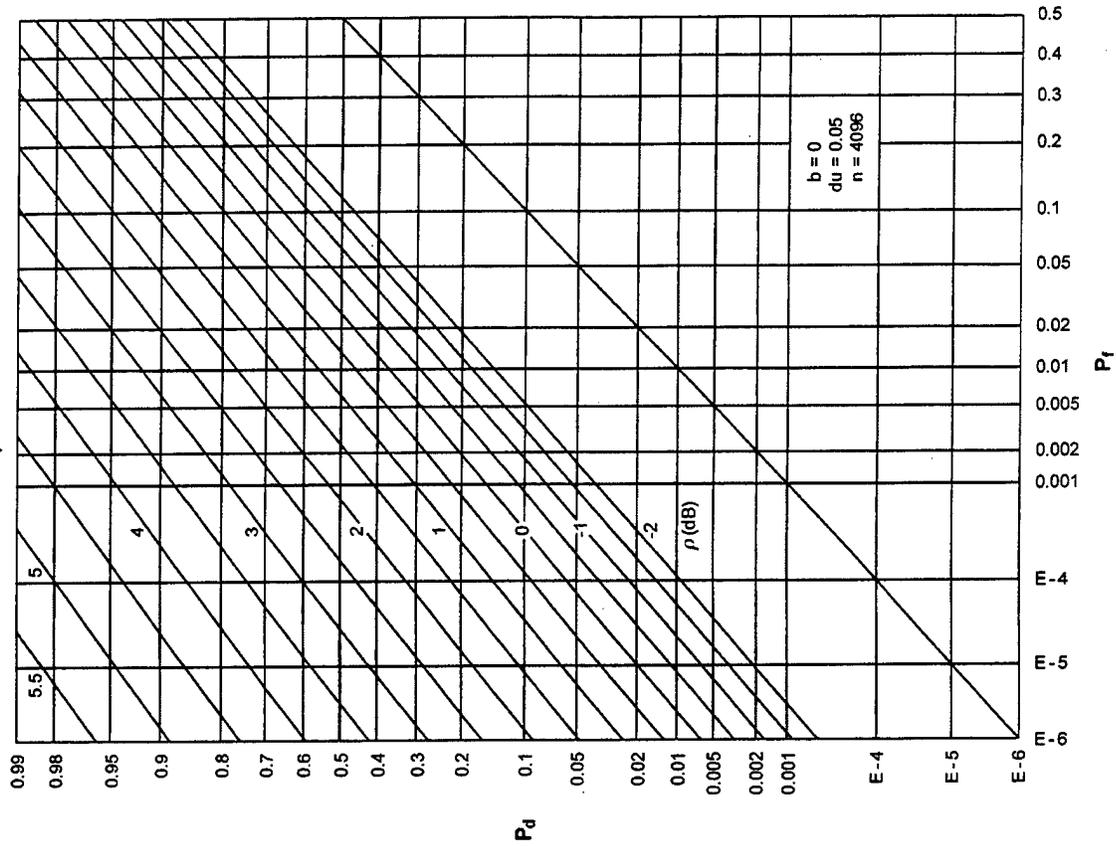
Figure D-18. ROCs for K = 2, N = 4, M = 8

Chart annotations: $b = 0$, $du = 0.05$, $n = 4096$. Axes labeled P_d (vertical) and P_f (horizontal), with ρ (dB) curves labeled 5.5, 5, 4, 3, 2, 1, 0, -1, -2.
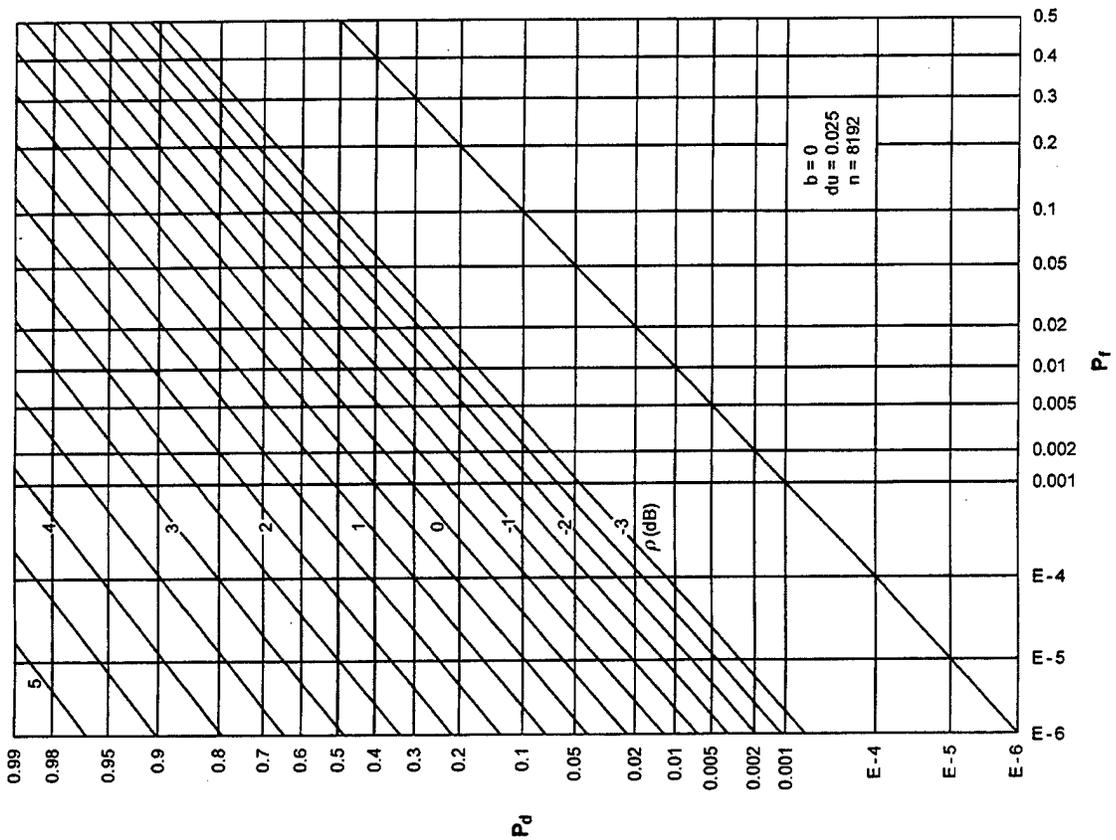
Figure D-17. ROCs for K = 2, N = 2, M = 8

Chart annotations: $b = 0$, $du = 0.025$, $n = 8192$. Axes labeled P_d (vertical) and P_f (horizontal), with ρ (dB) curves labeled 5, 4, 3, 2, 1, 0, -1, -2, -3.
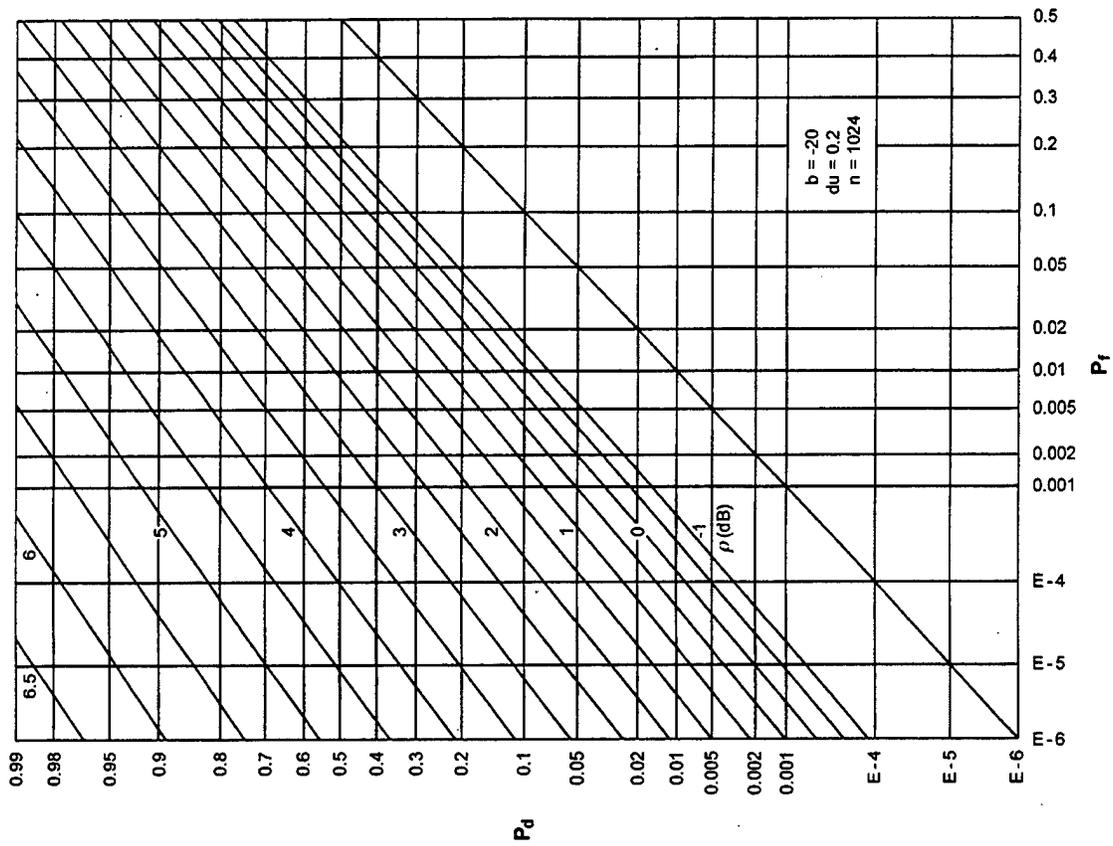
Figure D-20. ROCs for K = 2, N = 16, M = 8
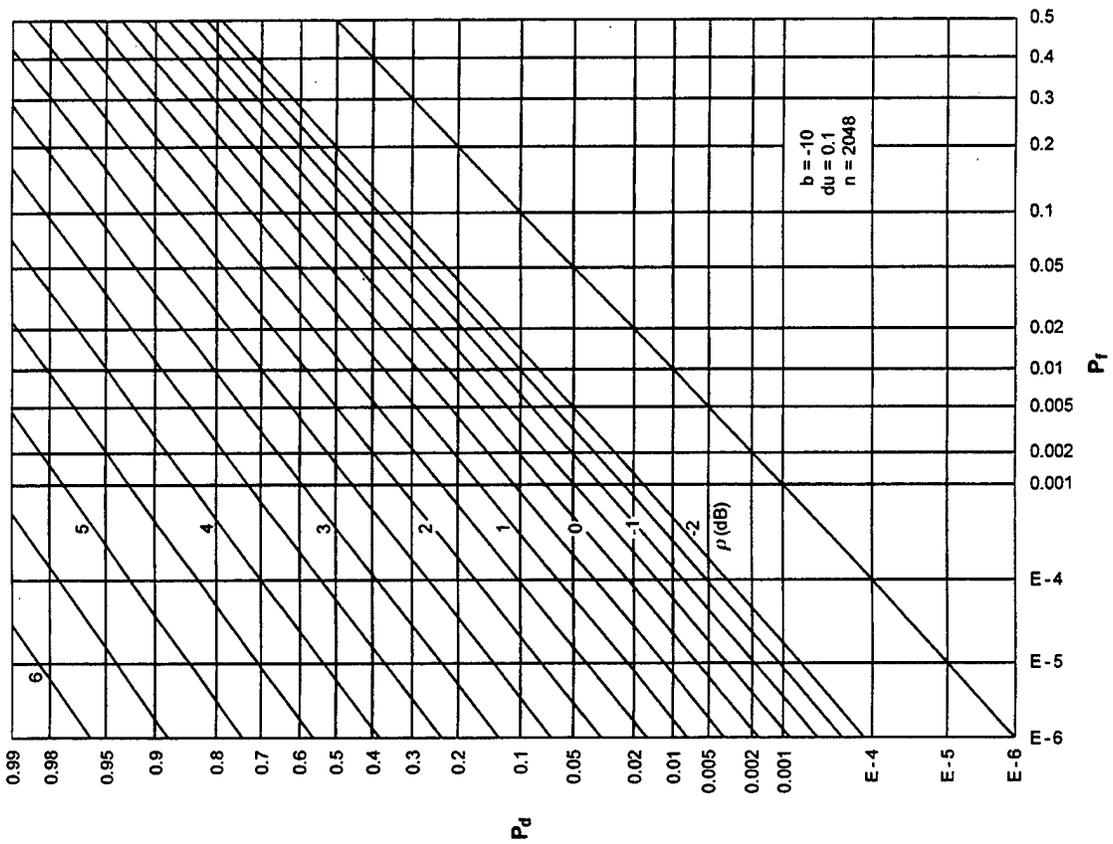
Figure D-19. ROCs for K = 2, N = 8, M = 8
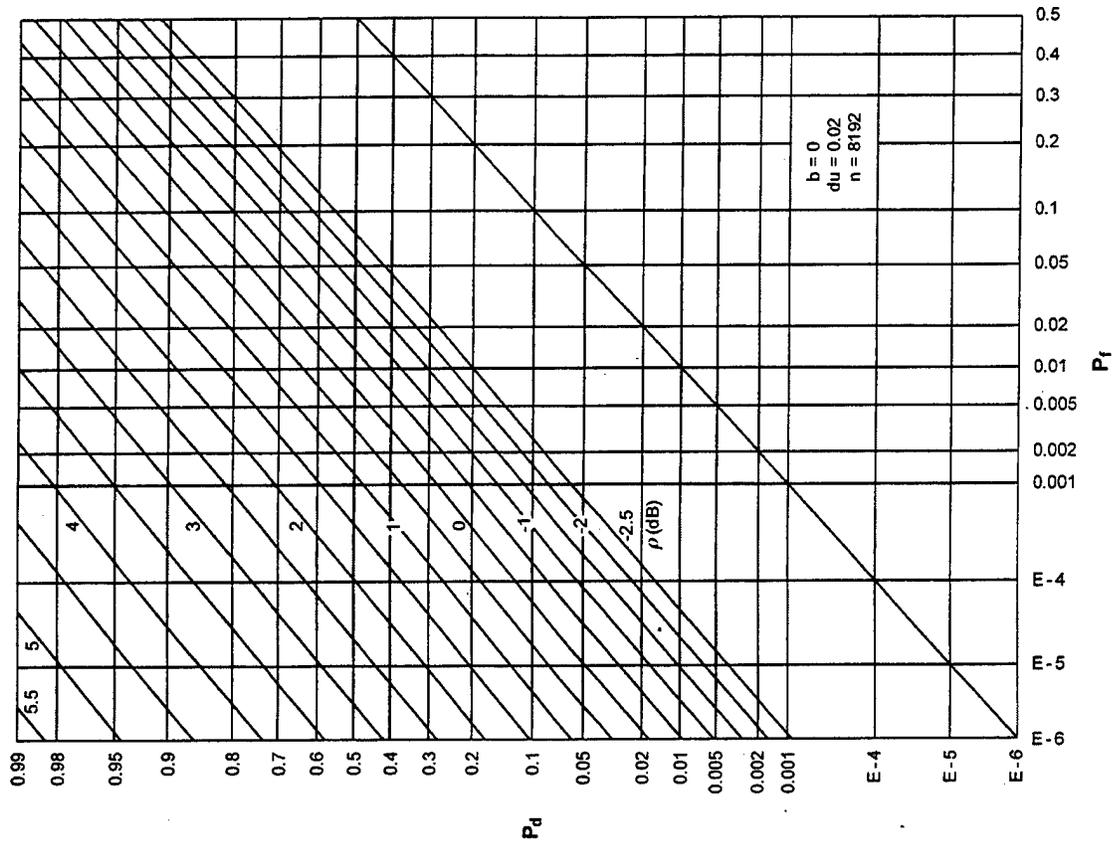
Figure D-22. ROCs for K = 1, N = 2, M = 16
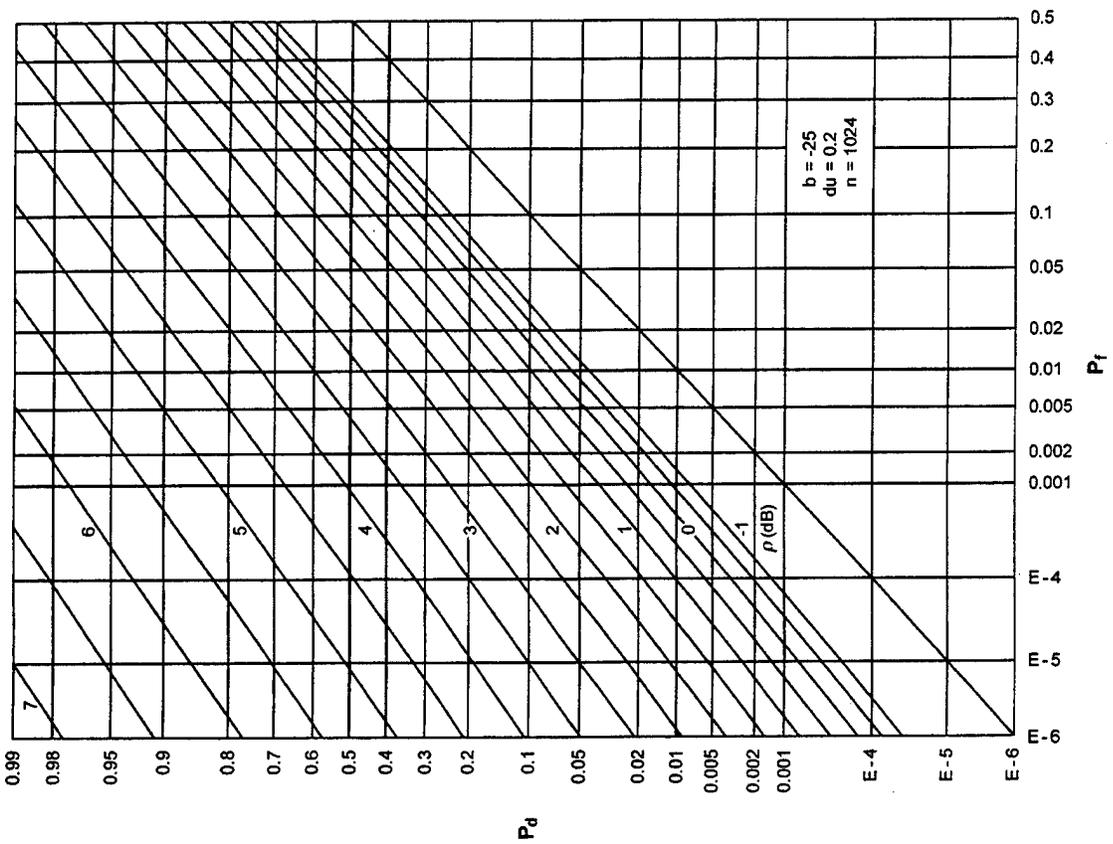
Figure D-21. ROCs for K = 2, N = 32, M = 8

D-12
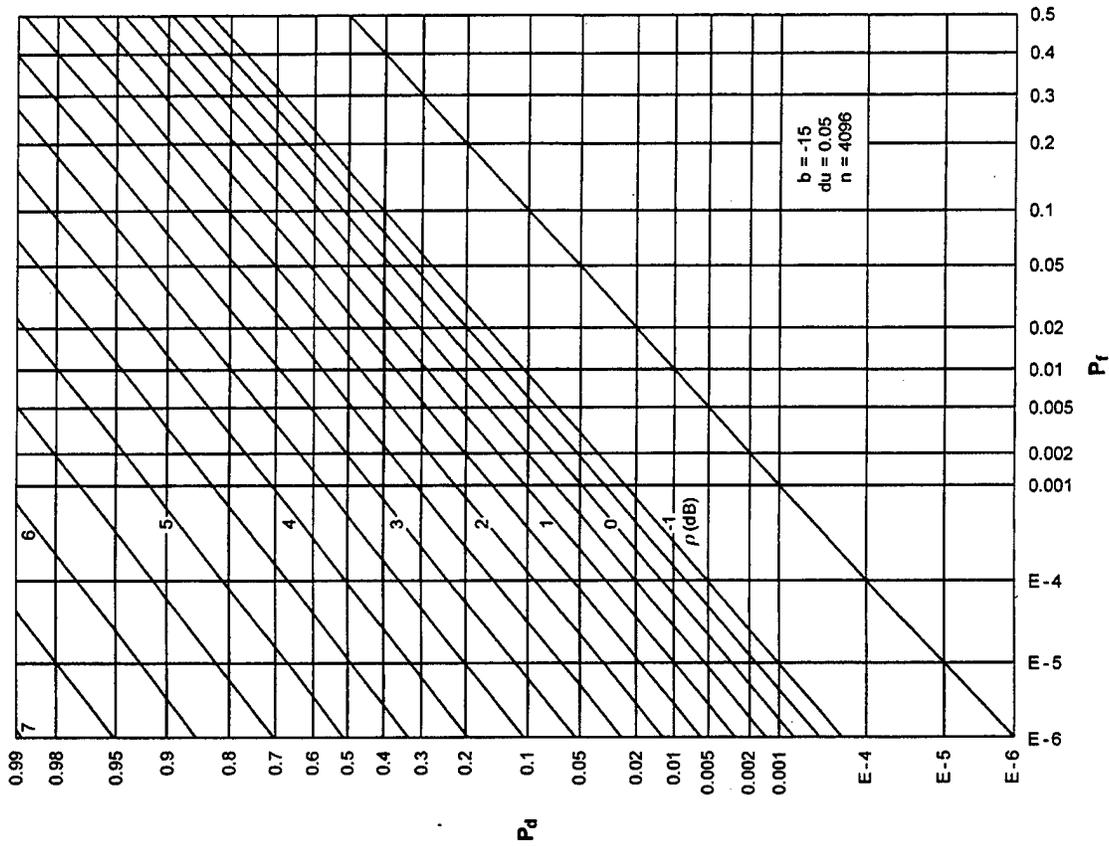
Figure D-24.   ROCs for K = 1, N = 8, M = 16
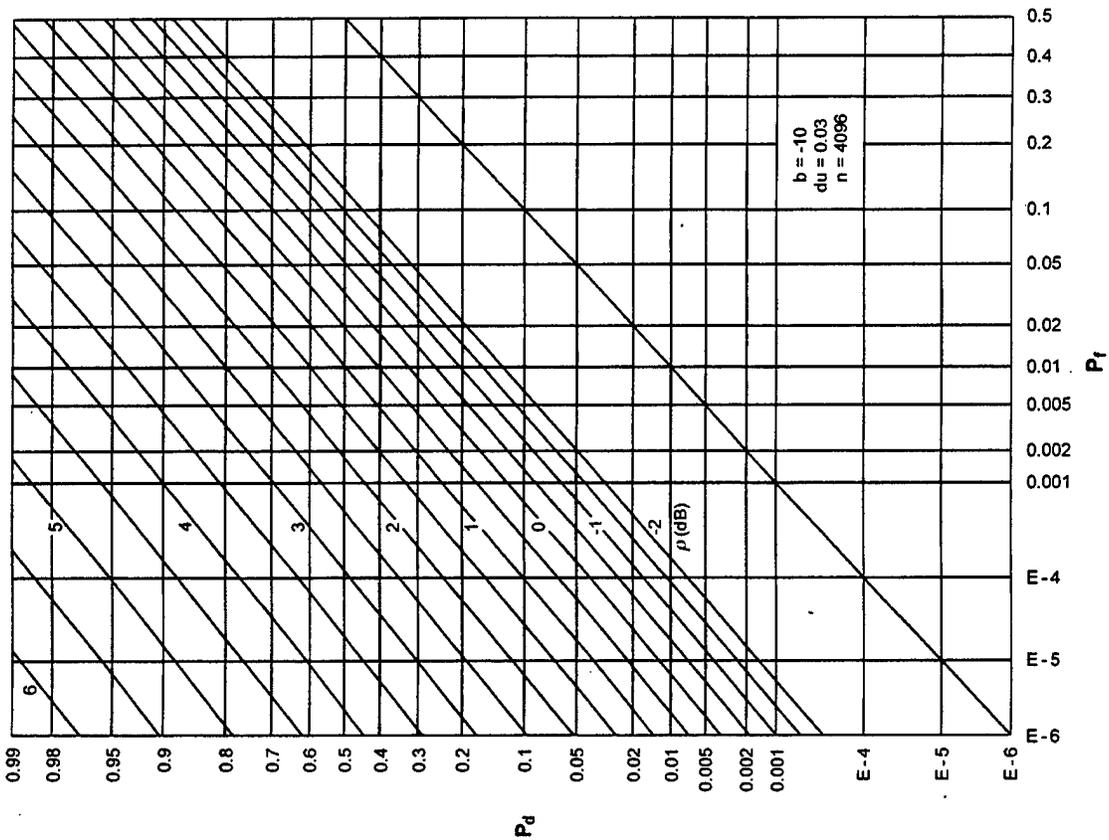
Figure D-23.   ROCs for K = 1, N = 4, M = 16
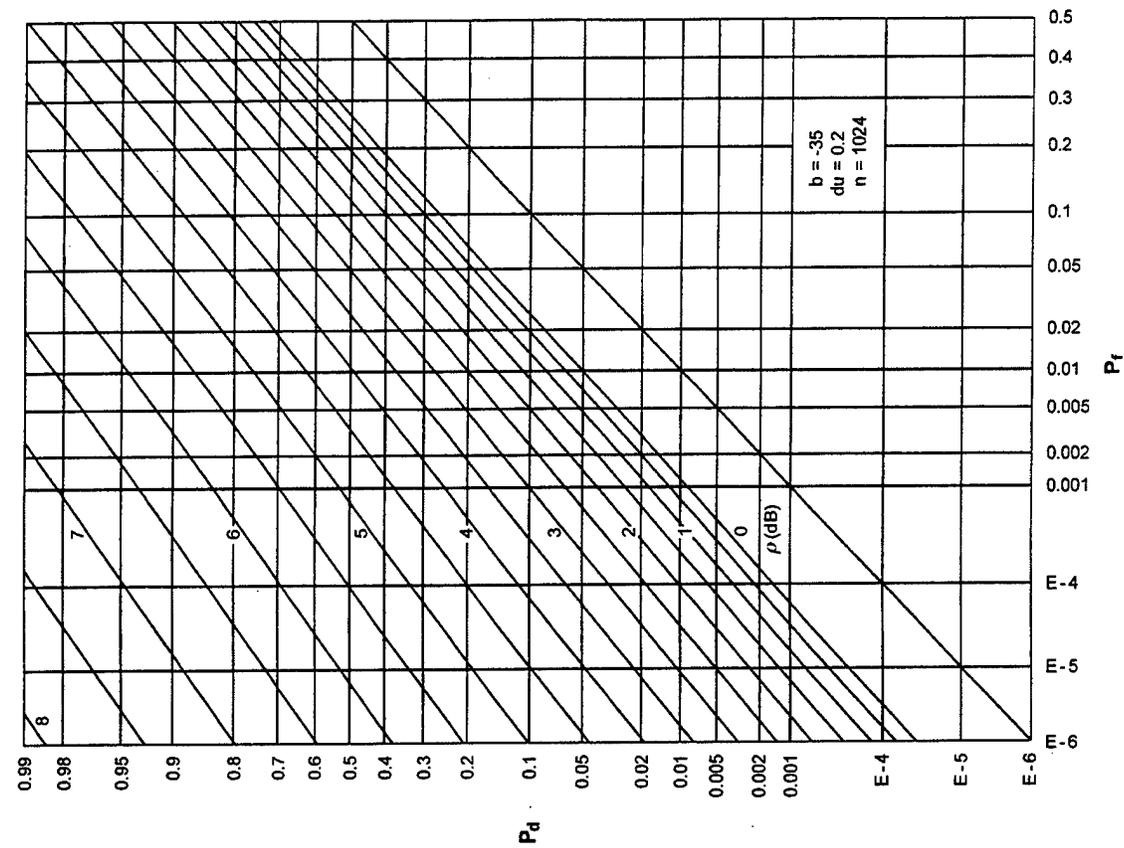
Figure D-26. ROCs for K = 1, N = 32, M = 16

b = -35
du = 0.2
n = 1024
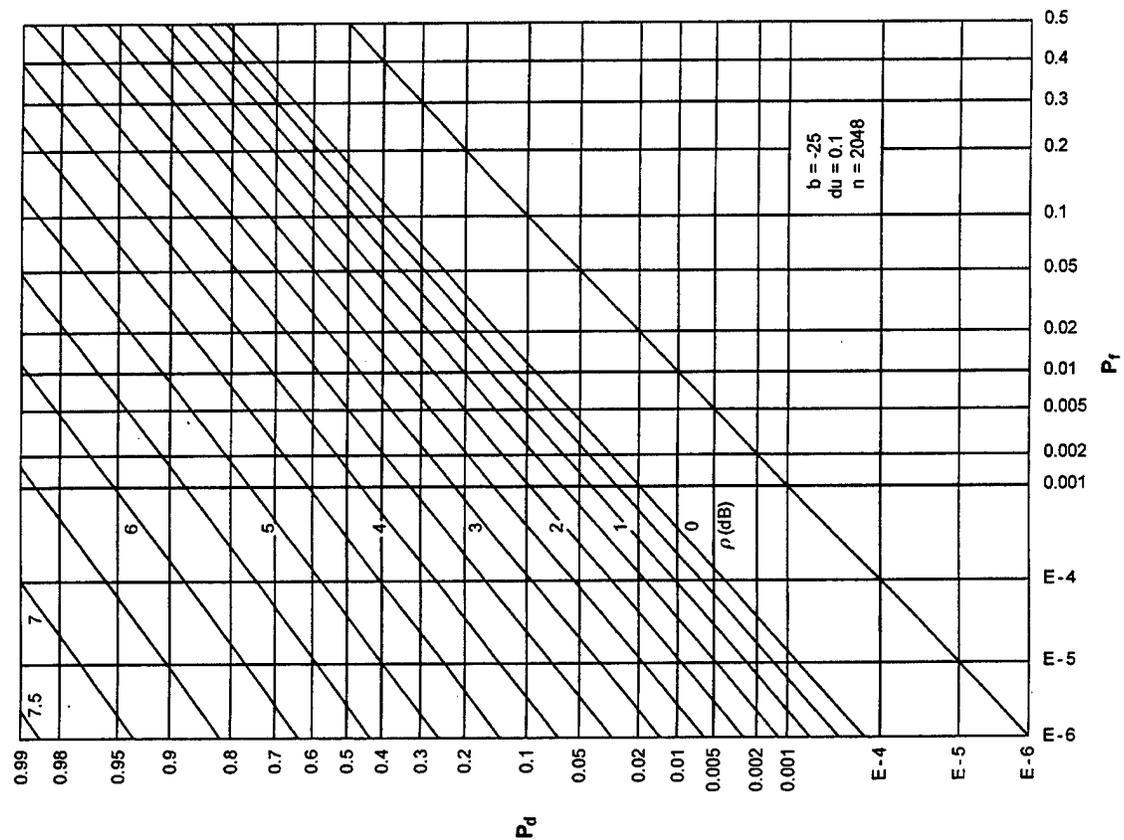
Figure D-25. ROCs for K = 1, N = 16, M = 16

b = -25
du = 0.1
n = 2048

APPENDIX E — ROCs FOR KM = 64, PHASE-INCOHERENT SIGNAL

This appendix contains the ROCs for or-ing with pre- and post-averaging when the time-bandwidth product KM is fixed at 64; the possible combinations (from table 1) are repeated here:

K	M	N
64	1	1,2,4,8,16,32
32	2	
16	4	
8	8	
4	16	
2	32	
1	64	

For N = 1, only the product KM matters; the first plot in this appendix covers this special case, under the labeling K = 64, N = 1, M = 1. The other 5 values of N, along with the 7 possible combinations of K and M, yield 35 additional ROCs, for a total of 36 ROCs in this appendix.

Figure E-2. ROCs for K = 64, N = 2, M = 1

Figure E-1. ROCs for K = 64, N = 1, M = 1
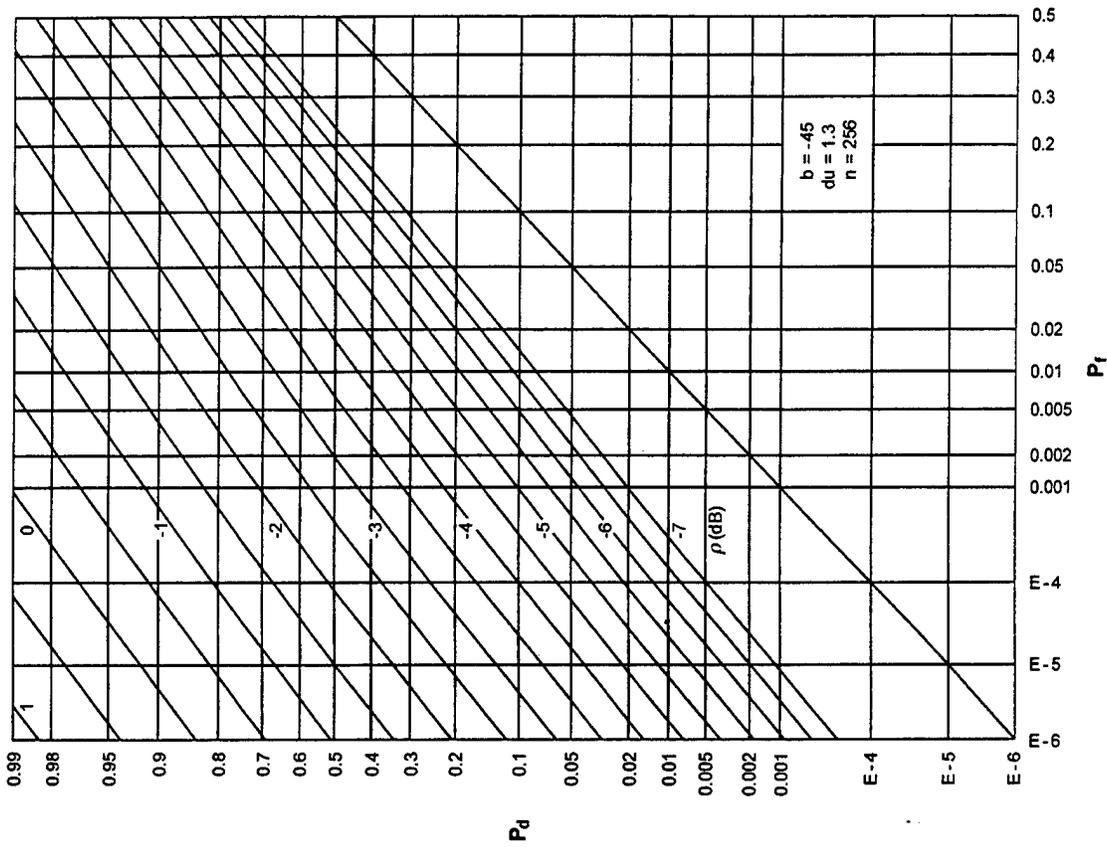
Figure E-4. ROCs for K = 64, N = 8, M = 1

b = -45
du = 1.3
n = 256
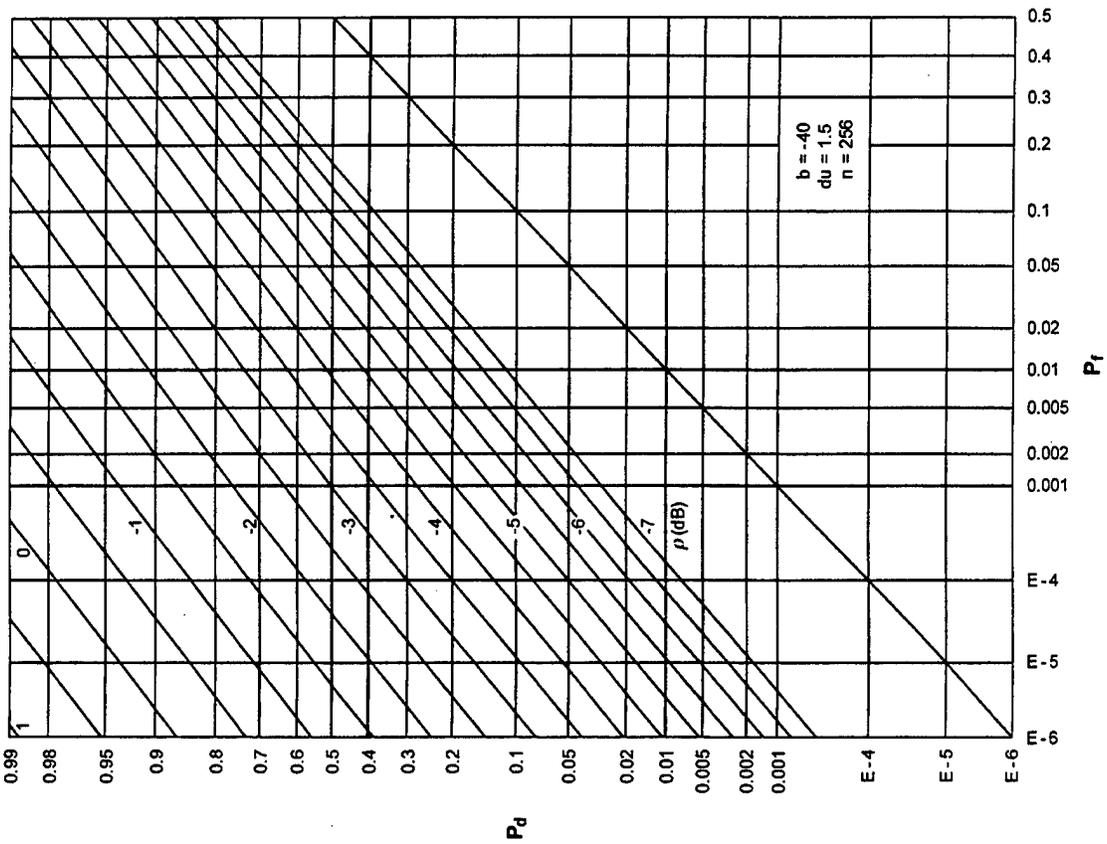
Figure E-3. ROCs for K = 64, N = 4, M = 1

b = -40
du = 1.5
n = 256
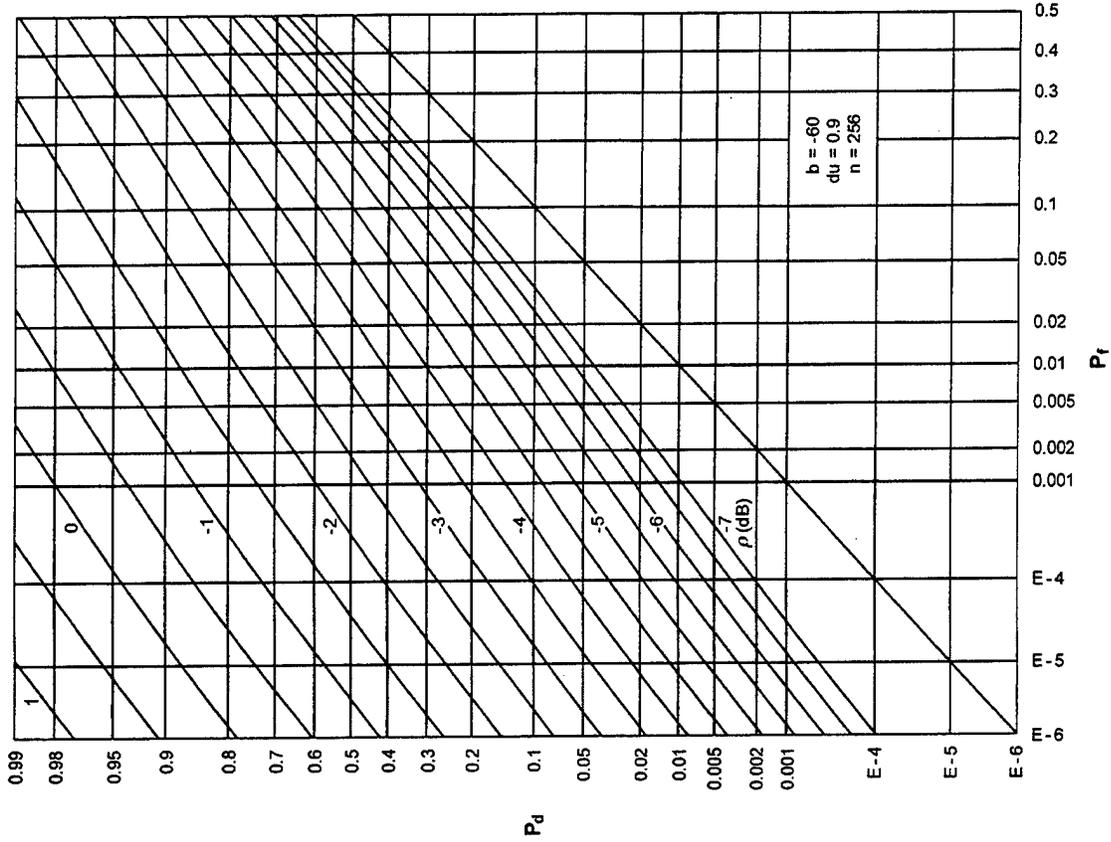
Figure E-6.   ROCs for K = 64, N = 32, M = 1
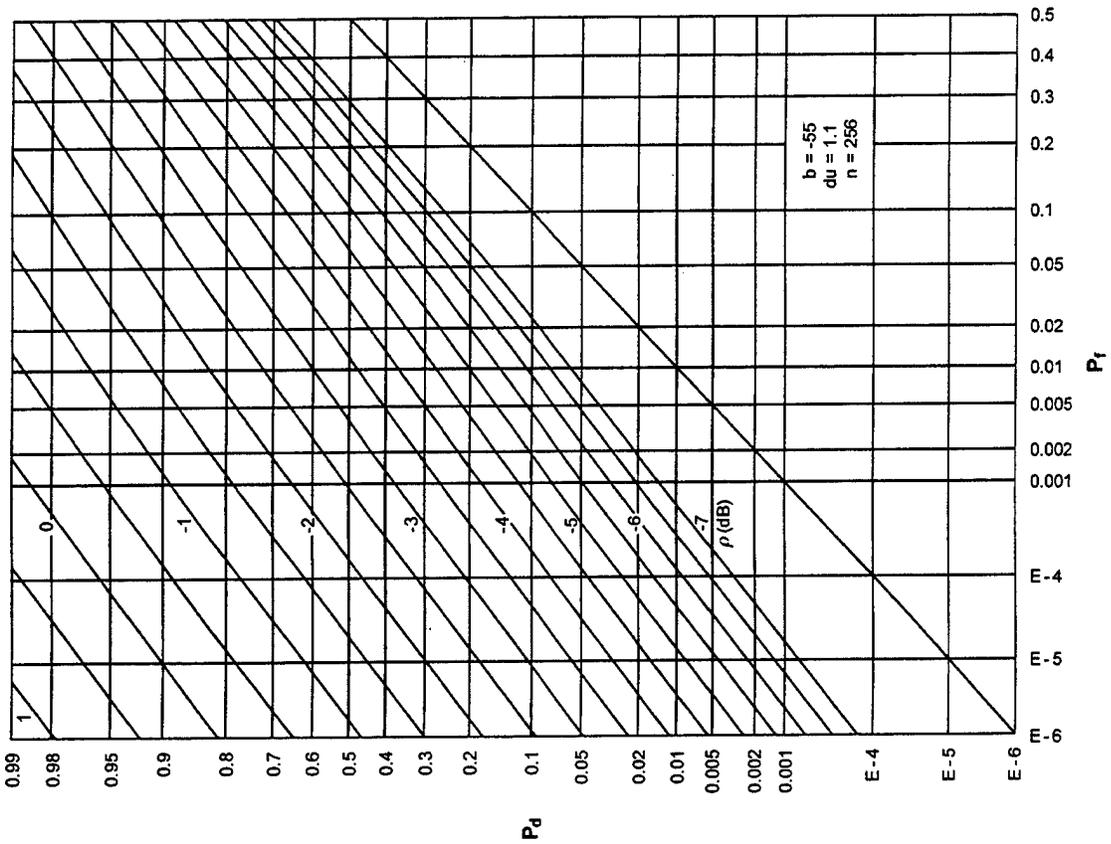
Figure E-5.   ROCs for K = 64, N = 16, M = 1

E−4
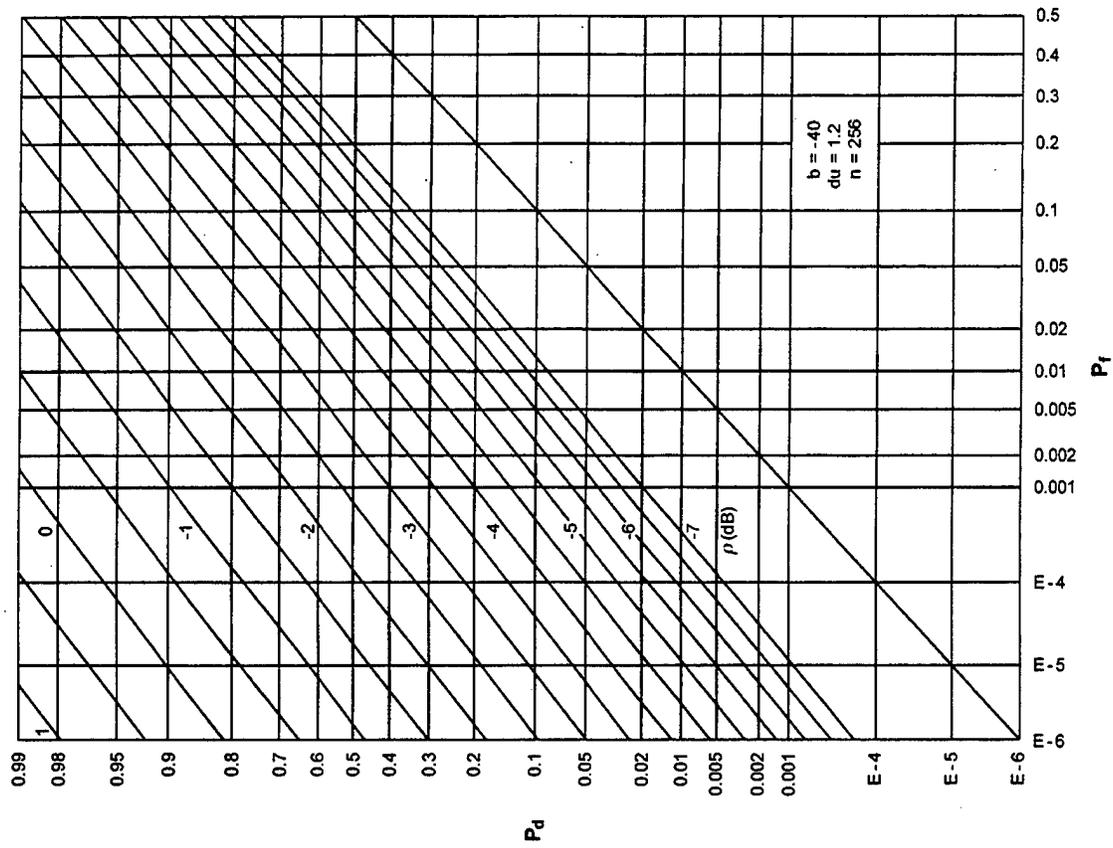
Figure E-8. ROCs for K = 32, N = 4, M = 2
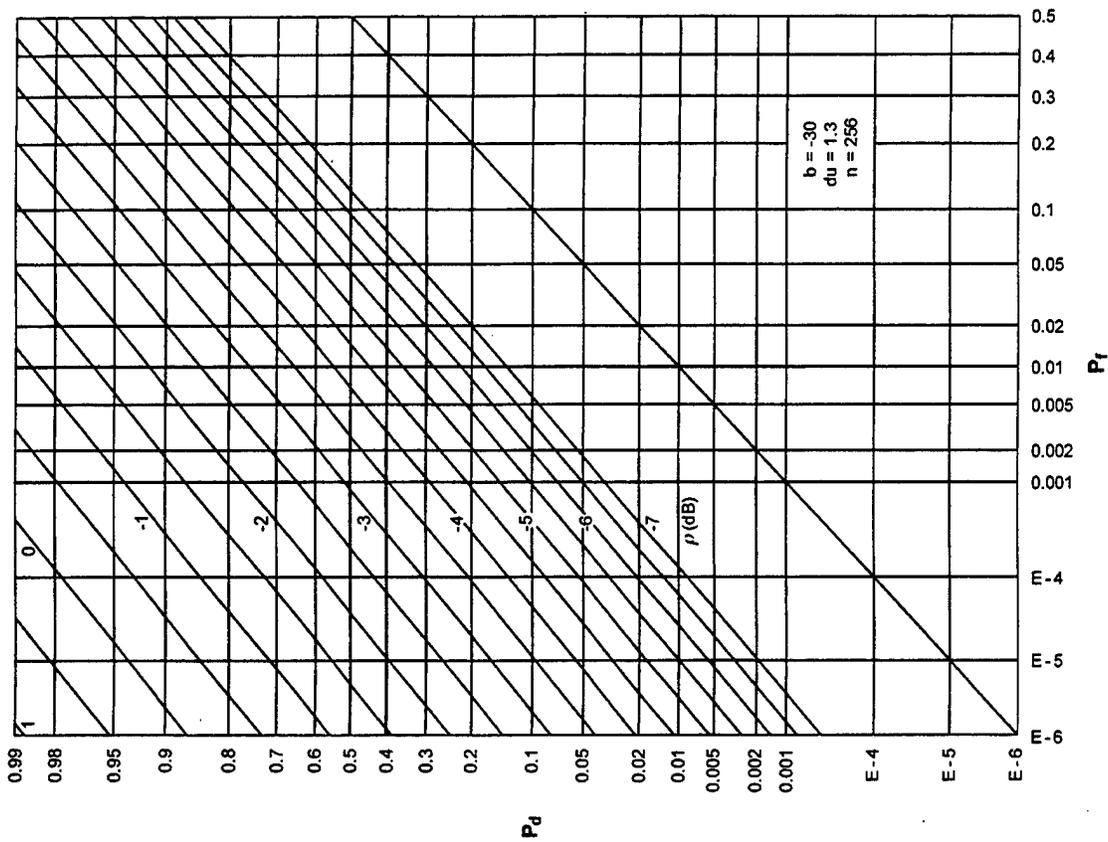
Figure E-7. ROCs for K = 32, N = 2, M = 2
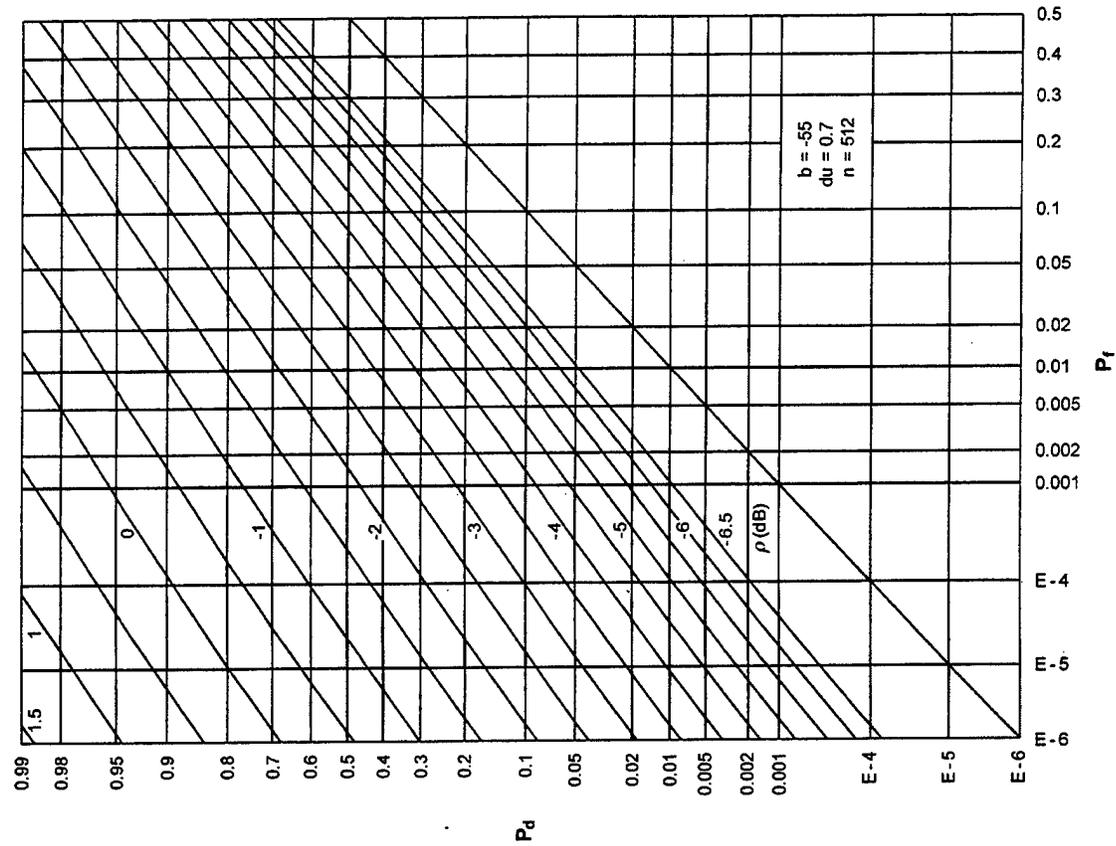
Figure E-10.   ROCs for K = 32, N = 16, M = 2
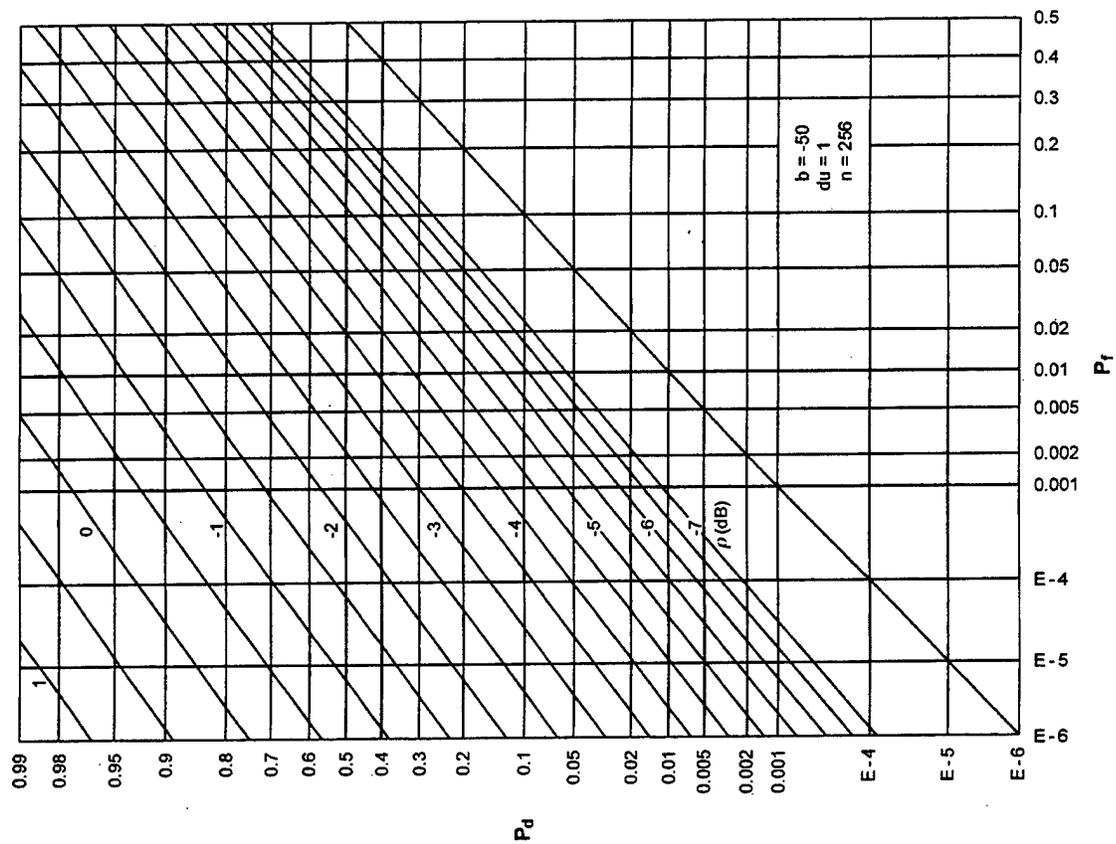
Figure E-9.   ROCs for K = 32, N = 8, M = 2
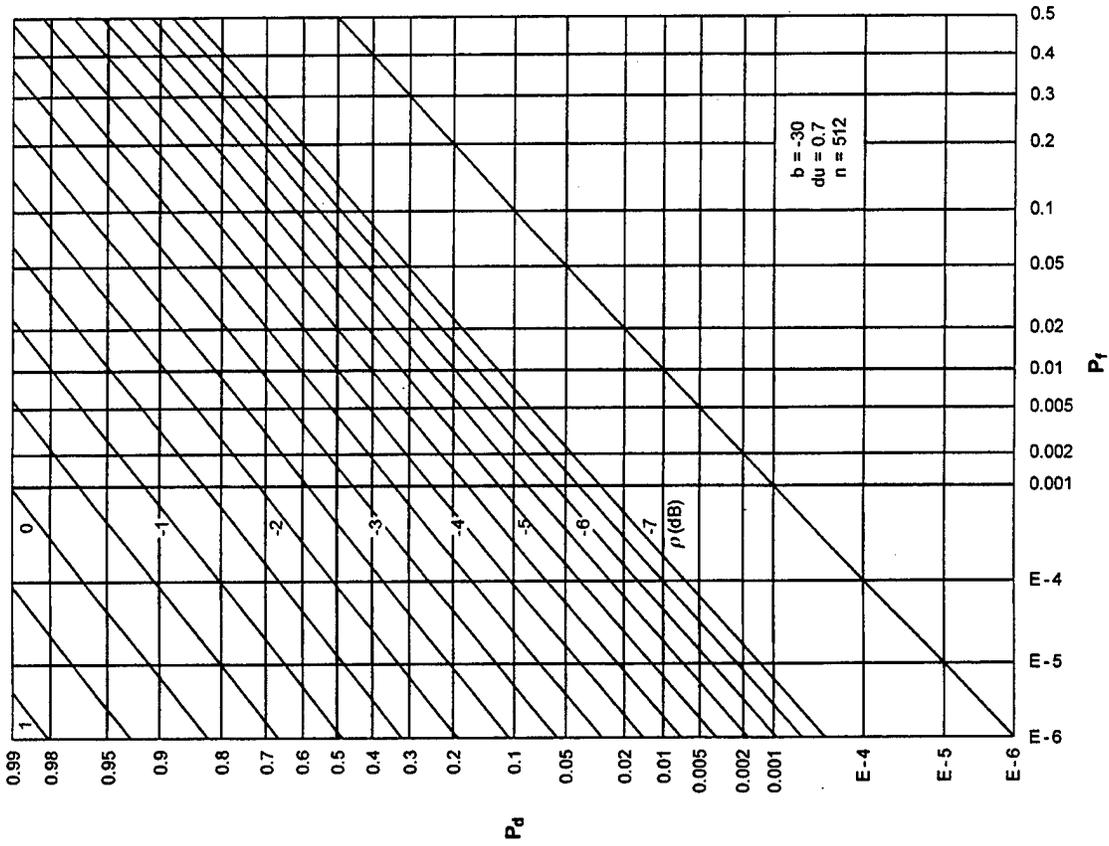
Figure E-12. ROCs for K = 16, N = 2, M = 4
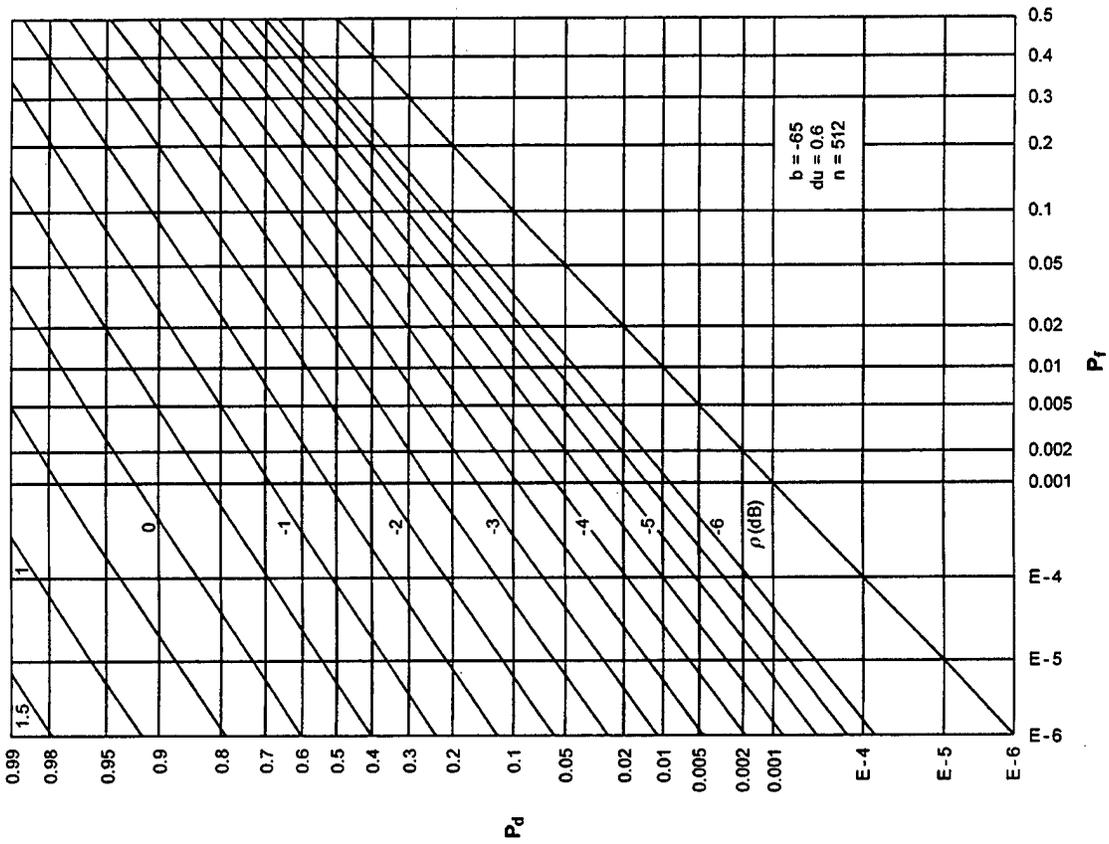
Figure E-11. ROCs for K = 32, N = 32, M = 2

Figure E-14. ROCs for K = 16, N = 8, M = 4

Figure E-13. ROCs for K = 16, N = 4, M = 4

E-8
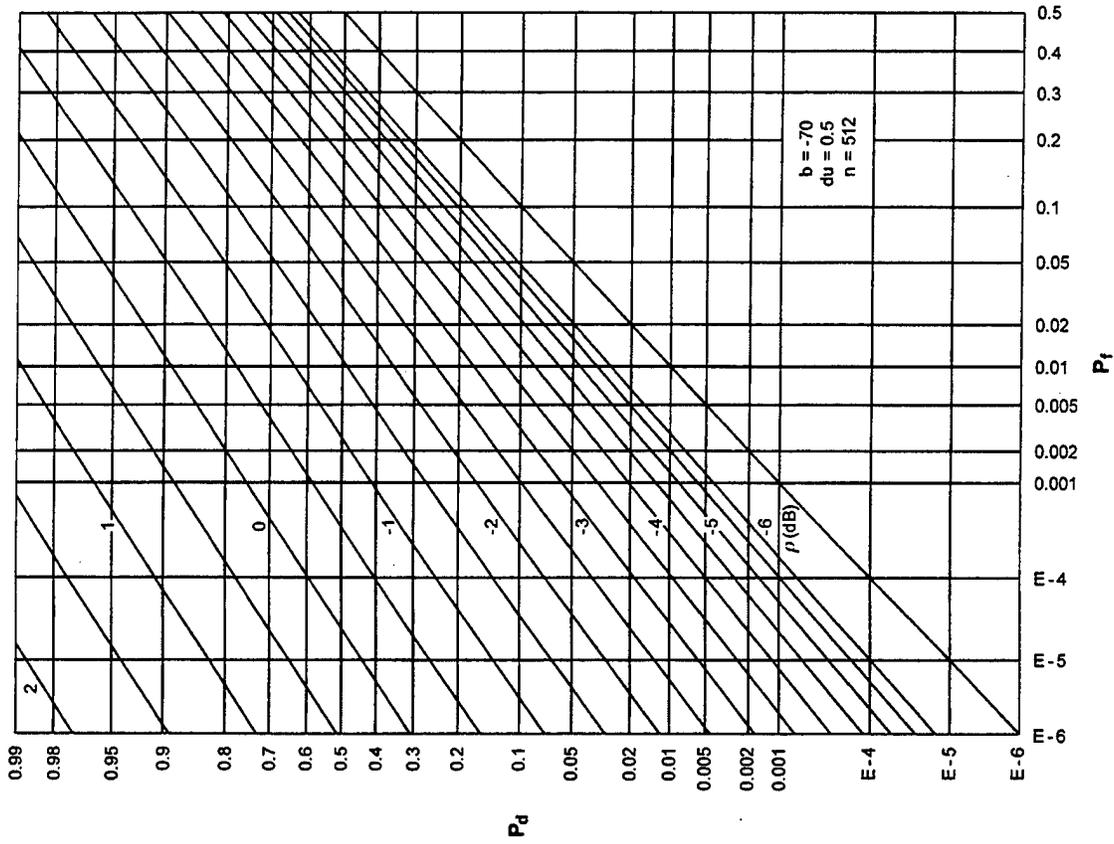
Figure E-16. ROCs for K = 16, N = 32, M = 4
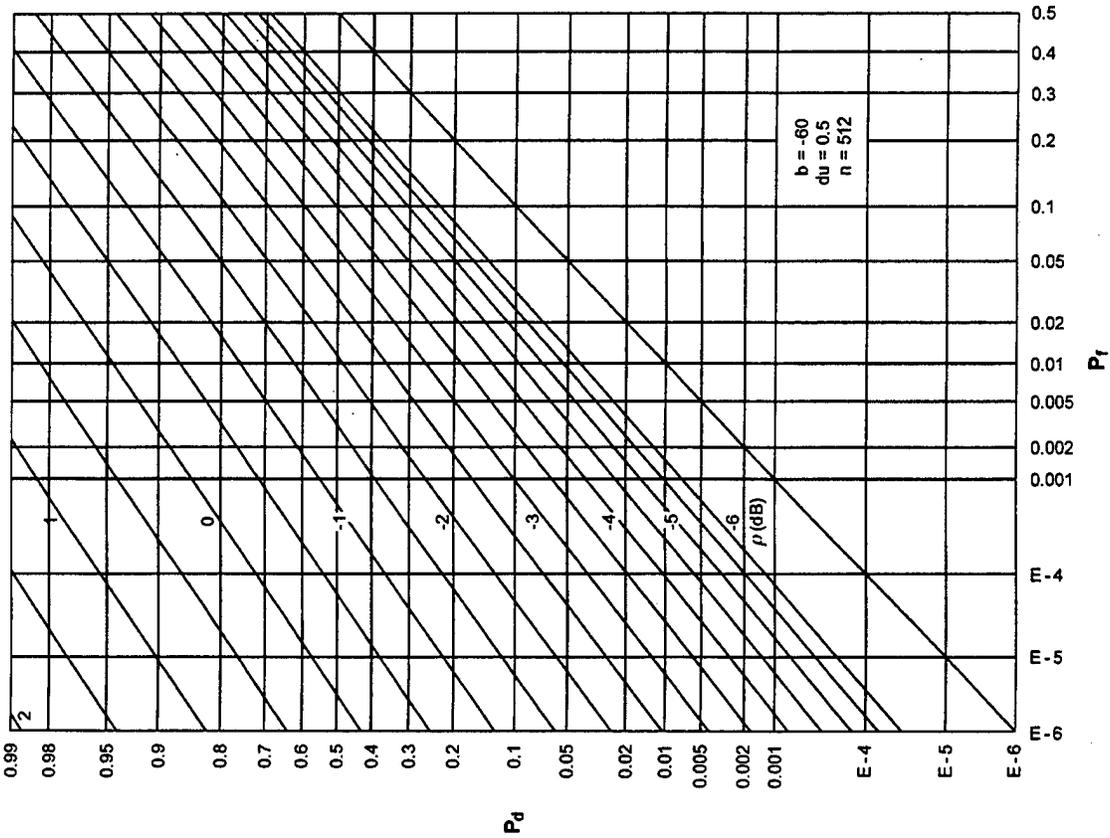
Figure E-15. ROCs for K = 16, N = 16, M = 4
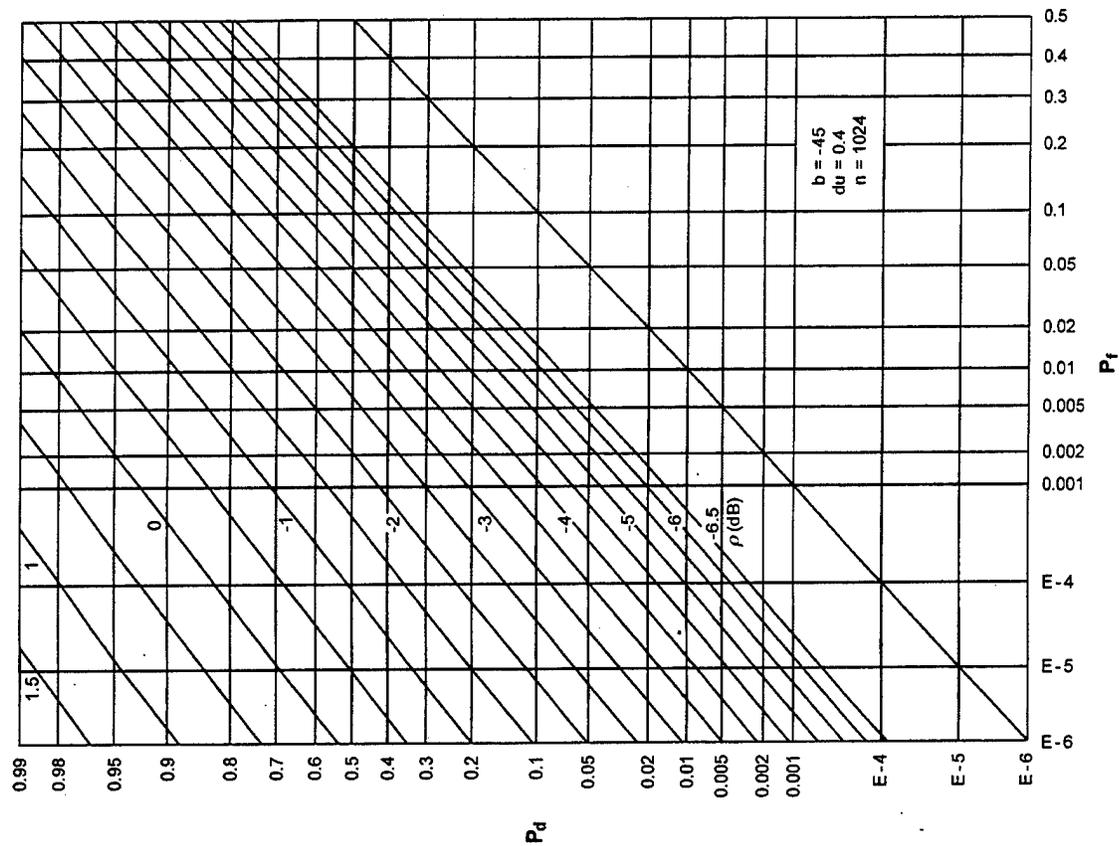
Figure E-18. ROCs for K = 8, N = 4, M = 8
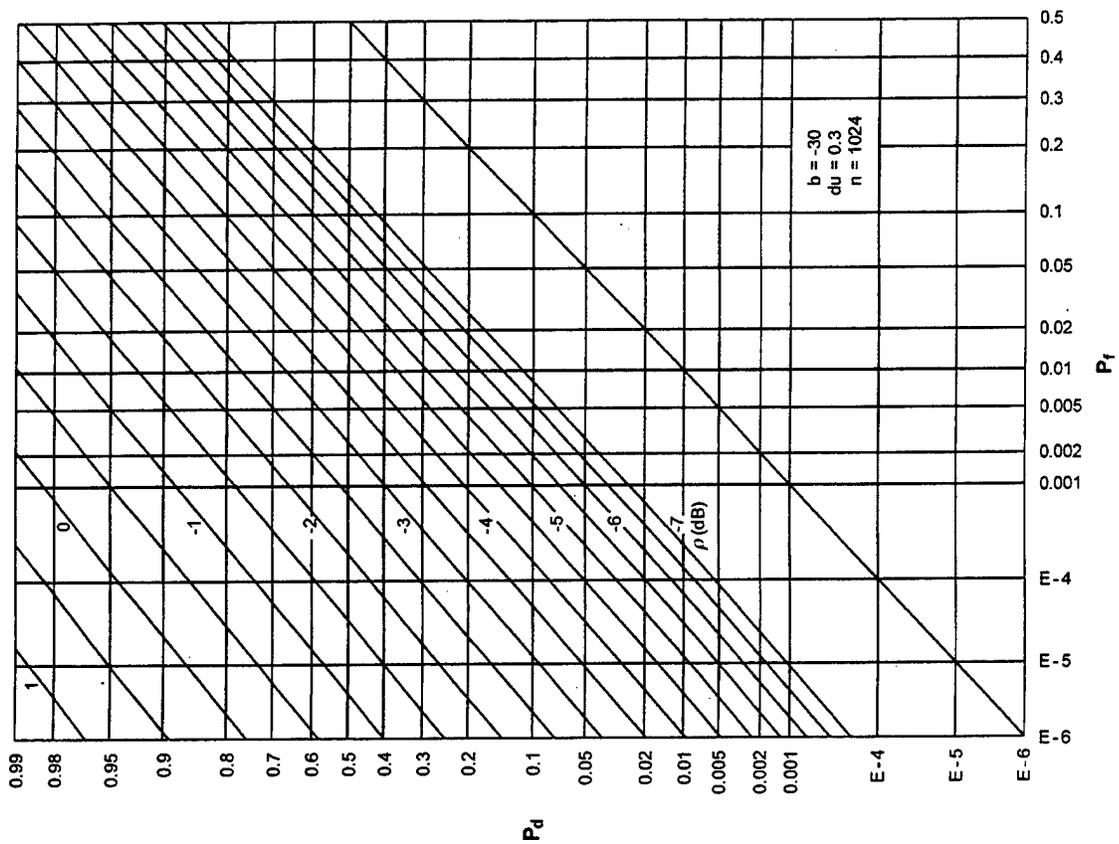
Figure E-17. ROCs for K = 8, N = 2, M = 8

E-10
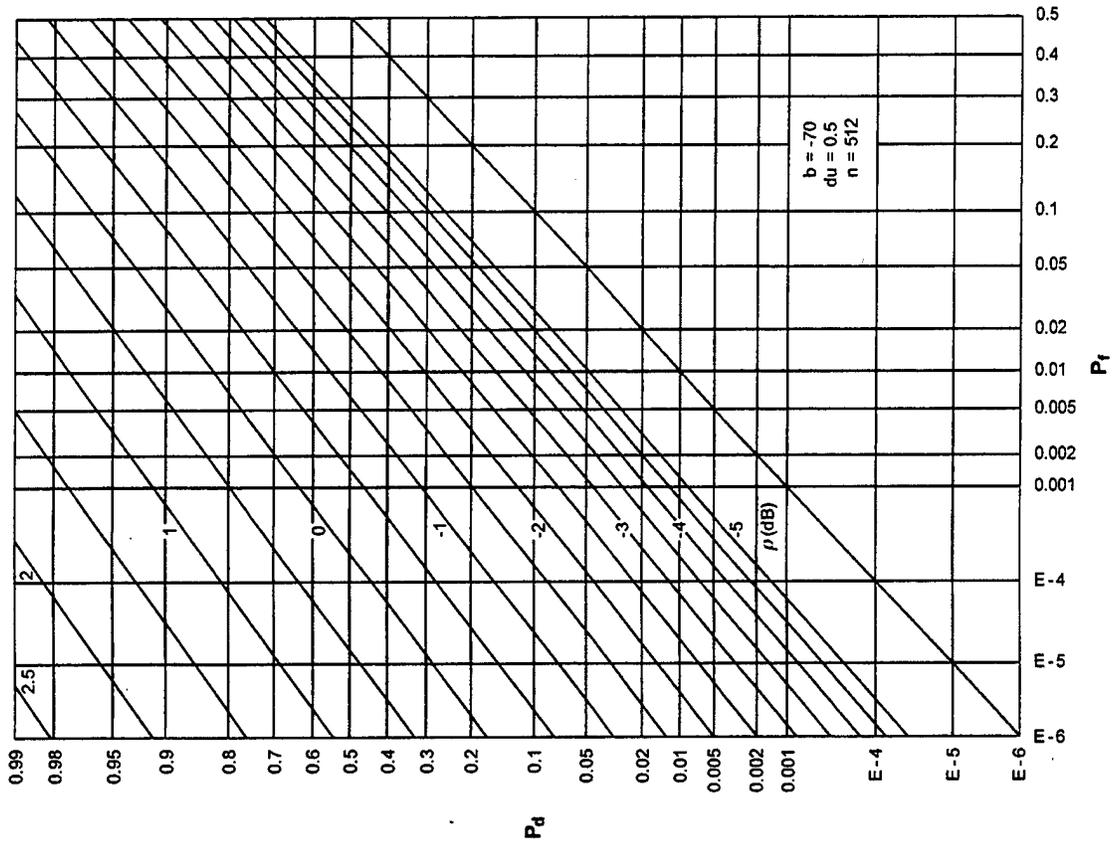
**Figure E-20. ROCs for K = 8, N = 16, M = 8**

b = -70
du = 0.5
n = 512

ρ (dB)
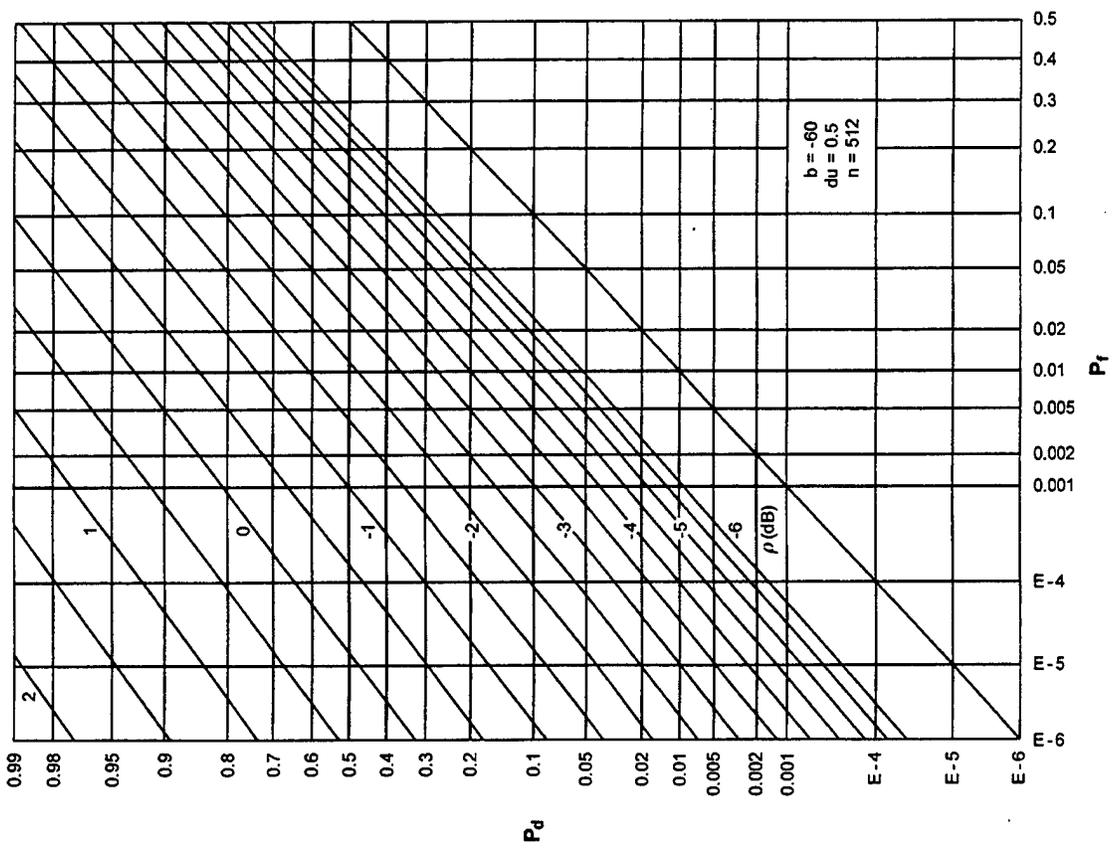
Figure E-19. ROCs for K = 8, N = 8, M = 8

b = -60
du = 0.5
n = 512

ρ (dB)
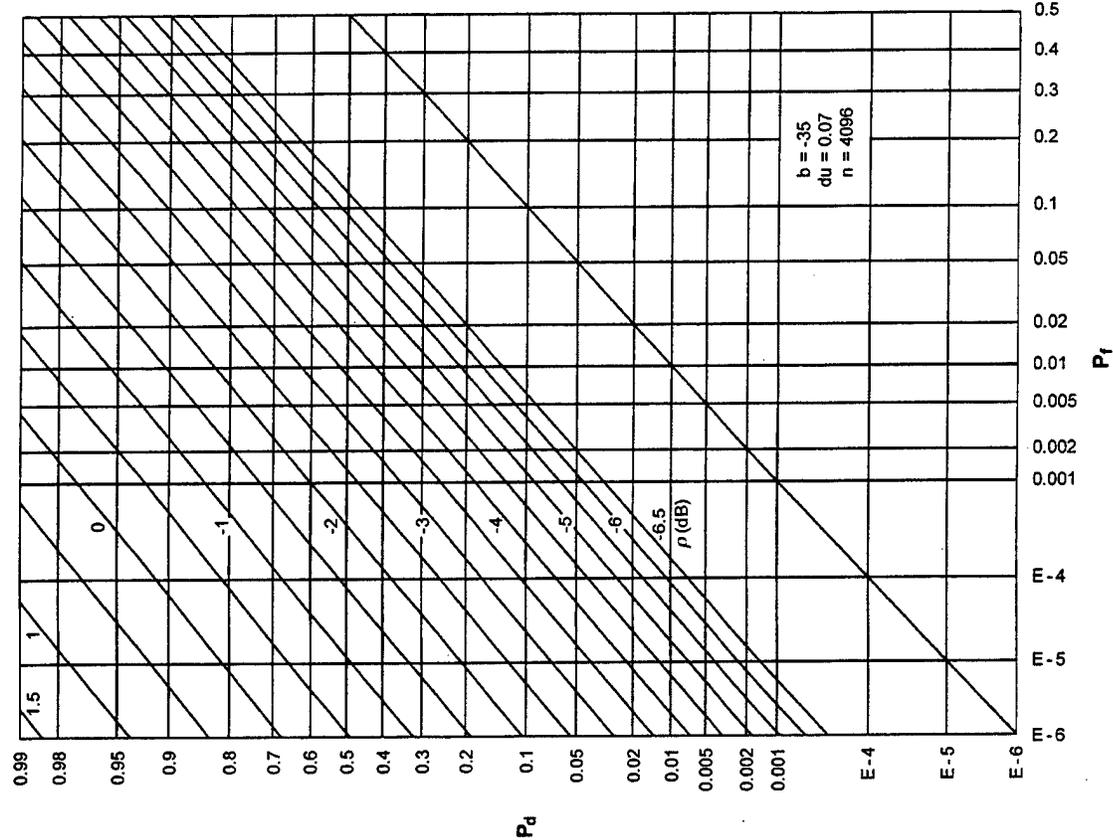
Figure E-22. ROCs for K = 4, N = 2, M = 16

b = -35
du = 0.07
n = 4096
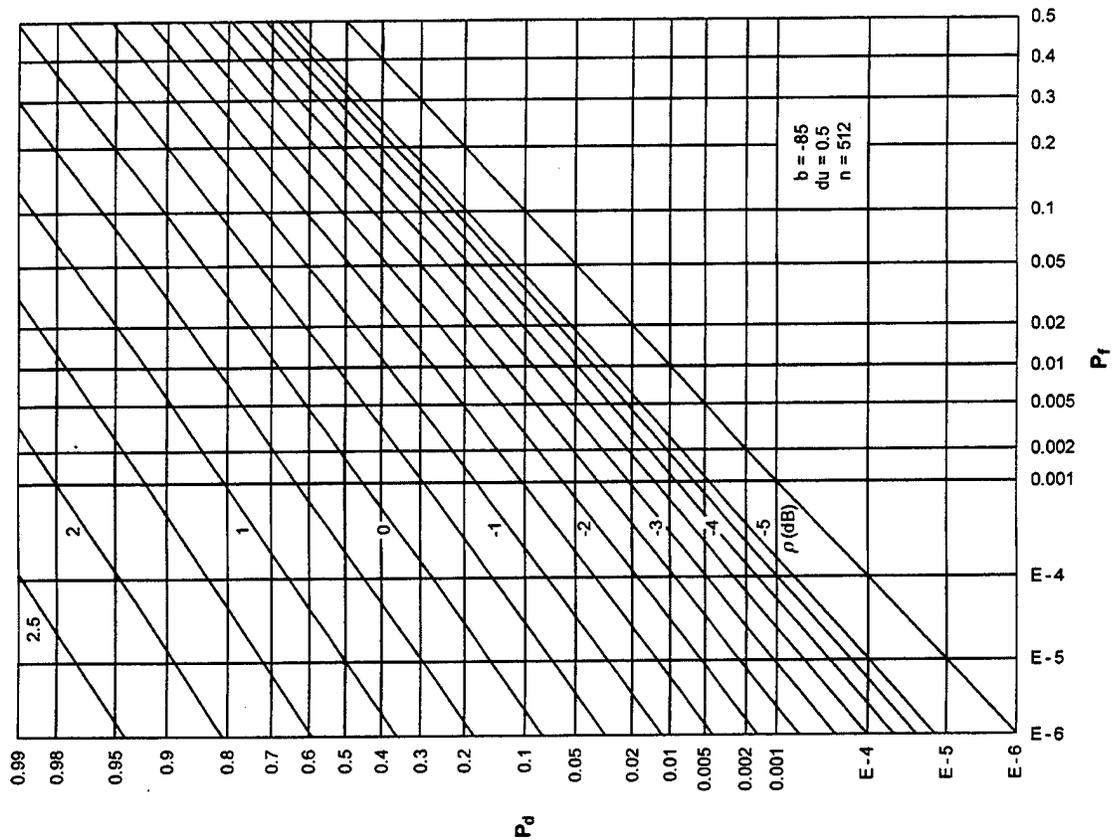
Figure E-21. ROCs for K = 8, N = 32, M = 8

b = -85
du = 0.5
n = 512

E-12
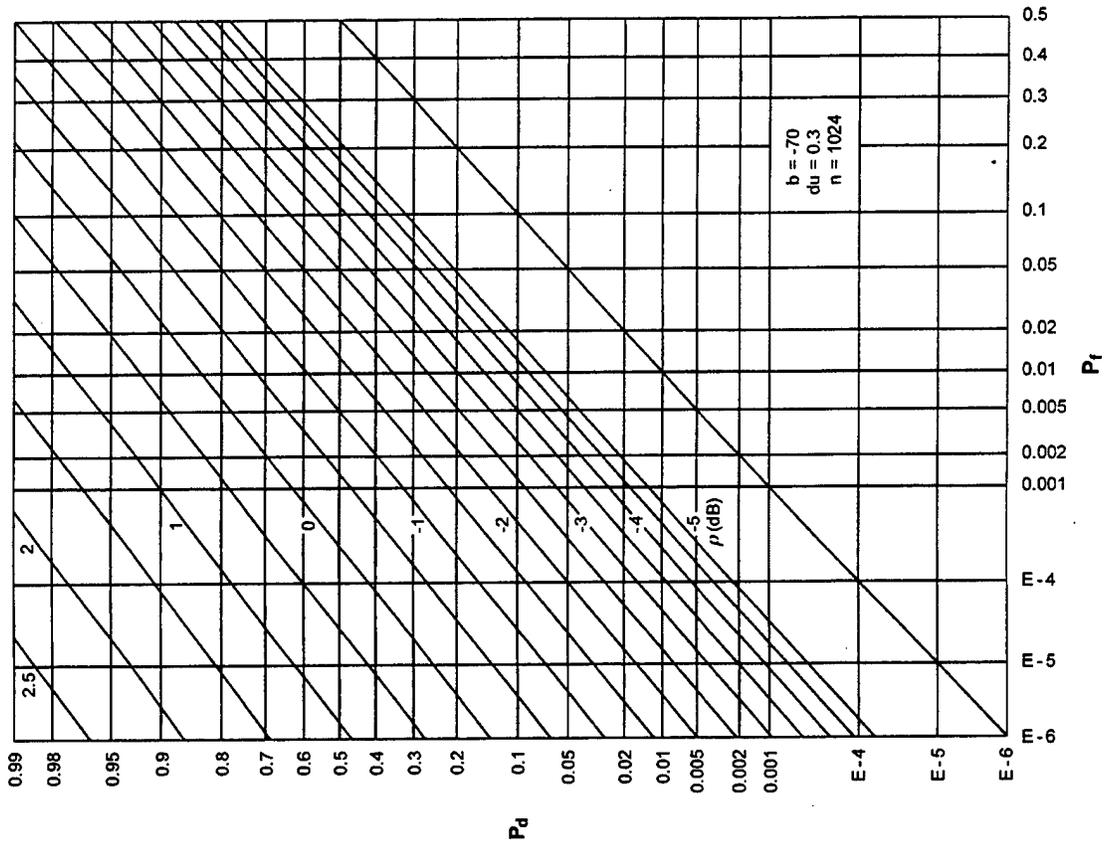
Figure E-24.   ROCs for K = 4, N = 8, M = 16

$b = -70$
$du = 0.3$
$n = 1024$
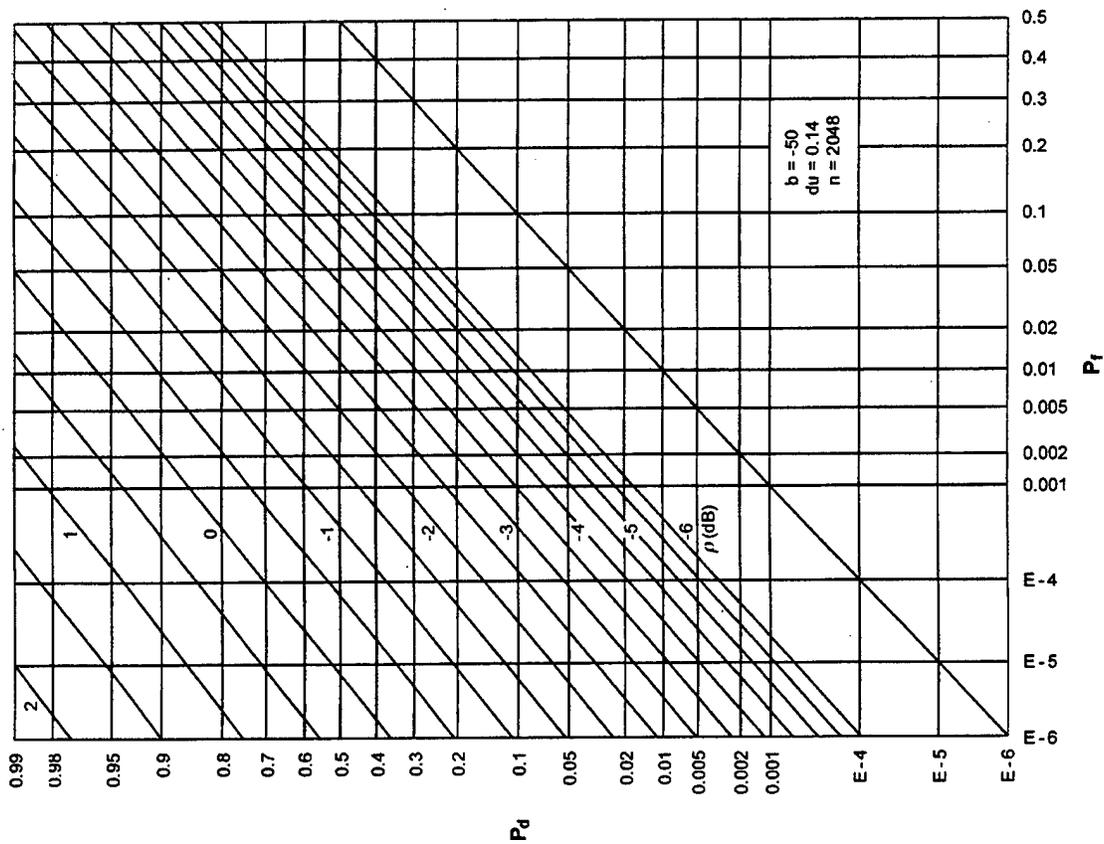
Figure E-23.   ROCs for K = 4, N = 4, M = 16

$b = -50$
$du = 0.14$
$n = 2048$
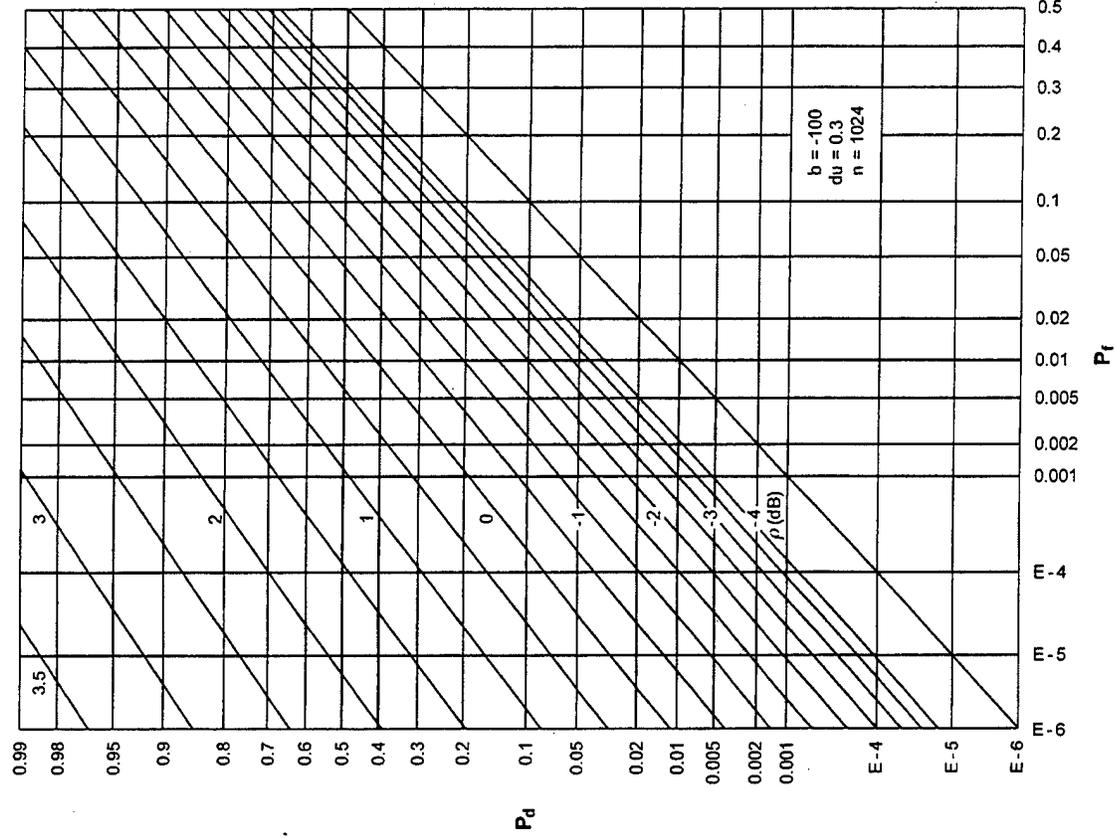
Figure E-26. ROCs for K = 4, N = 32, M = 16
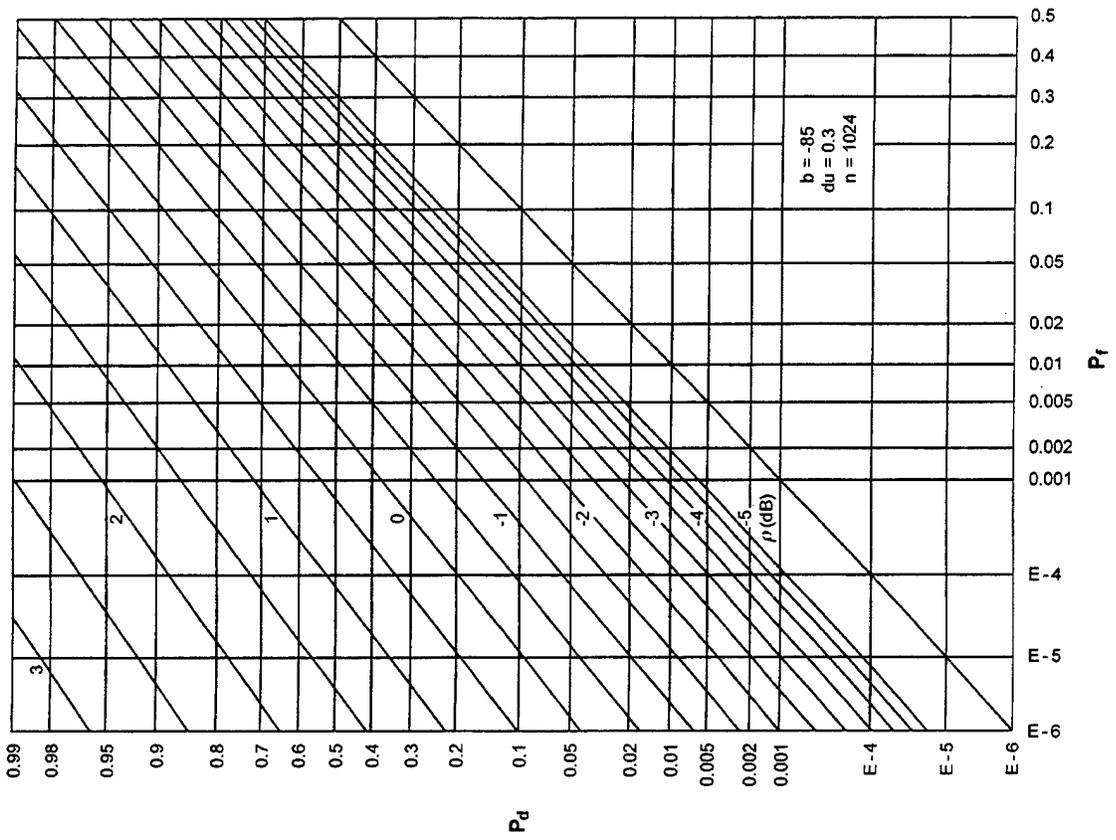
Figure E-25. ROCs for K = 4, N = 16, M = 16

E-14
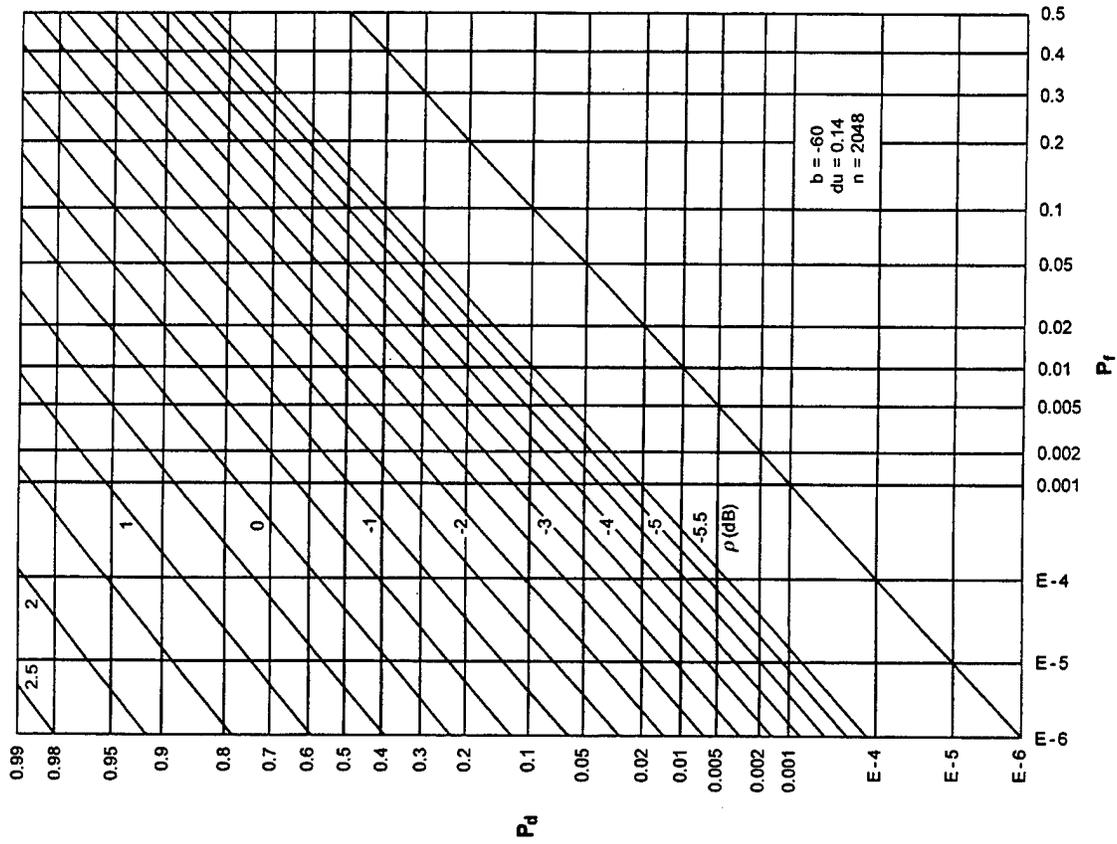
Figure E-28. ROCs for K = 2, N = 4, M = 32

b = -60
du = 0.14
n = 2048
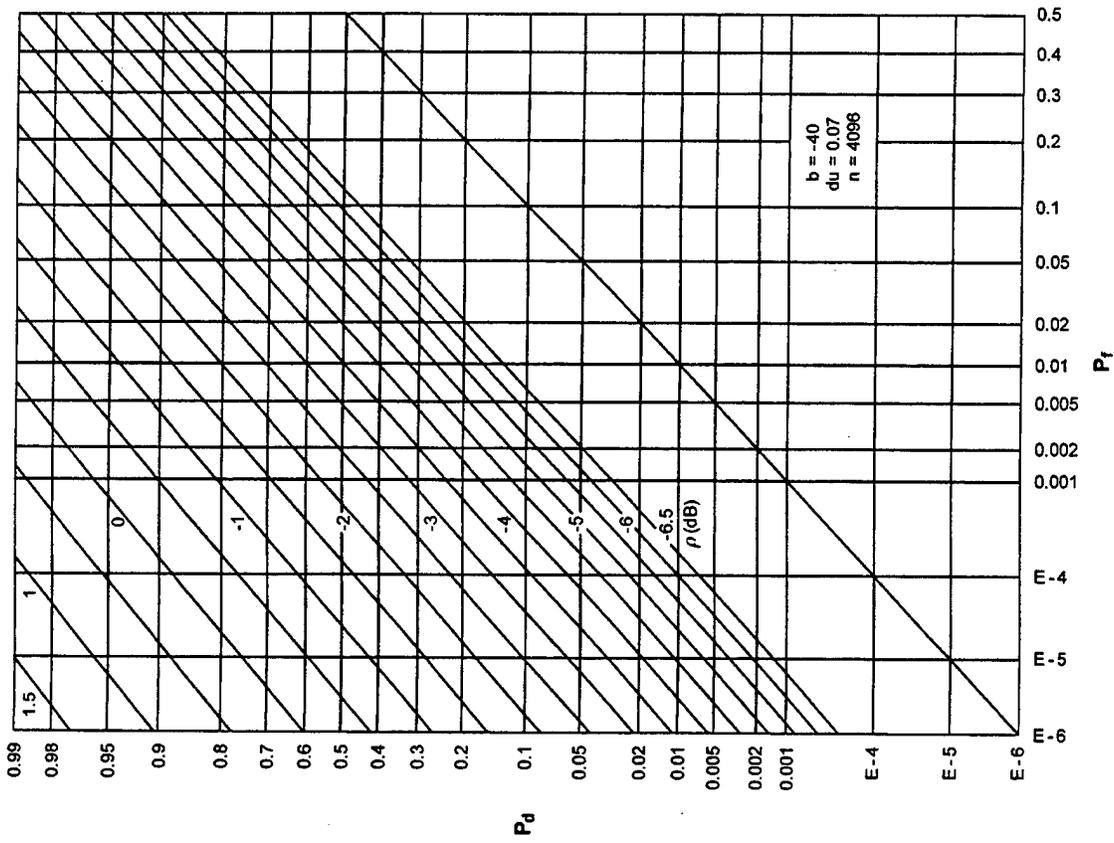
Figure E-27. ROCs for K = 2, N = 2, M = 32

b = -40
du = 0.07
n = 4096
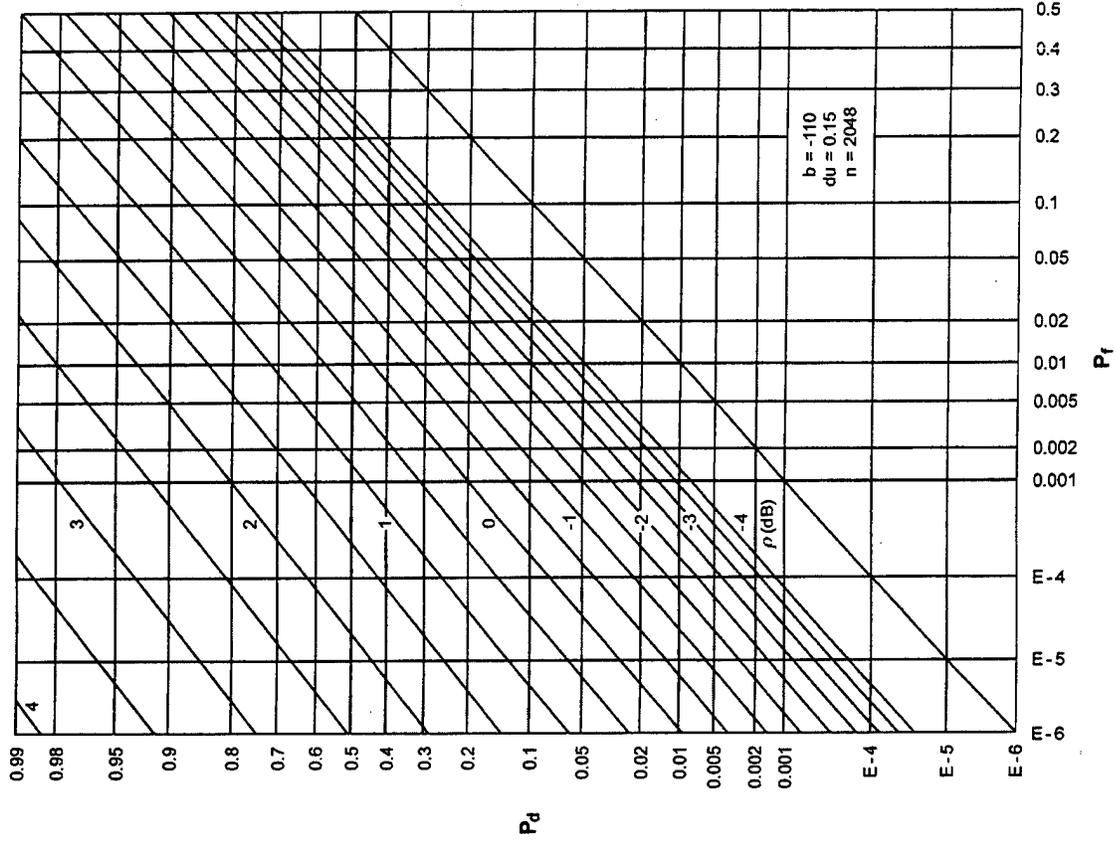
Figure E-30. ROCs for K = 2, N = 16, M = 32

b = -110
du = 0.15
n = 2048

P_f

P_d

ρ (dB)
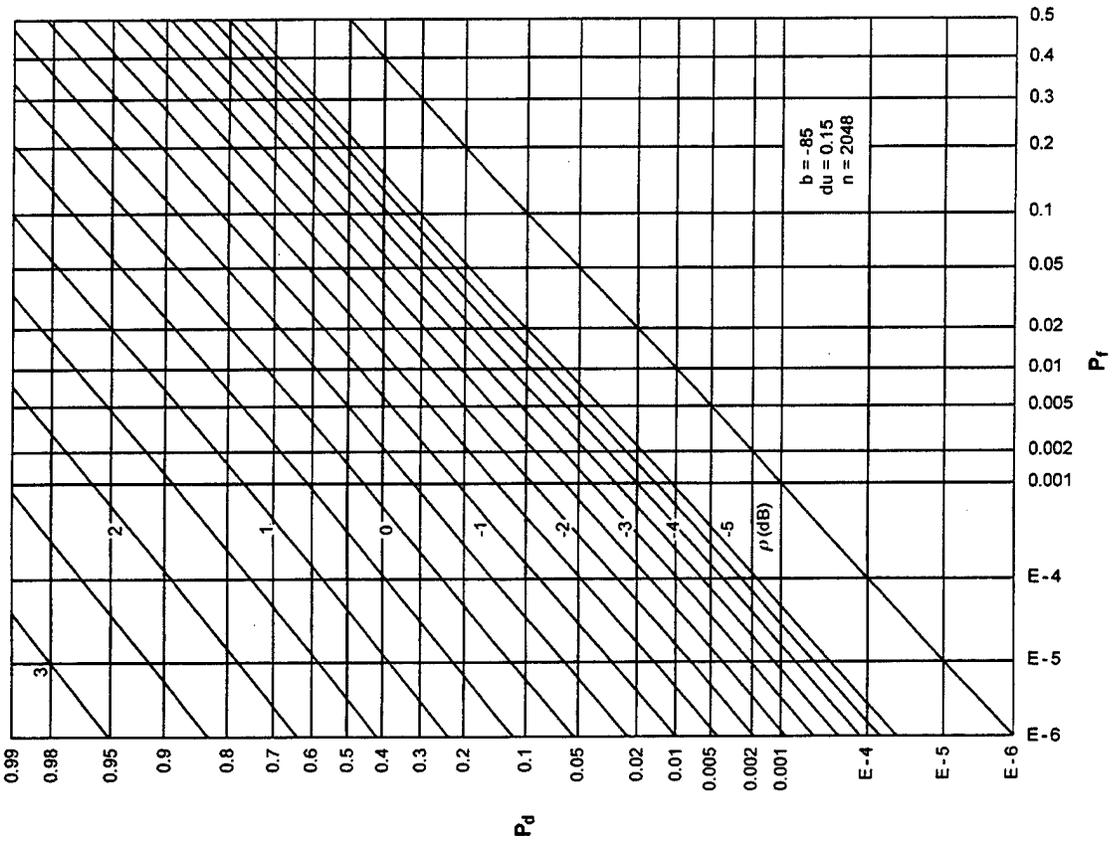
Figure E-29. ROCs for K = 2, N = 8, M = 32

b = -85
du = 0.15
n = 2048

P_f

P_d

ρ (dB)
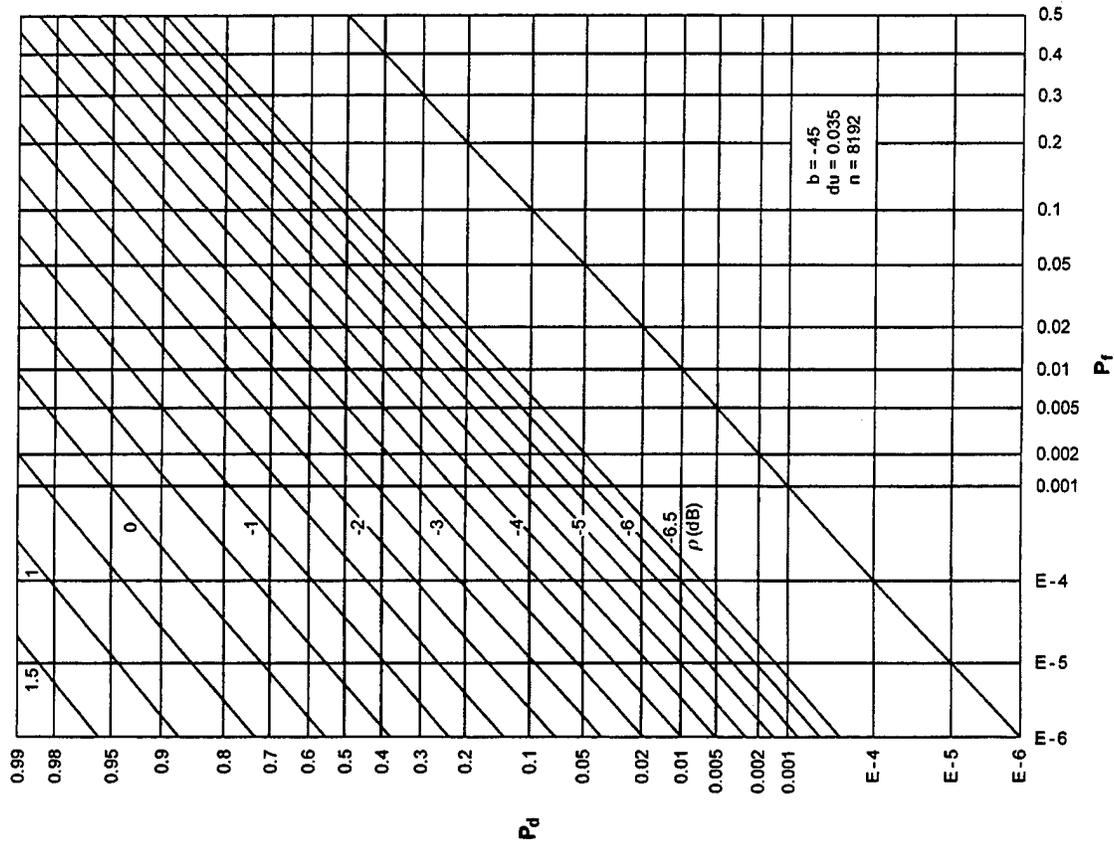
Figure E-32. ROCs for K = 1, N = 2, M = 64
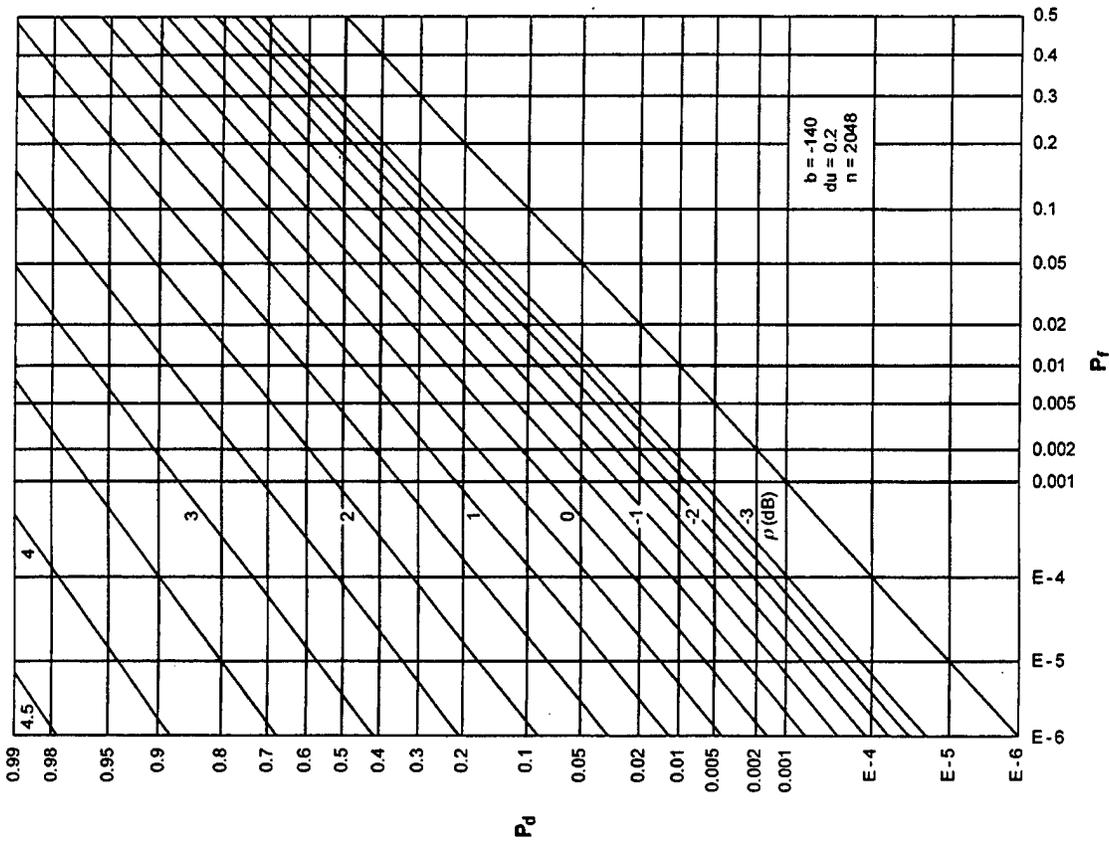
Figure E-31. ROCs for K = 2, N = 32, M = 32

E-17
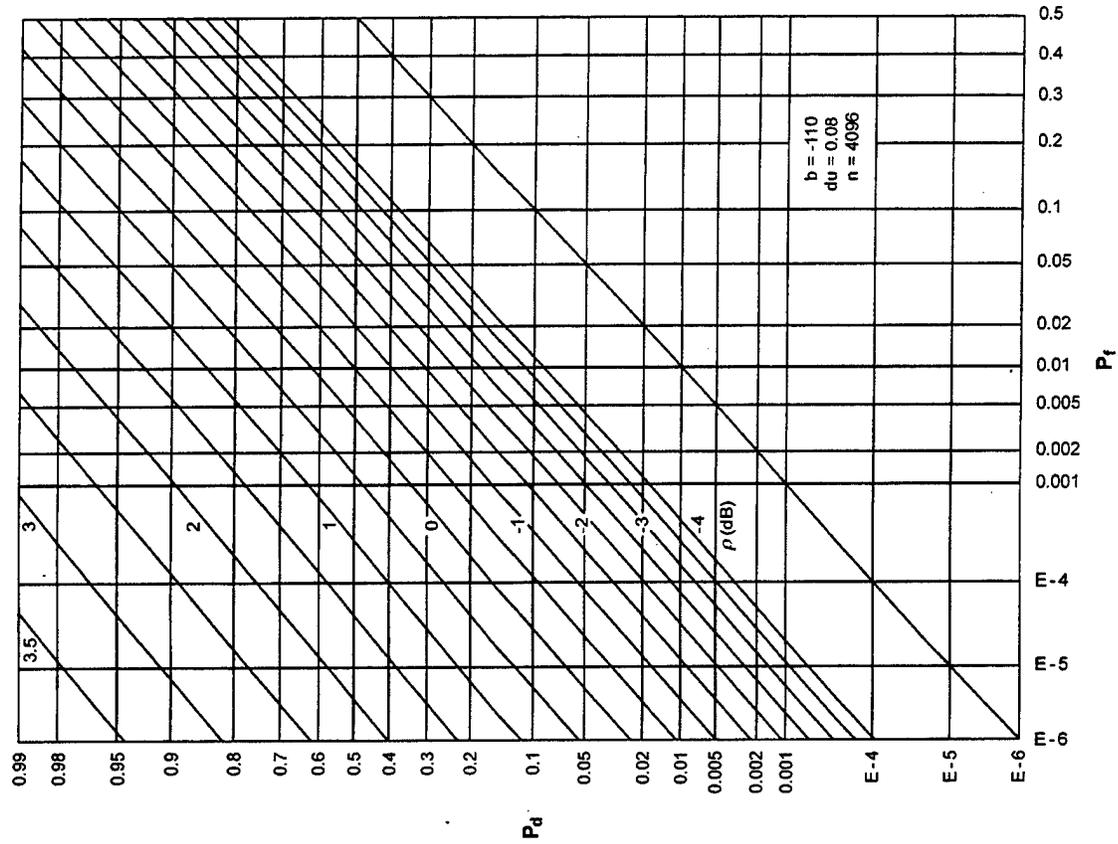
Figure E-34. ROCs for K = 1, N = 8, M = 64

P_f

P_d

$b = -110$
$du = 0.08$
$n = 4096$

ρ (dB)
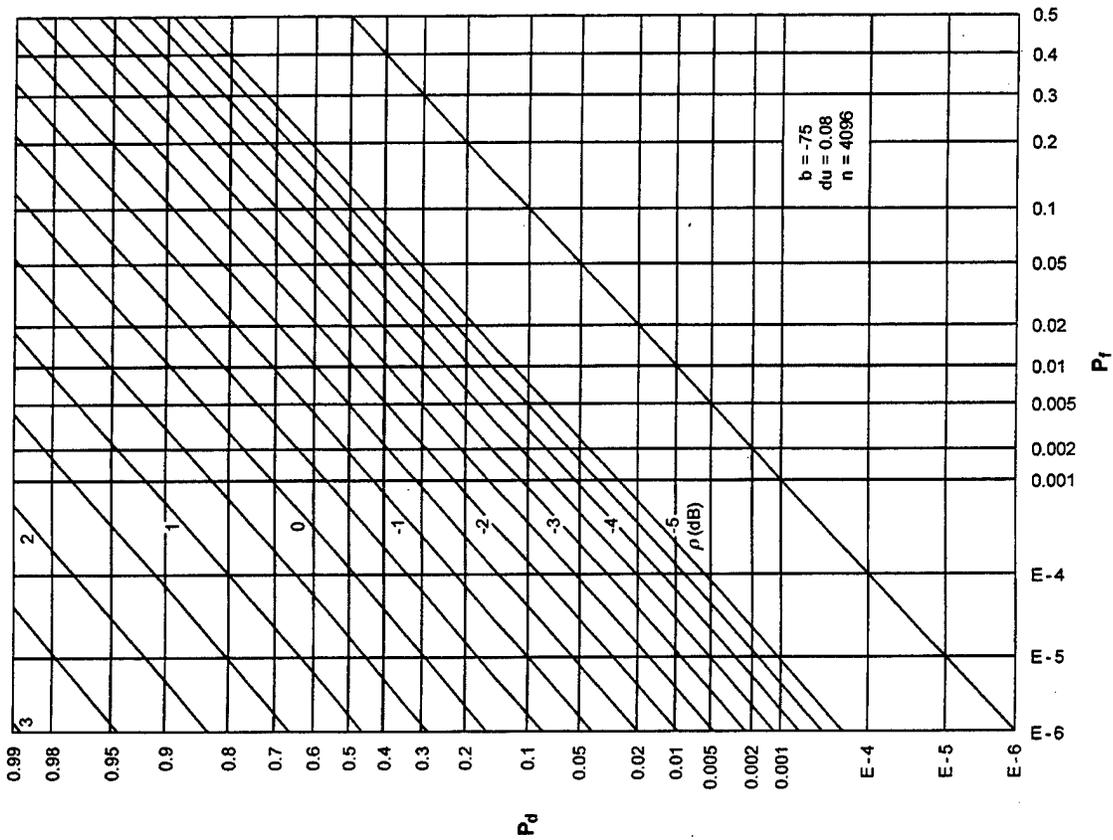
Figure E-33. ROCs for K = 1, N = 4, M = 64

P_f

P_d

$b = -75$
$du = 0.08$
$n = 4096$

ρ (dB)
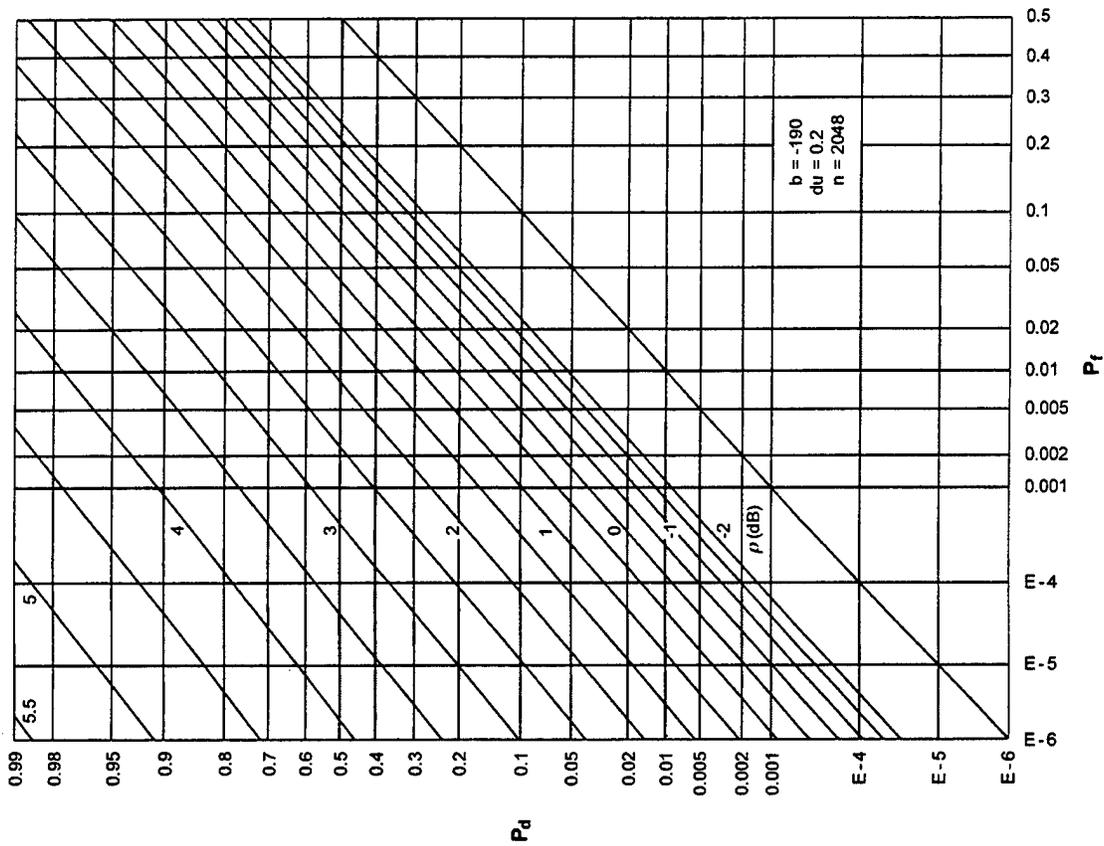
Figure E-36. ROCs for K = 1, N = 32, M = 64

b = -190
du = 0.2
n = 2048
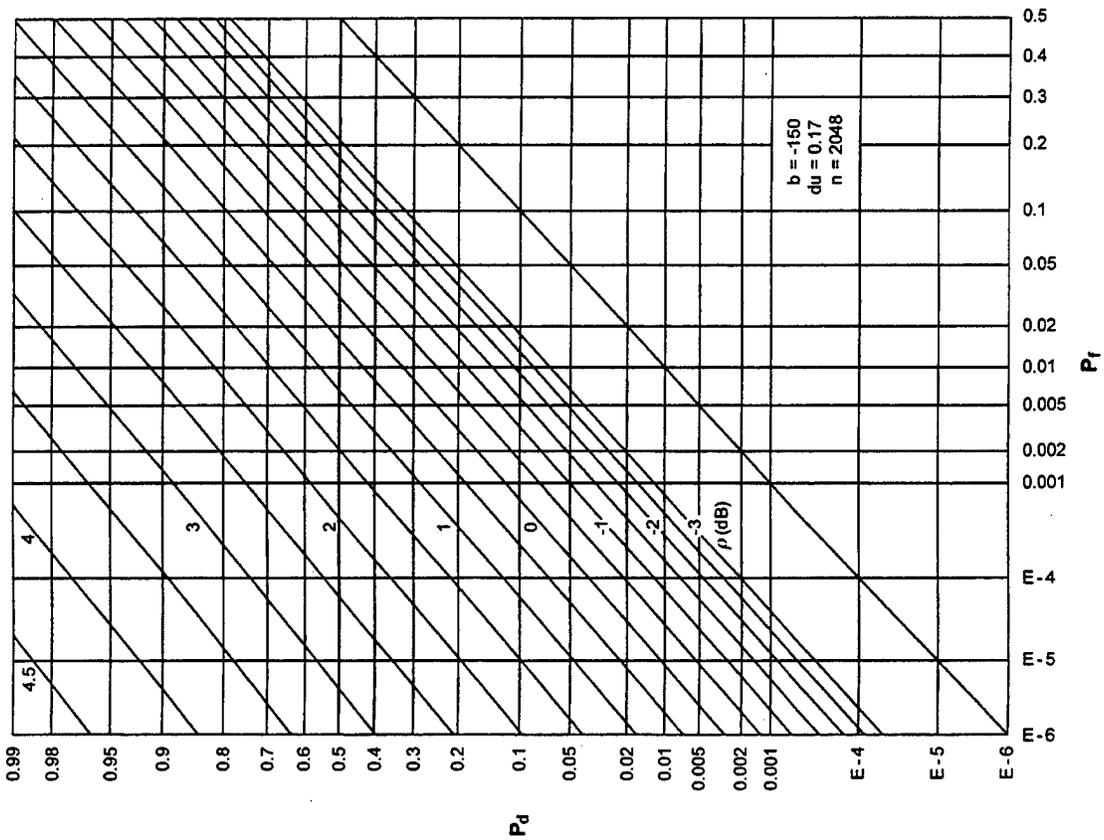
Figure E-35. ROCs for K = 1, N = 16, M = 64

b = -150
du = 0.17
n = 2048

APPENDIX F — ROCs FOR KM = 256, PHASE-INCOHERENT SIGNAL

This appendix contains the ROCs for or-ing with pre- and post-averaging when the time-bandwidth product KM is fixed at 256; the possible combinations (from table 1) are repeated here:

K	M	N
256	1	1,2,4,8,16,32
128	2	
64	4	
32	8	
16	16	
8	32	
4	64	
2	128	
1	256	

For N = 1, only the product KM matters; the first plot in this appendix covers this special case, under the labeling K = 256, N = 1, M = 1. The other 5 values of N, along with the 9 possible combinations of K and M, yield 45 additional ROCs, for a total of 46 ROCs in this appendix.
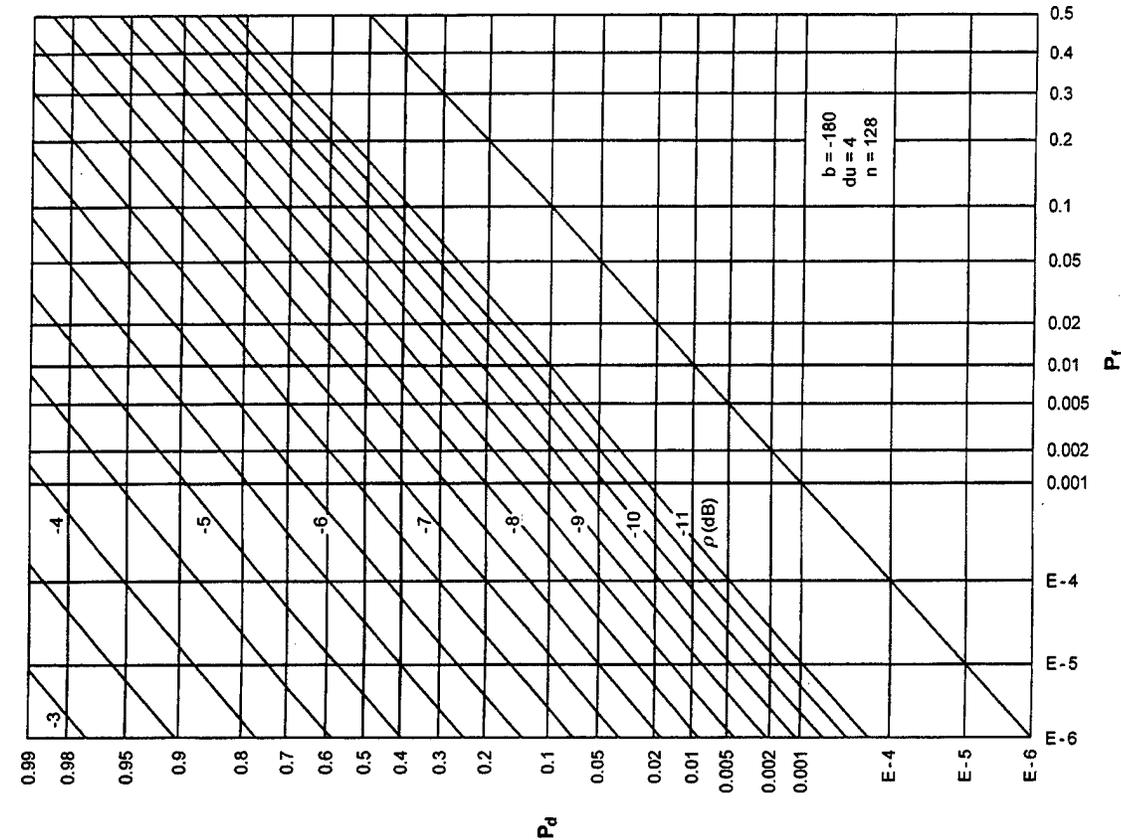
Figure F-2. ROCs for K = 256, N = 2, M = 1
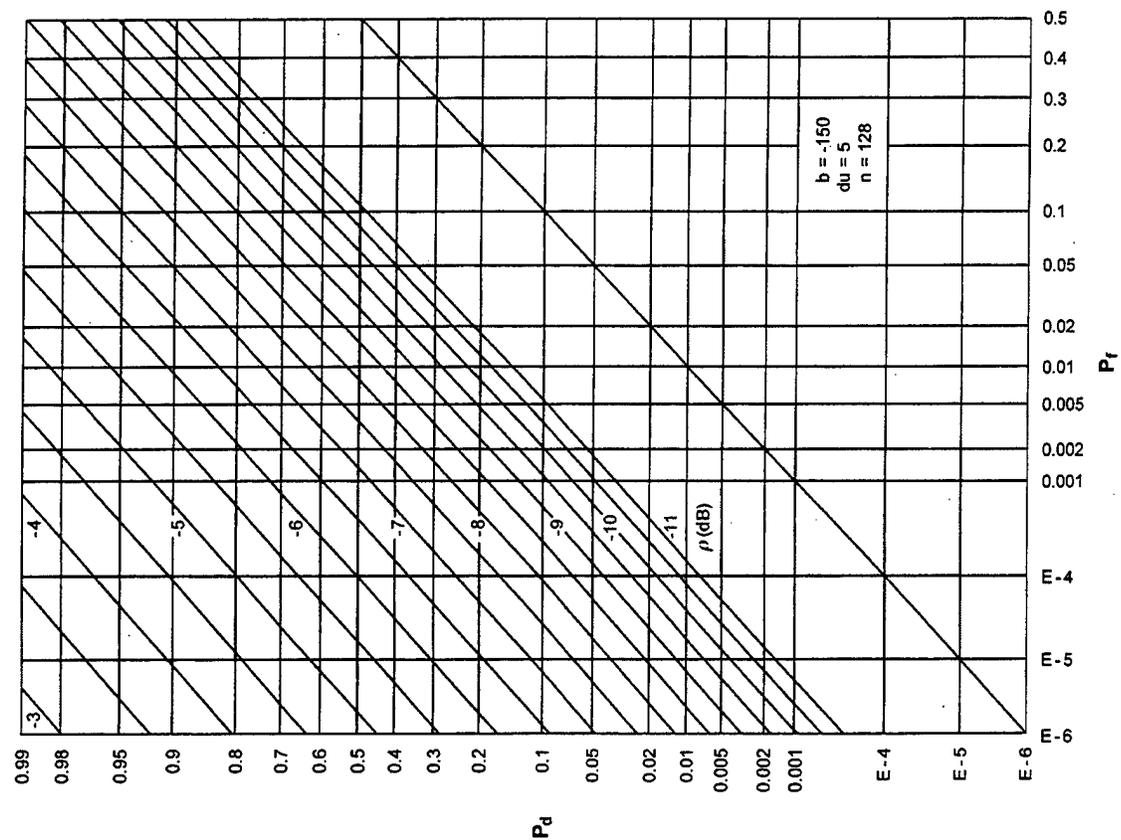
Figure F-1. ROCs for K = 256, N = 1, M = 1

F-2
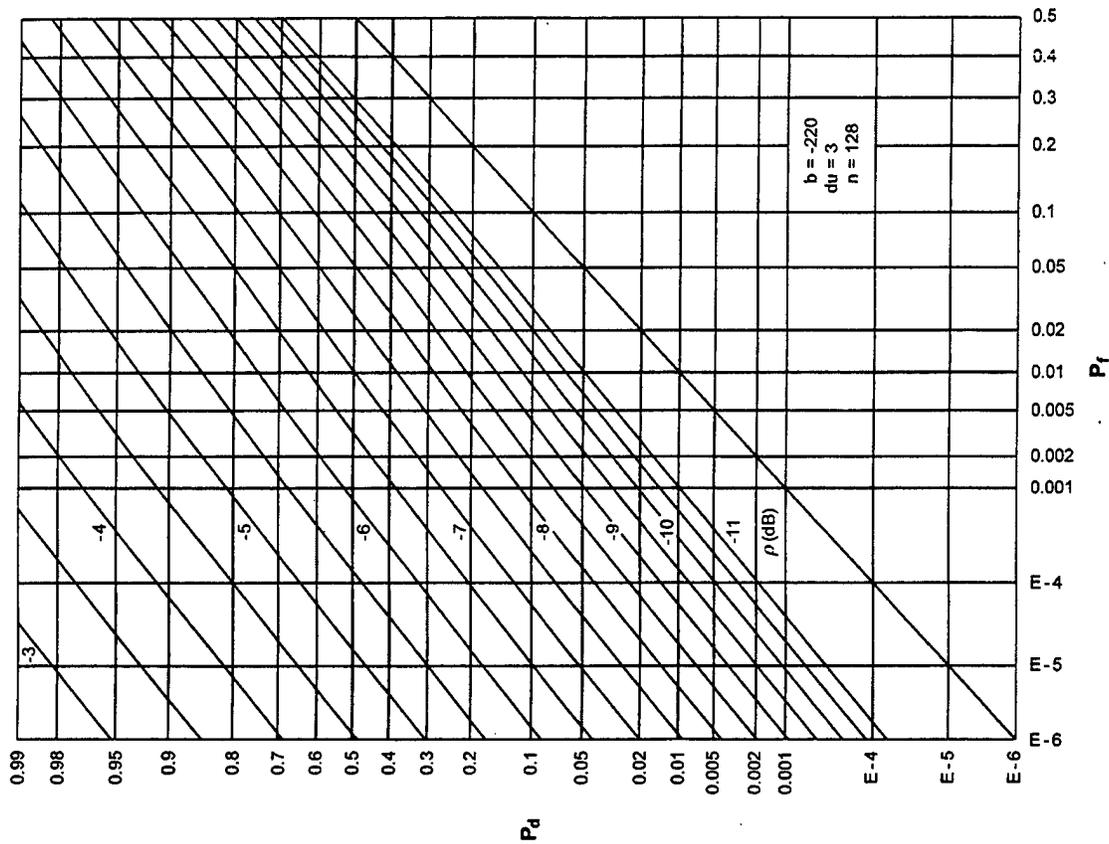
Figure F-4. ROCs for K = 256, N = 8, M = 1
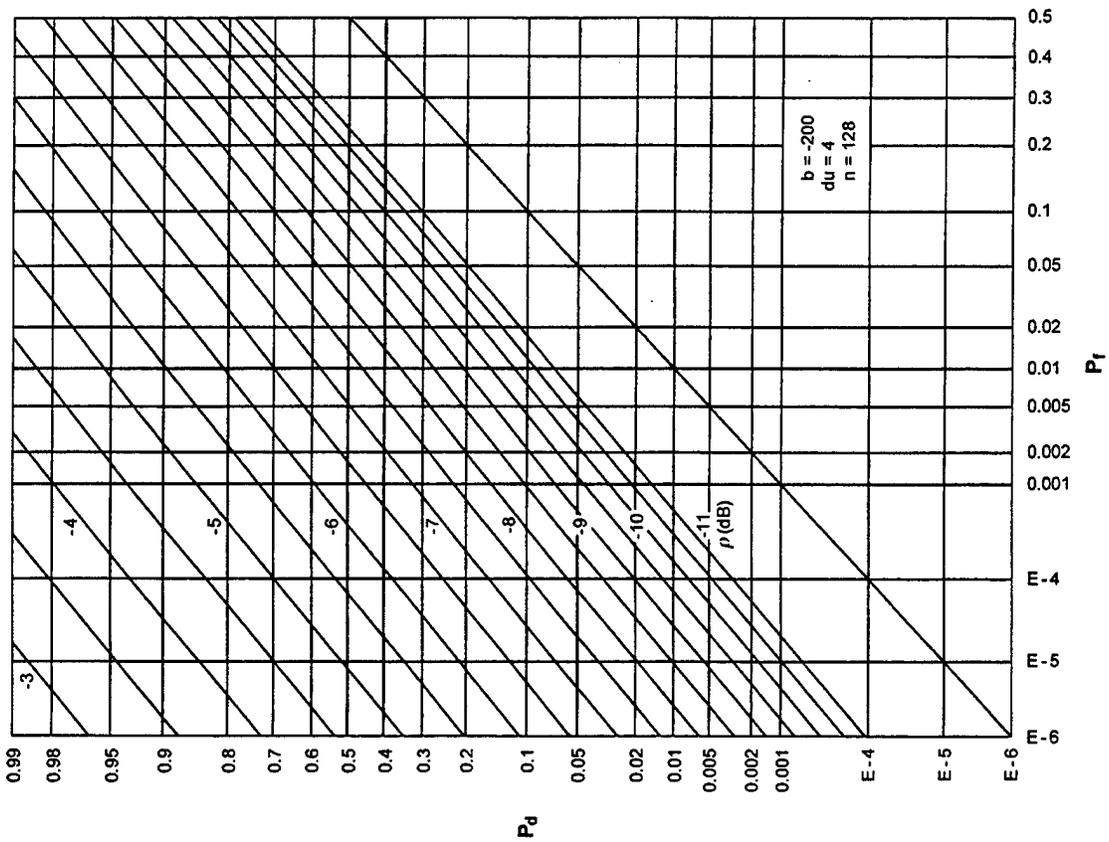
Figure F-3. ROCs for K = 256, N = 4, M = 1

F-3
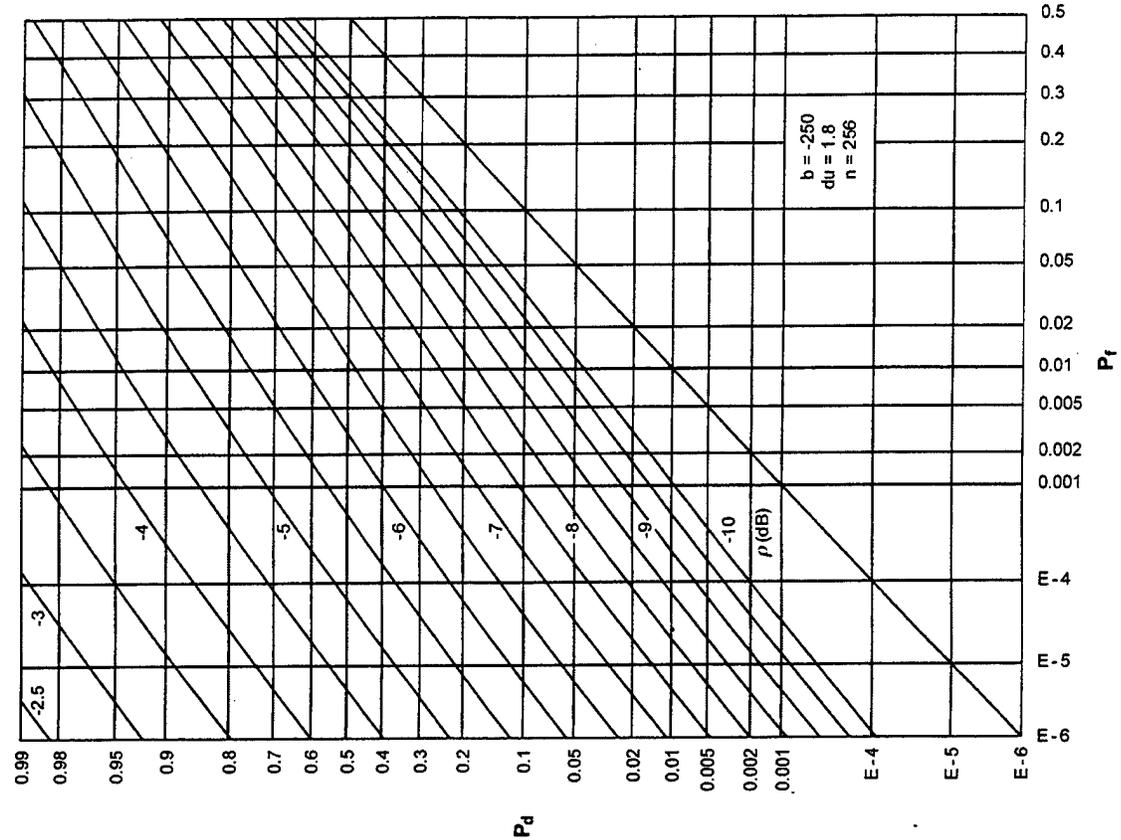
Figure F-6. ROCs for $K = 256$, $N = 32$, $M = 1$

$b = -250$
$du = 1.8$
$n = 256$
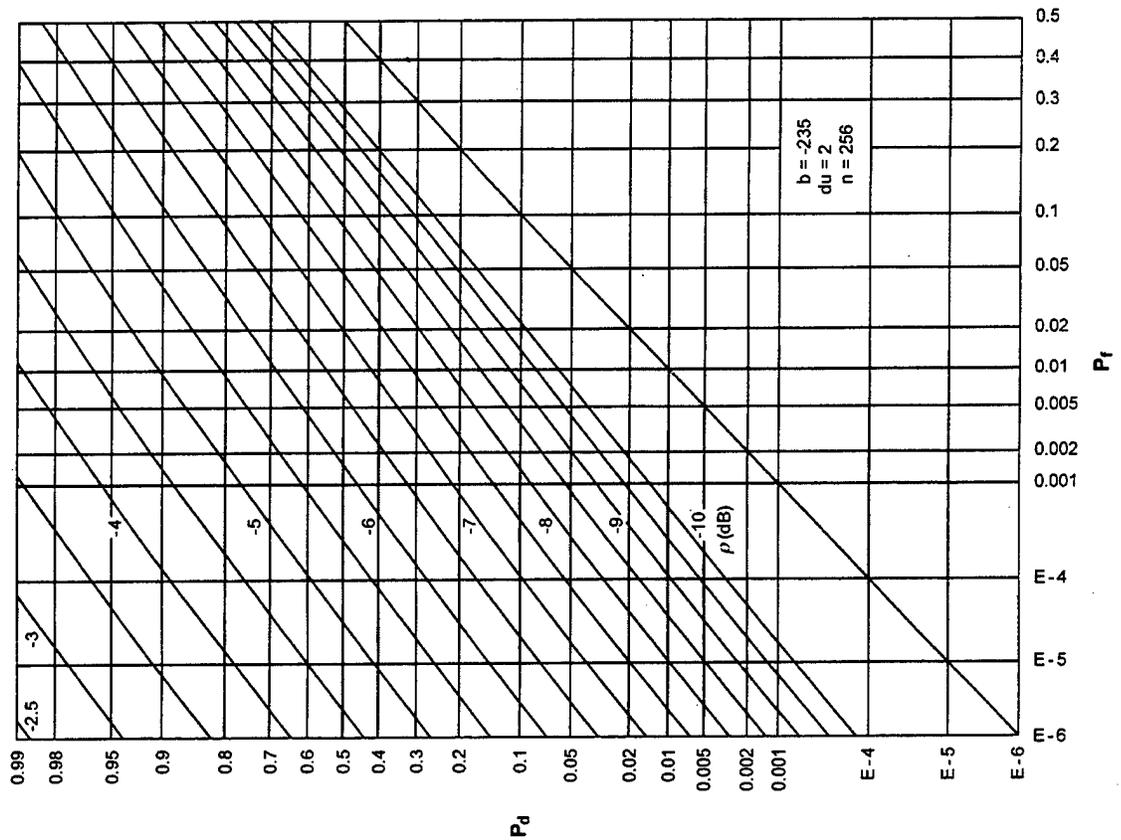
Figure F-5. ROCs for $K = 256$, $N = 16$, $M = 1$

$b = -235$
$du = 2$
$n = 256$

F-4
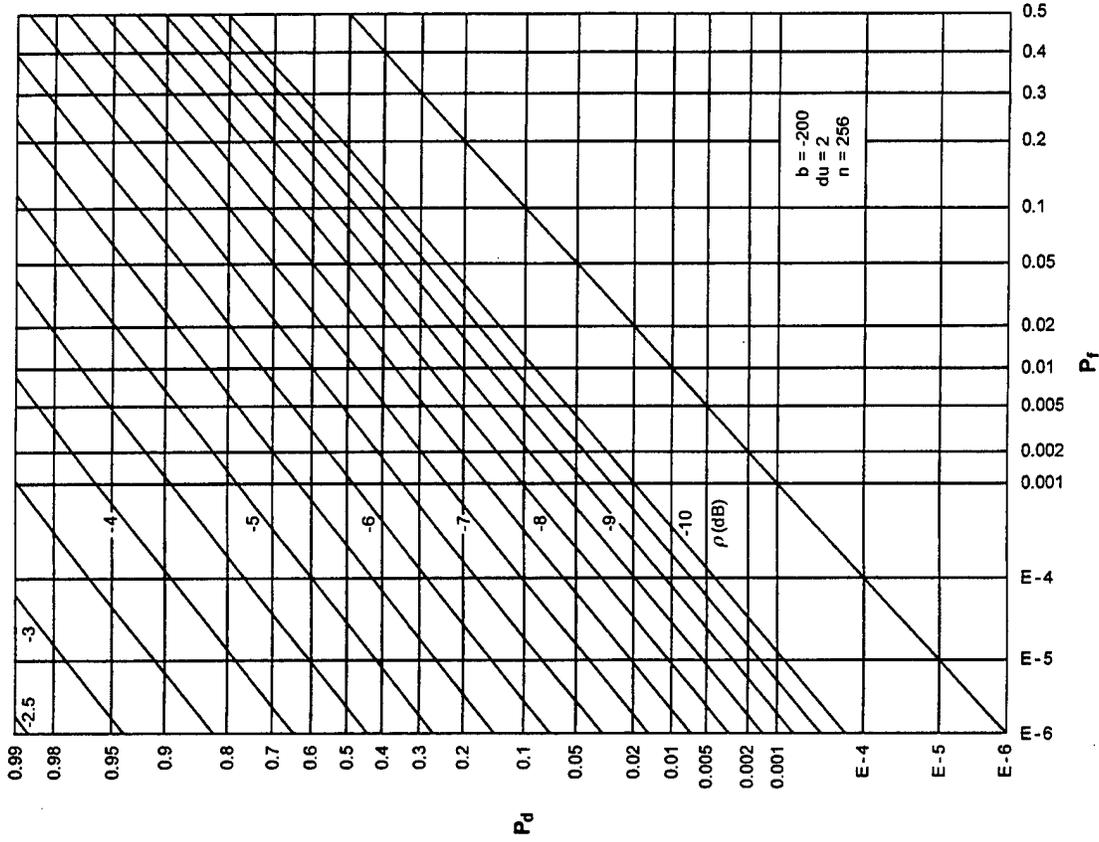
Figure F-8. ROCs for K = 128, N = 4, M = 2

b = -200
du = 2
n = 256

P_f

P_d

ρ(dB)

-2.5 -3 -4 -5 -6 -7 -8 -9 -10

0.5 0.4 0.3 0.2 0.1 0.05 0.02 0.01 0.005 0.002 0.001 E-4 E-5 E-6

0.99 0.98 0.95 0.9 0.8 0.7 0.6 0.5 0.4 0.3 0.2 0.1 0.05 0.02 0.01 0.005 0.002 0.001 E-4 E-5 E-6
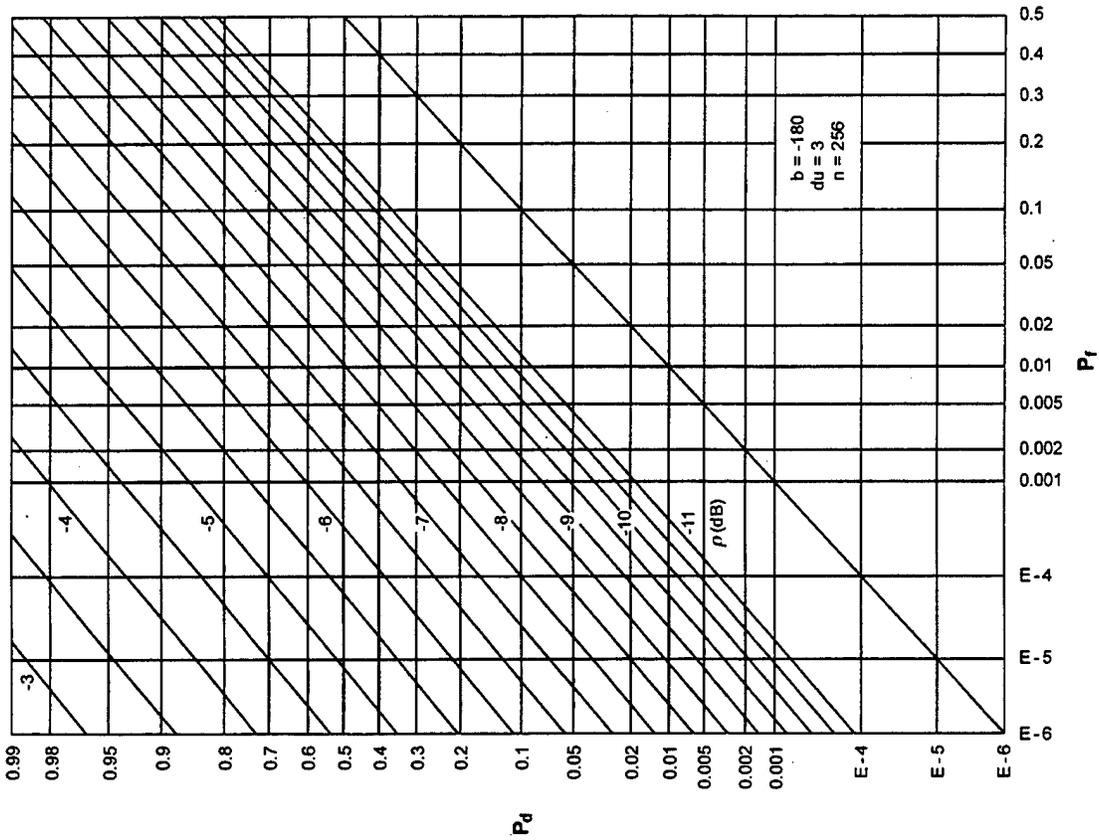
Figure F-7. ROCs for K = 128, N = 2, M = 2

b = -180
du = 3
n = 256

P_f

P_d

ρ(dB)

-3 -4 -5 -6 -7 -8 -9 -10 -11

Figure F-10. ROCs for K = 128, N = 16, M = 2

b = -240
du = 1.6
n = 256

Figure F-9. ROCs for K = 128, N = 8, M = 2

b = -225
du = 1.8
n = 256
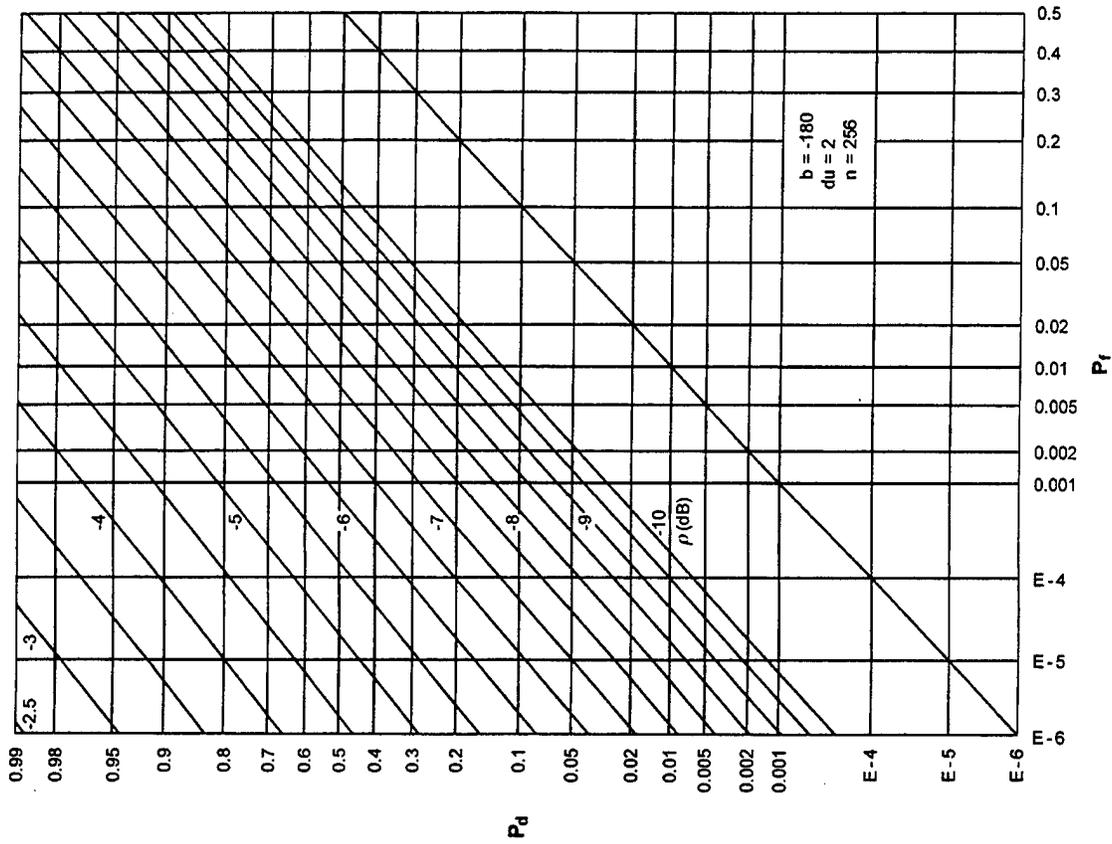
Figure F-12. ROCs for K = 64, N = 2, M = 4
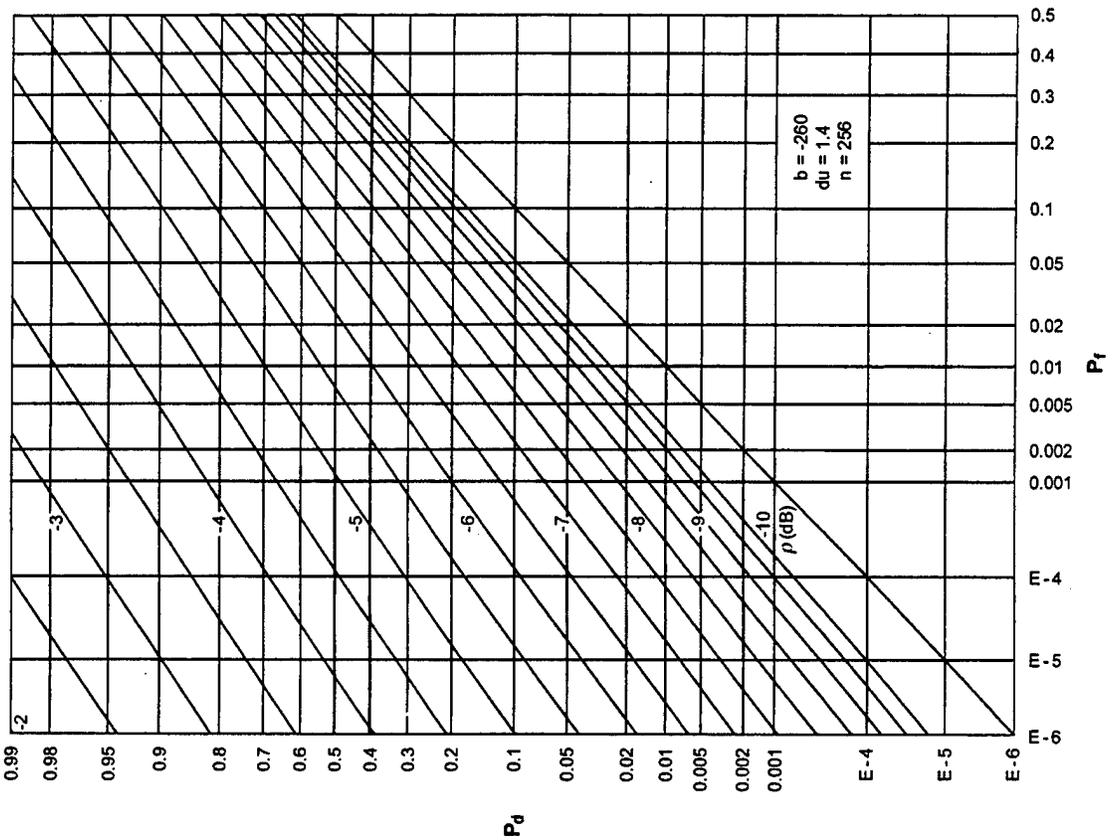
Figure F-11. ROCs for K = 128, N = 32, M = 2

Figure F-14. ROCs for K = 64, N = 8, M = 4

Figure F-13. ROCs for K = 64, N = 4, M = 4

F-8
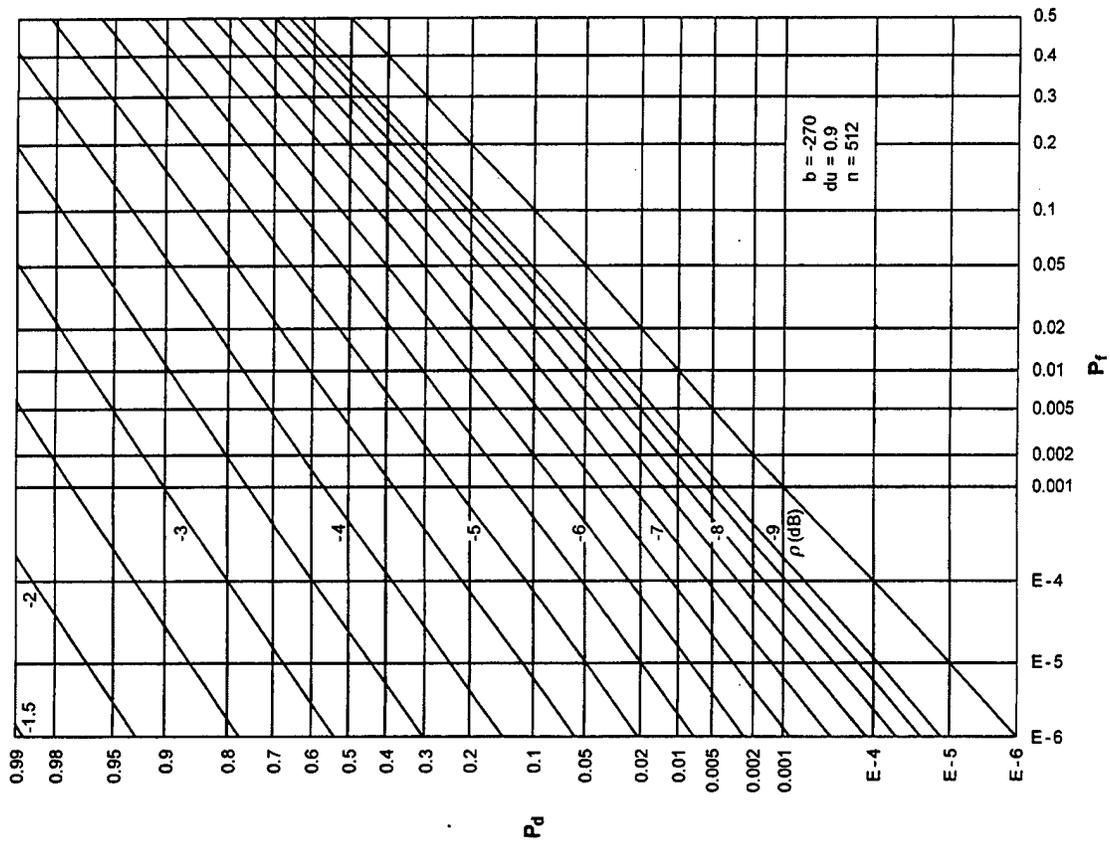
Figure F-16. ROCs for K = 64, N = 32, M = 4

b = -270
du = 0.9
n = 512
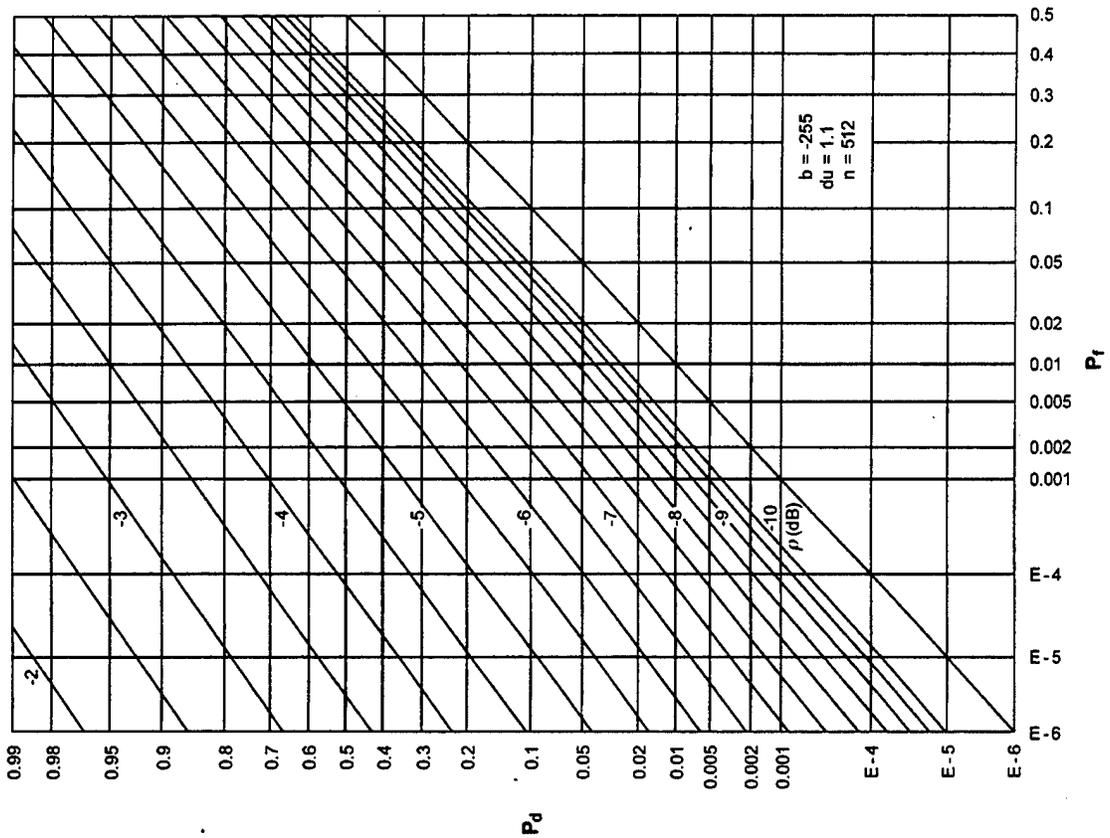
Figure F-15. ROCs for K = 64, N = 16, M = 4

b = -255
du = 1.1
n = 512

Figure F-18. ROCs for K = 32, N = 4, M = 8

b = -220
du = 1.2
n = 512

ρ (dB)

Figure F-17. ROCs for K = 32, N = 2, M = 8

b = -180
du = 1.4
n = 512

ρ (dB)
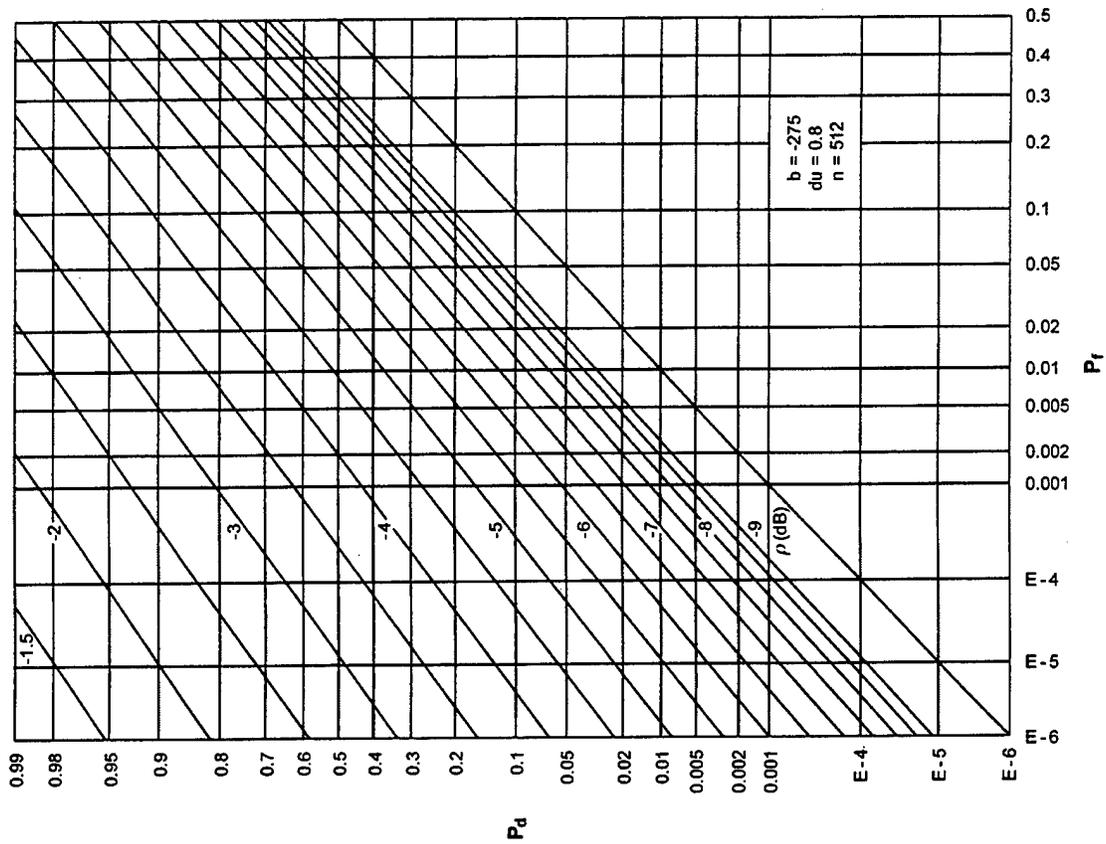
Figure F-20. ROCs for K = 32, N = 16, M = 8

b = -275
du = 0.8
n = 512
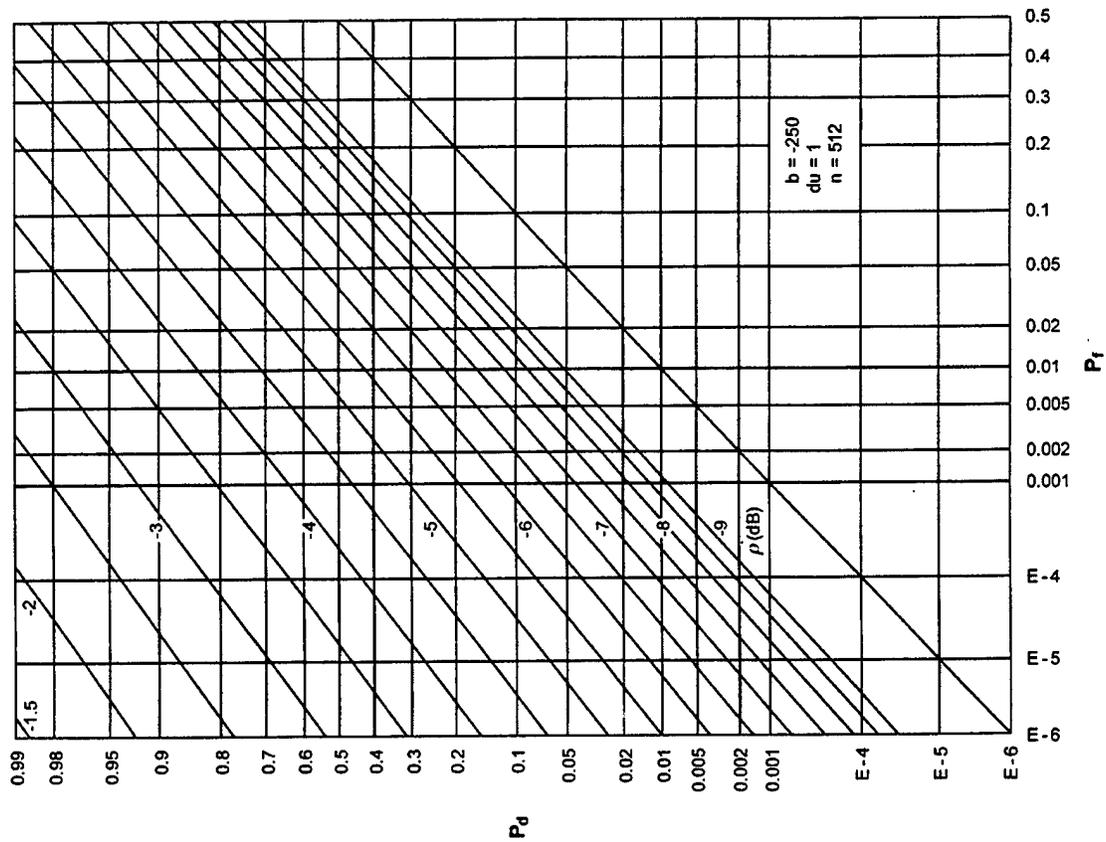
Figure F-19. ROCs for K = 32, N = 8, M = 8

b = -250
du = 1
n = 512

F-11

Figure F-22. ROCs for K = 16, N = 2, M = 16

Figure F-21. ROCs for K = 32, N = 32, M = 8

F-12
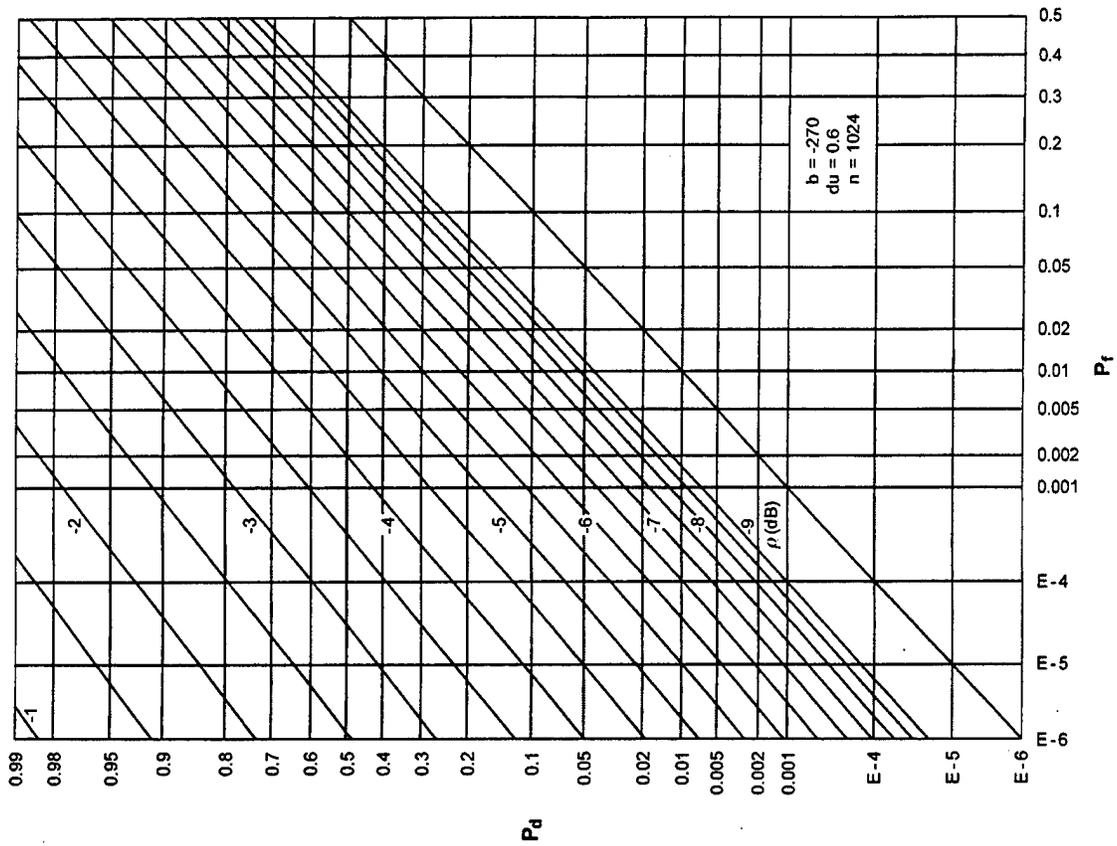
Figure F-24. ROCs for K = 16, N = 8, M = 16

b = -270
du = 0.6
n = 1024
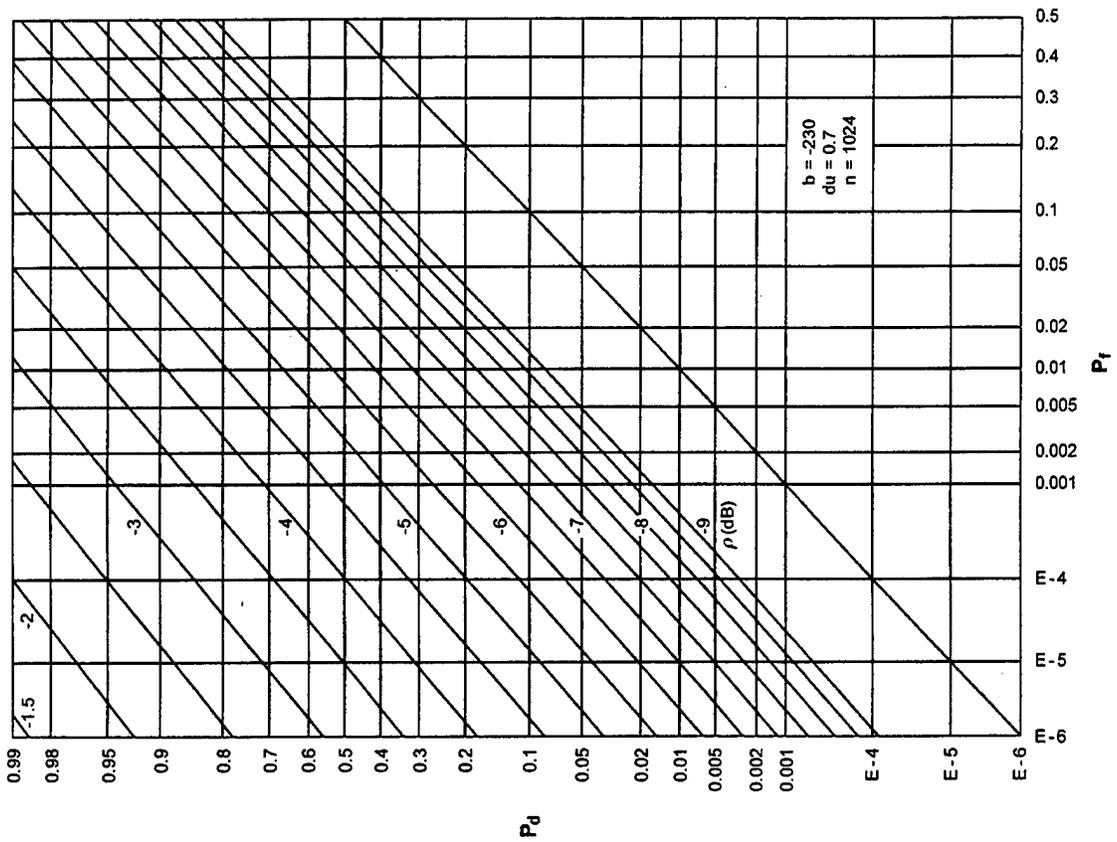
Figure F-23. ROCs for K = 16, N = 4, M = 16

b = -230
du = 0.7
n = 1024

F-13

Figure F-26. ROCs for K = 16, N = 32, M = 16

Figure F-25. ROCs for K = 16, N = 16, M = 16

F-14
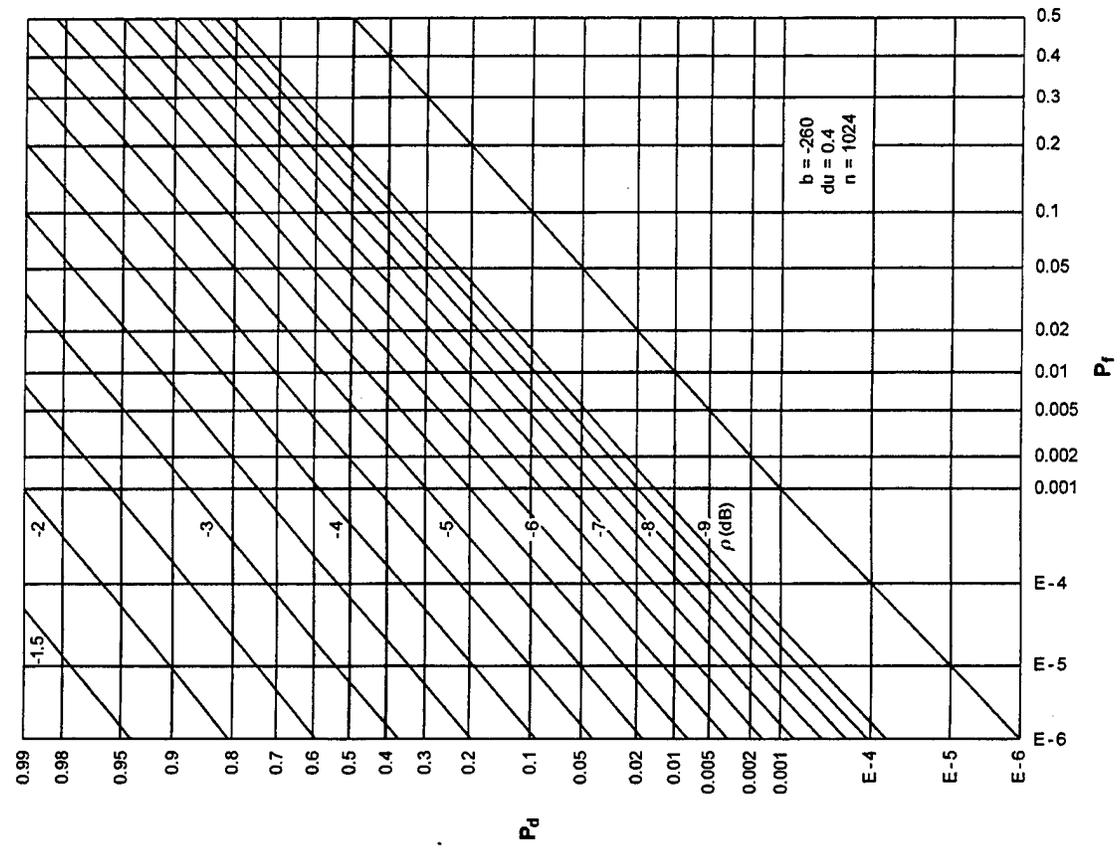
Figure F–28. ROCs for K = 8, N = 4, M = 32

b = -260
du = 0.4
n = 1024
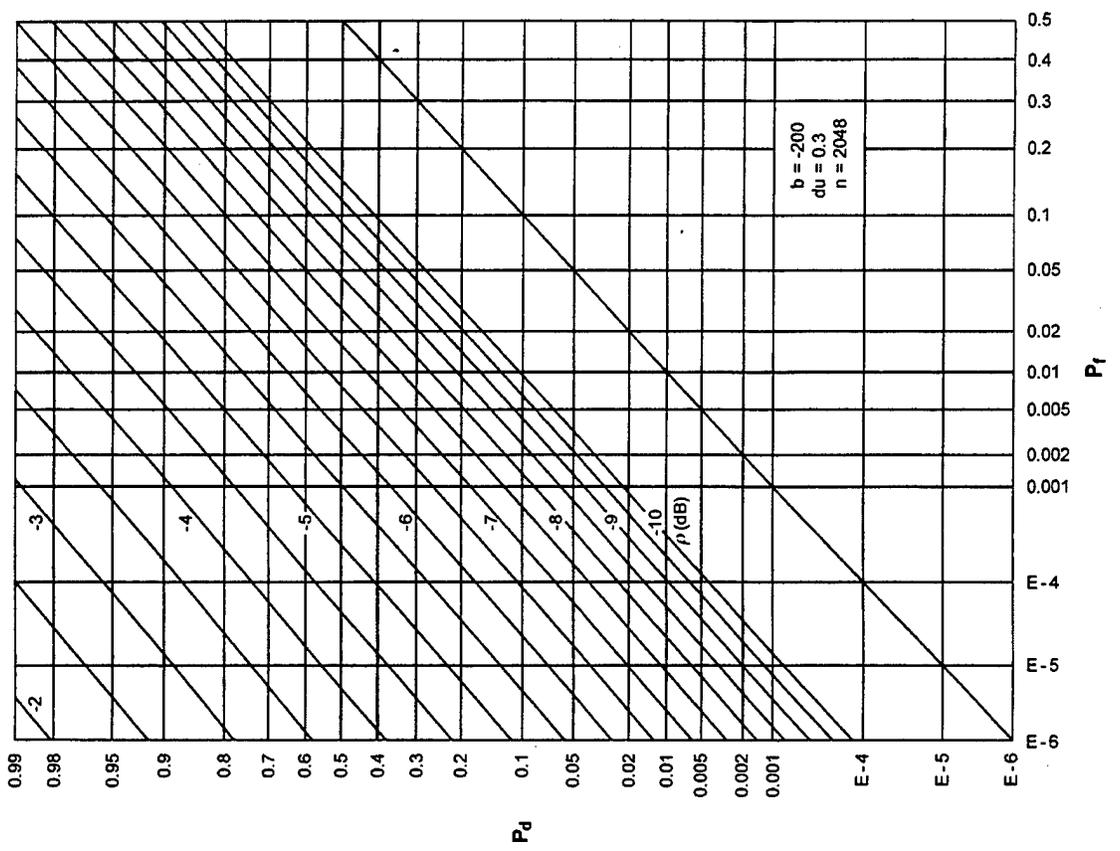
Figure F–27. ROCs for K = 8, N = 2, M = 32

b = -200
du = 0.3
n = 2048
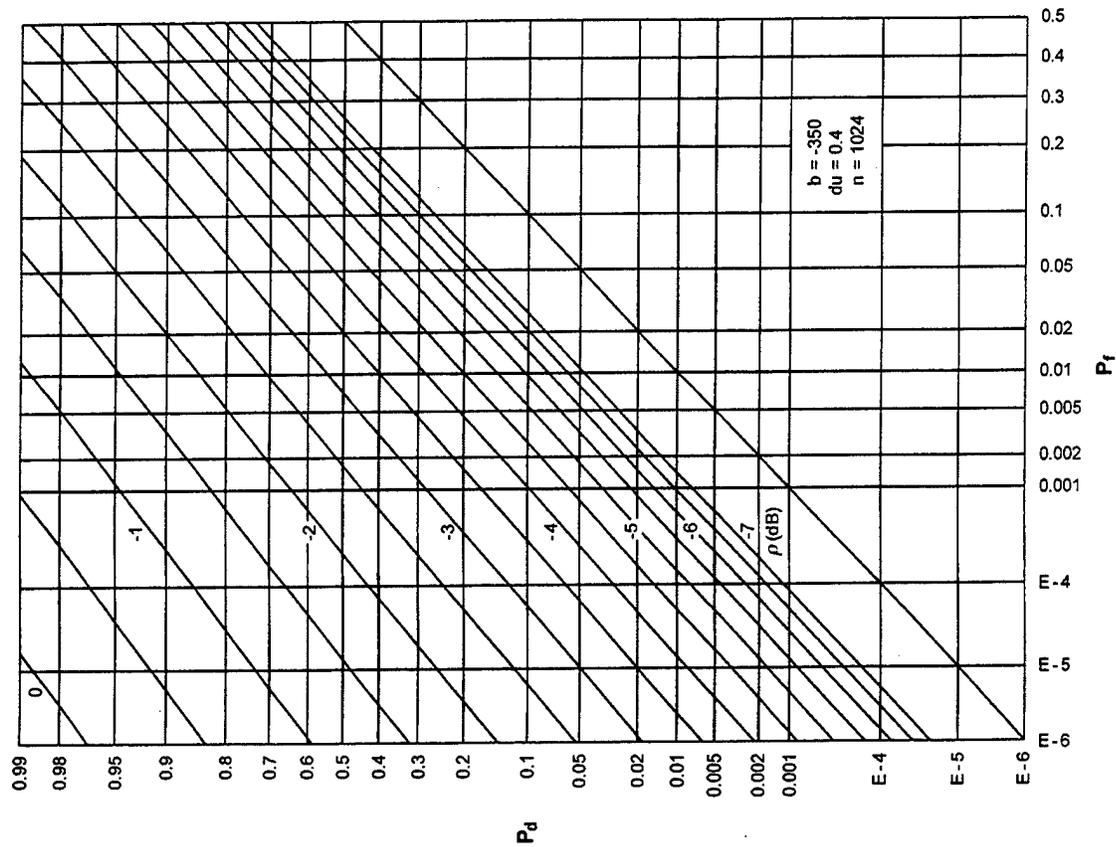
Figure F-30. ROCs for K = 8, N = 16, M = 32
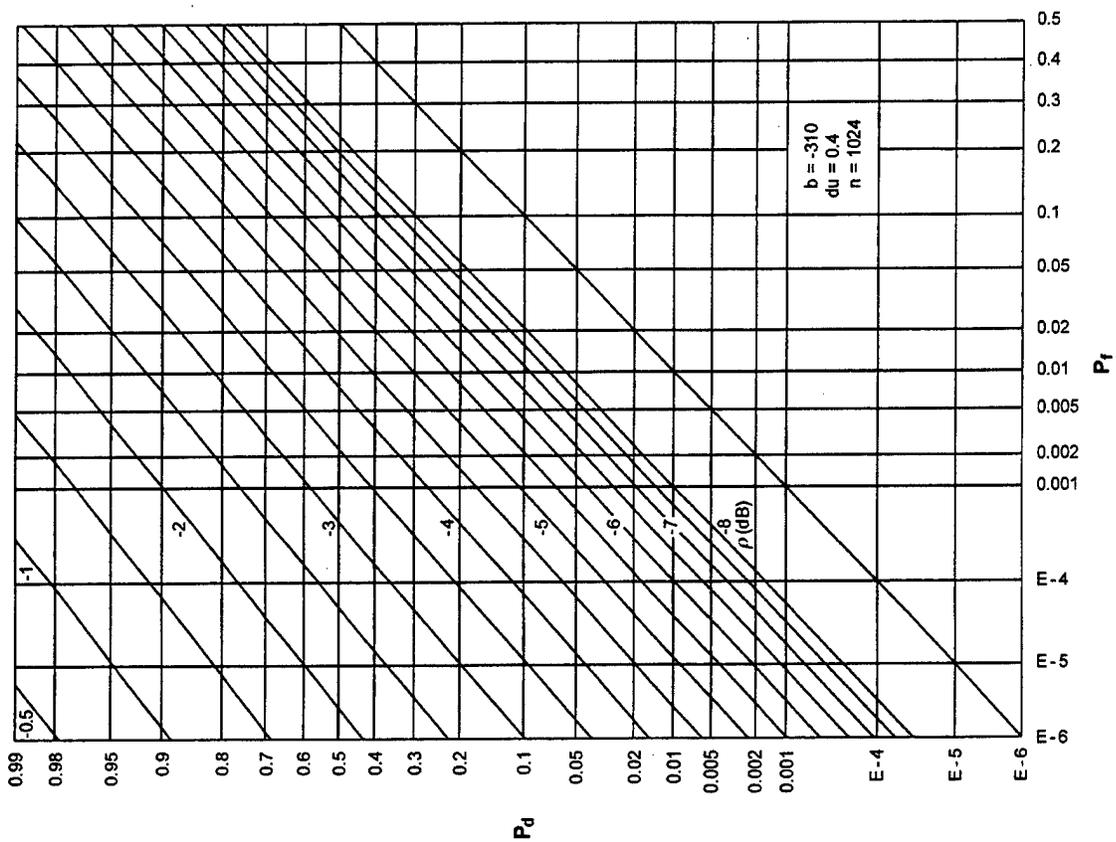
Figure F-29. ROCs for K = 8, N = 8, M = 32

F-16
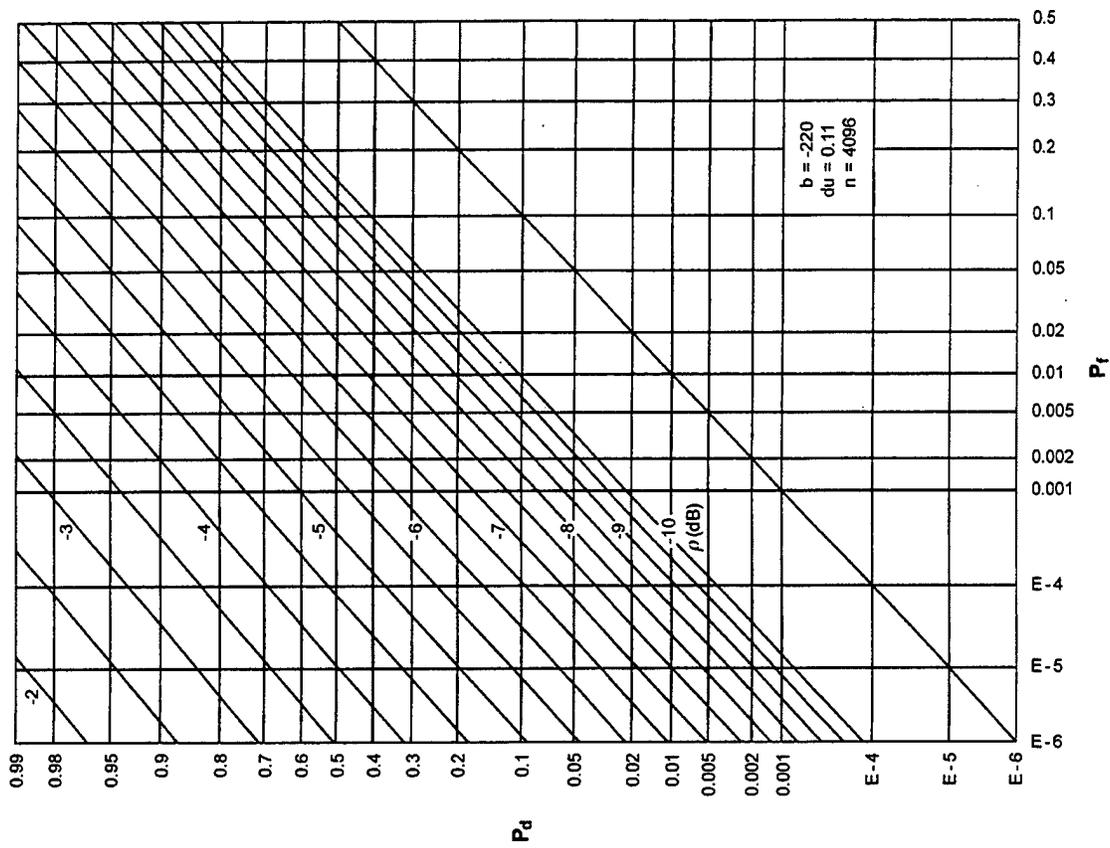
Figure F-32. ROCs for K = 4, N = 2, M = 64
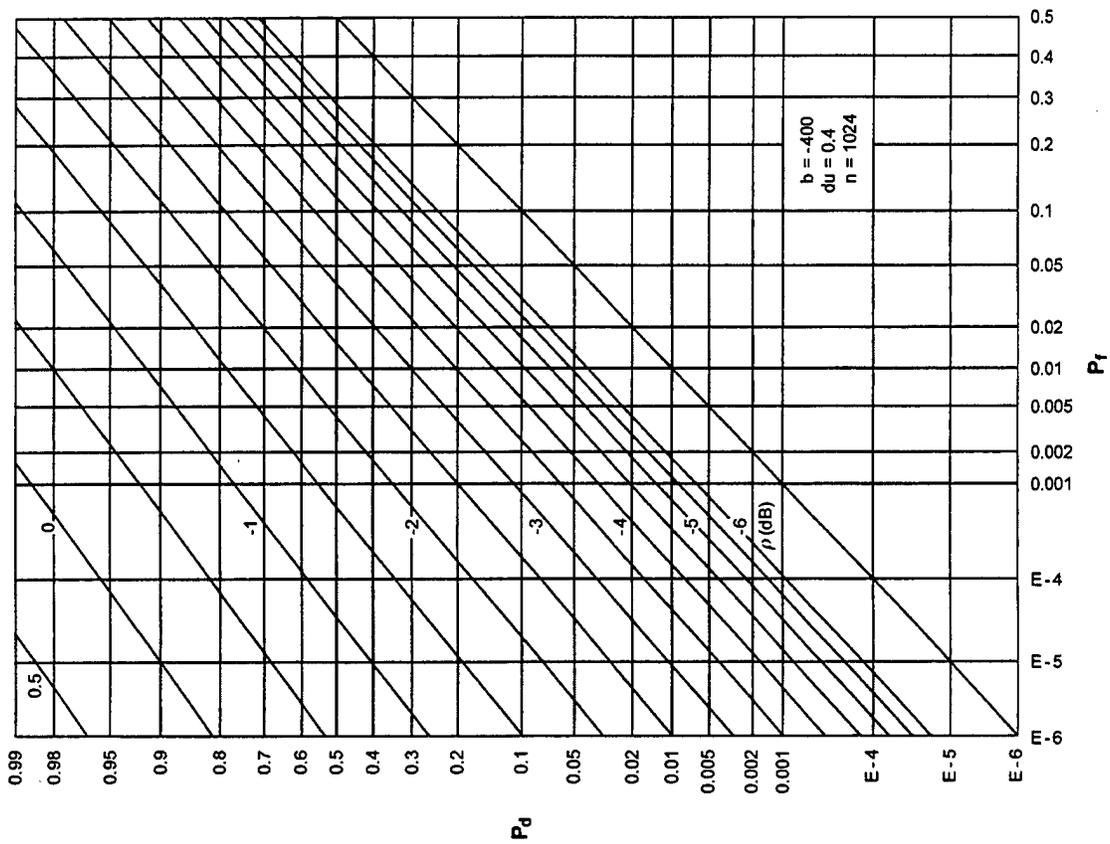
Figure F-31. ROCs for K = 8, N = 32, M = 32
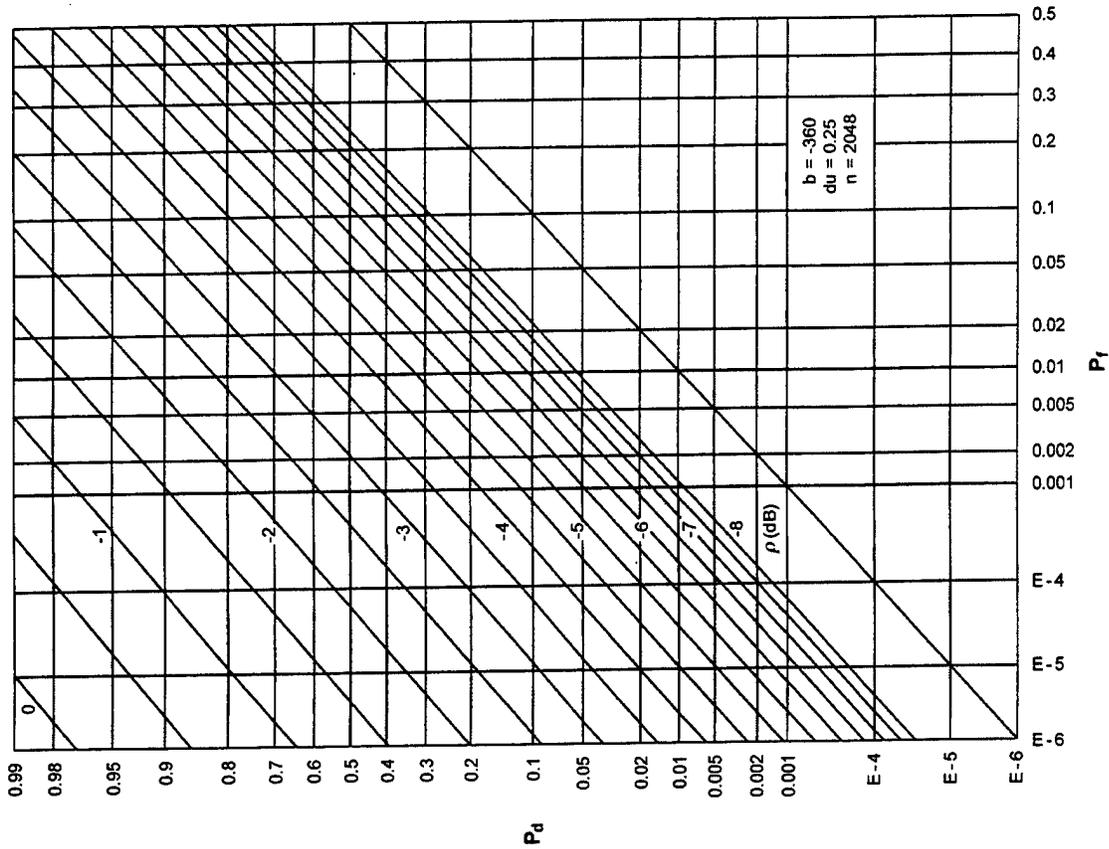
Figure F-34. ROCs for K = 4, N = 8, M = 64
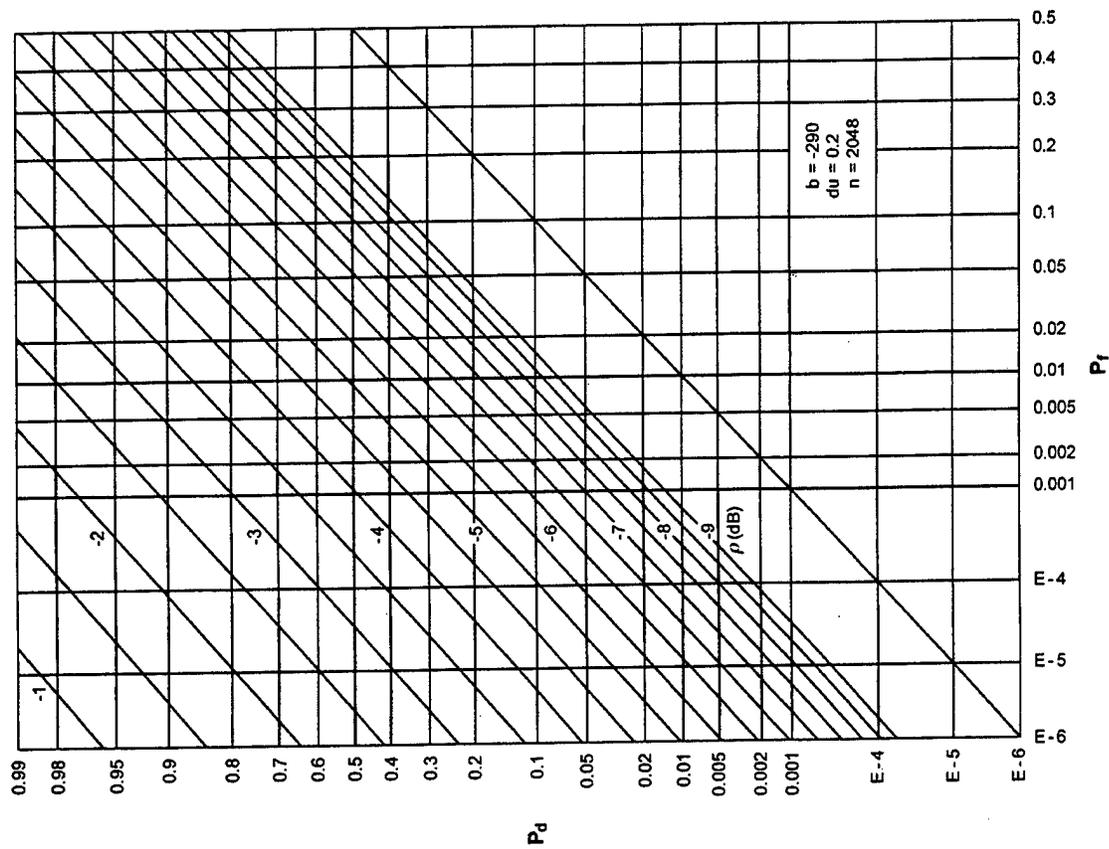
Figure F-33. ROCs for K = 4, N = 4, M = 64
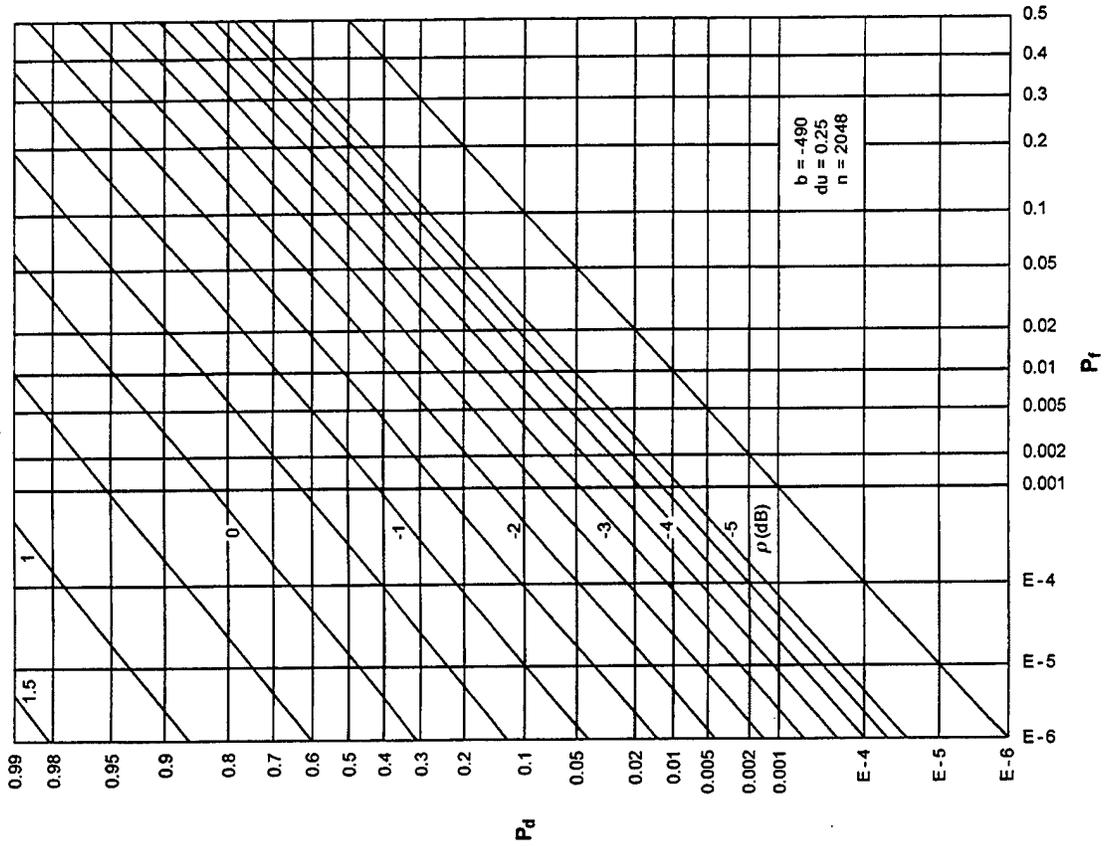
Figure F-36. ROCs for K = 4, N = 32, M = 64
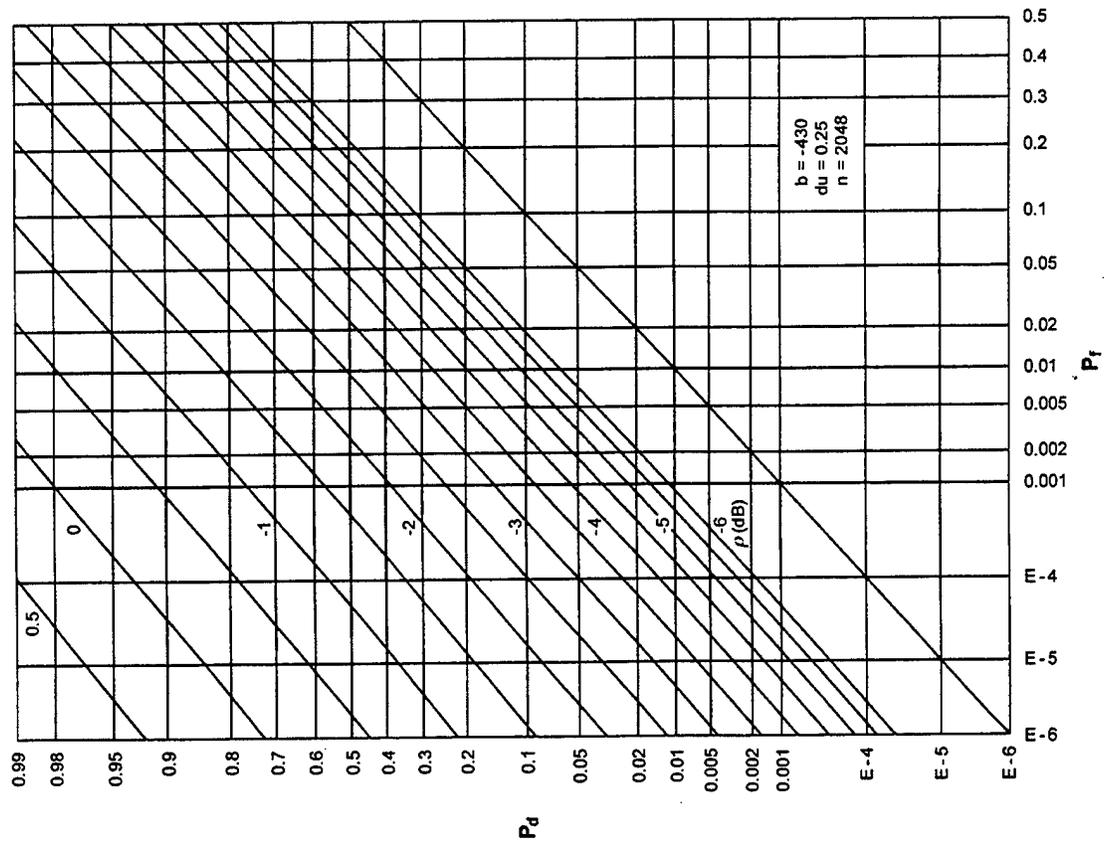
Figure F-35. ROCs for K = 4, N = 16, M = 64

F-19
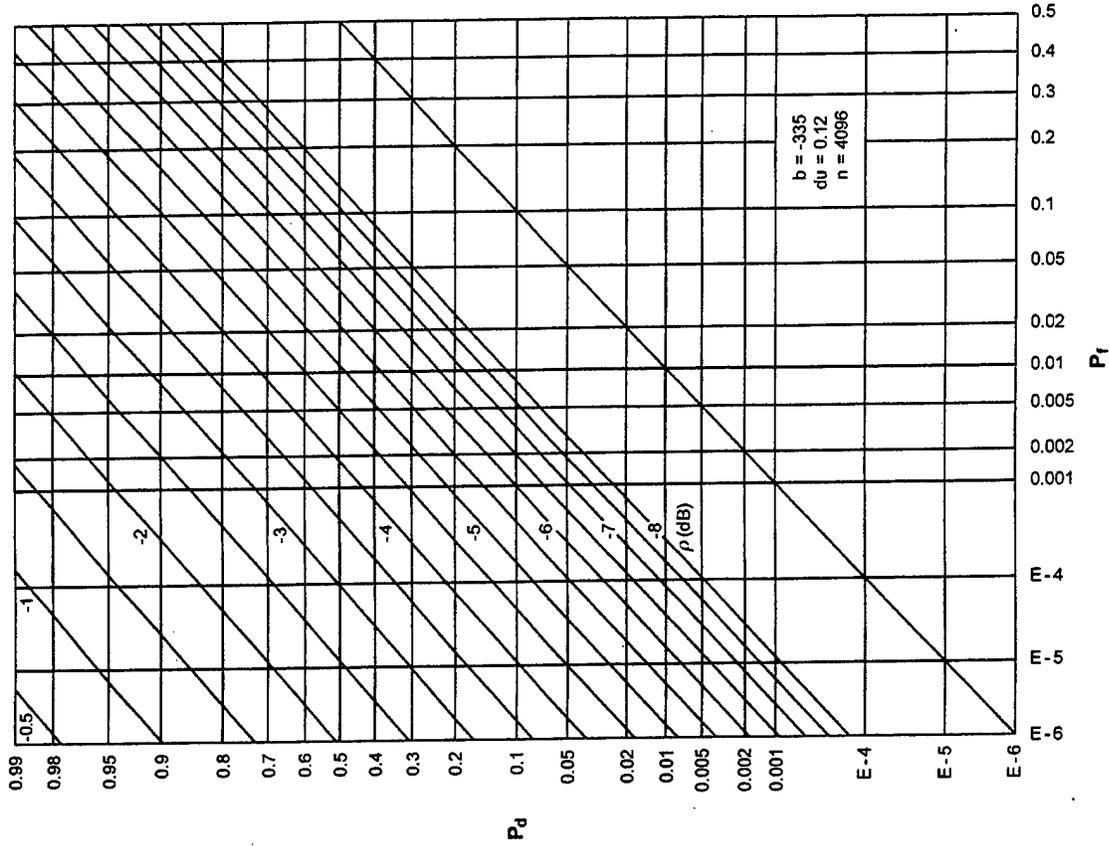
Figure F-38. ROCs for K = 2, N = 4, M = 128

Chart annotations: b = -335, du = 0.12, n = 4096
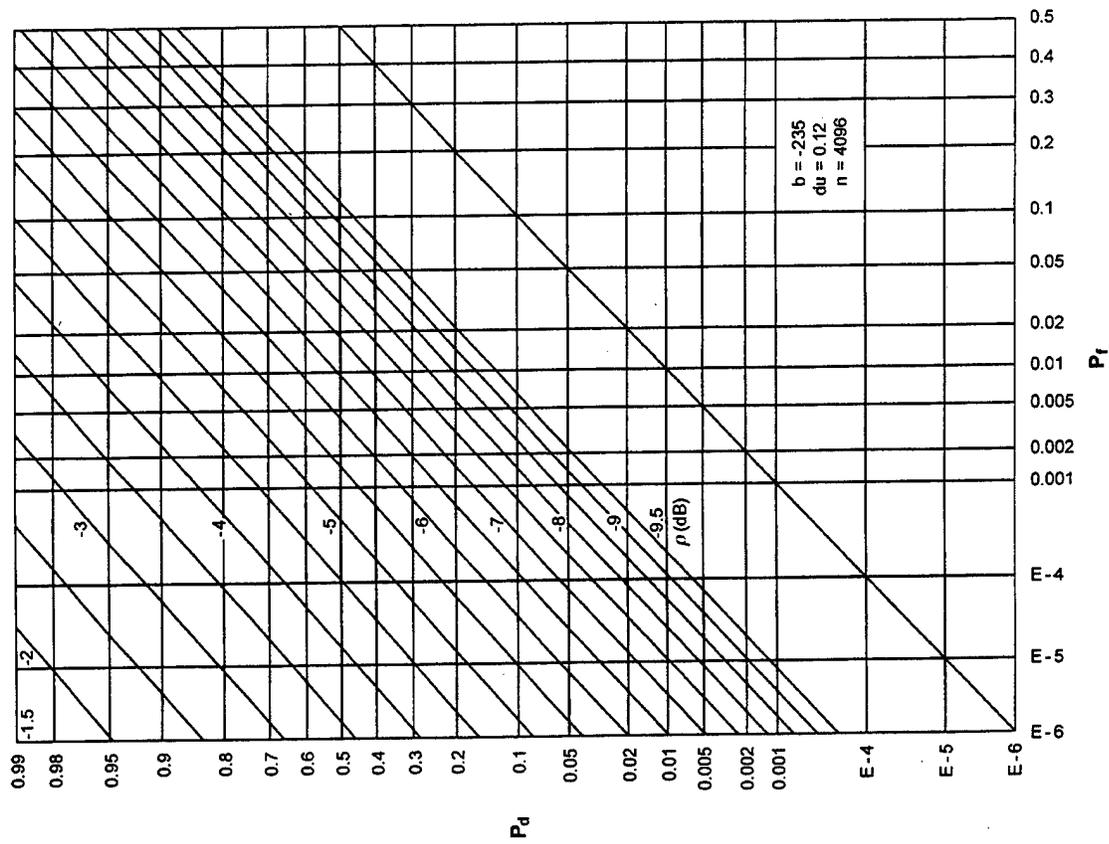
Figure F-37. ROCs for K = 2, N = 2, M = 128

Chart annotations: b = -235, du = 0.12, n = 4096
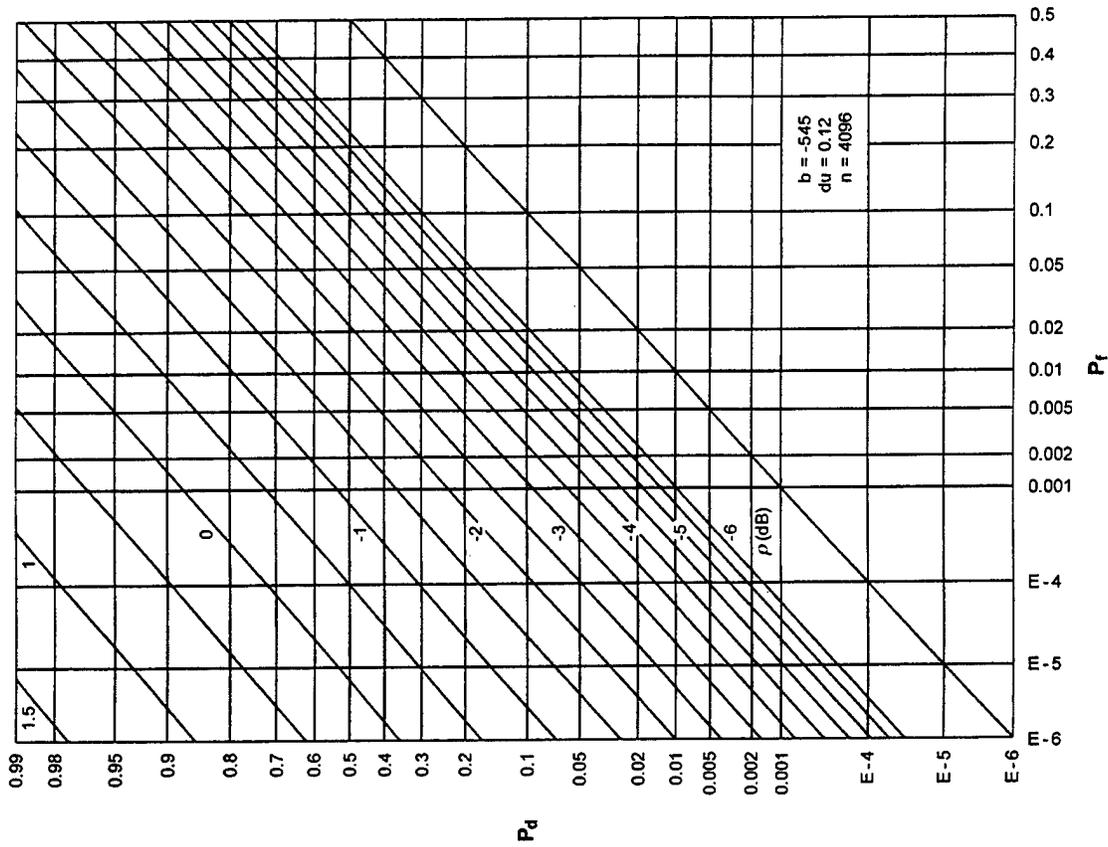
Figure F-40. ROCs for K = 2, N = 16, M = 128

b = -545
du = 0.12
n = 4096
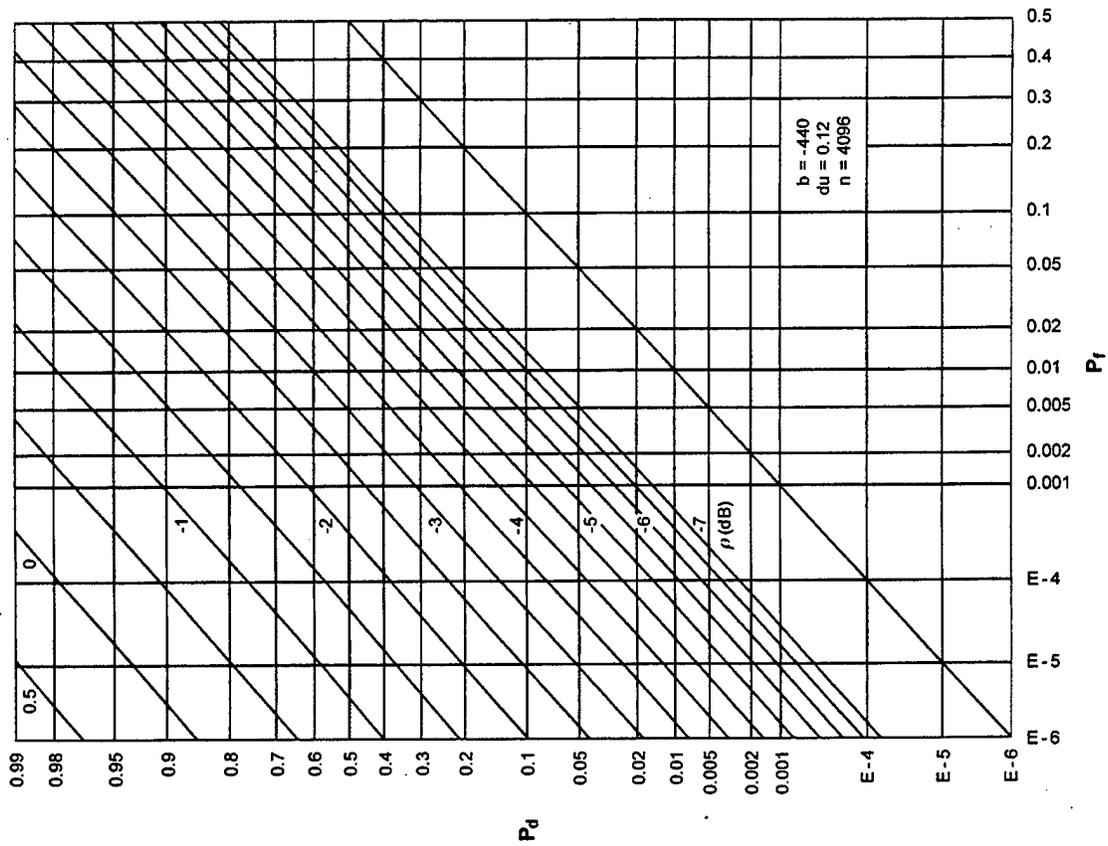
Figure F-39. ROCs for K = 2, N = 8, M = 128

b = -440
du = 0.12
n = 4096
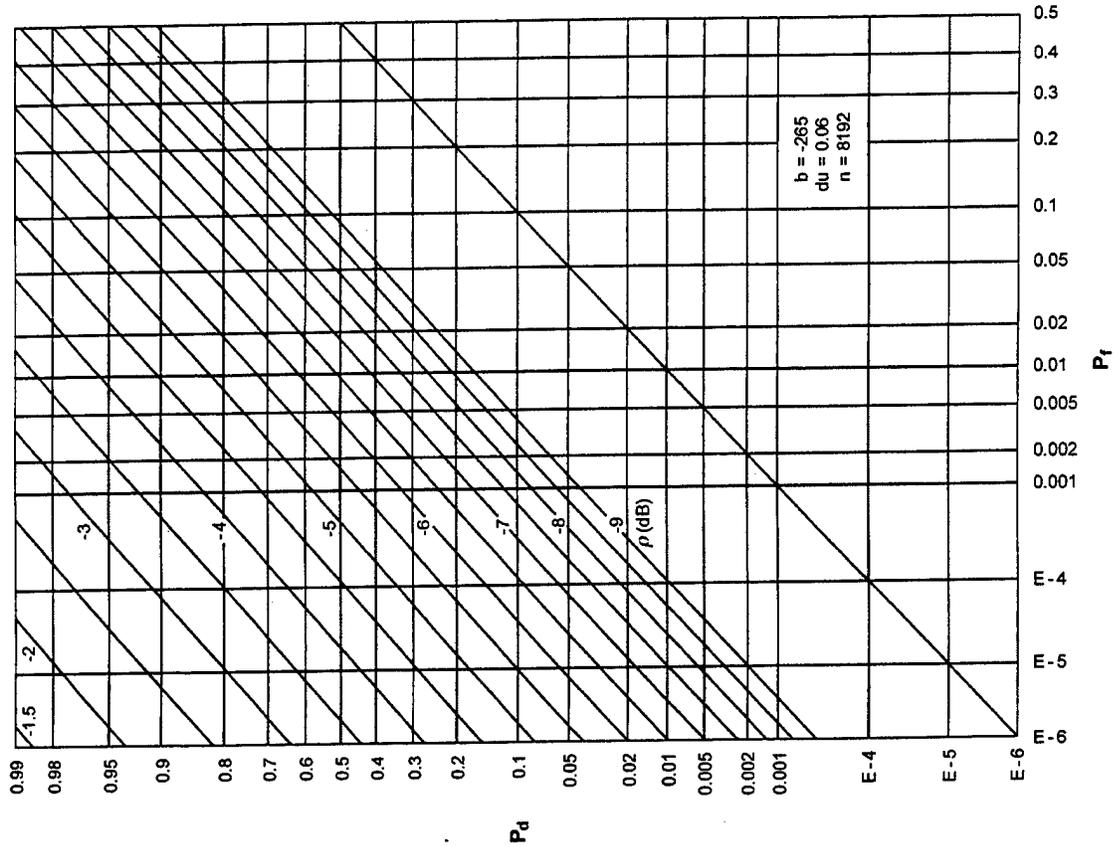
Figure F-42. ROCs for K = 1, N = 2, M = 256
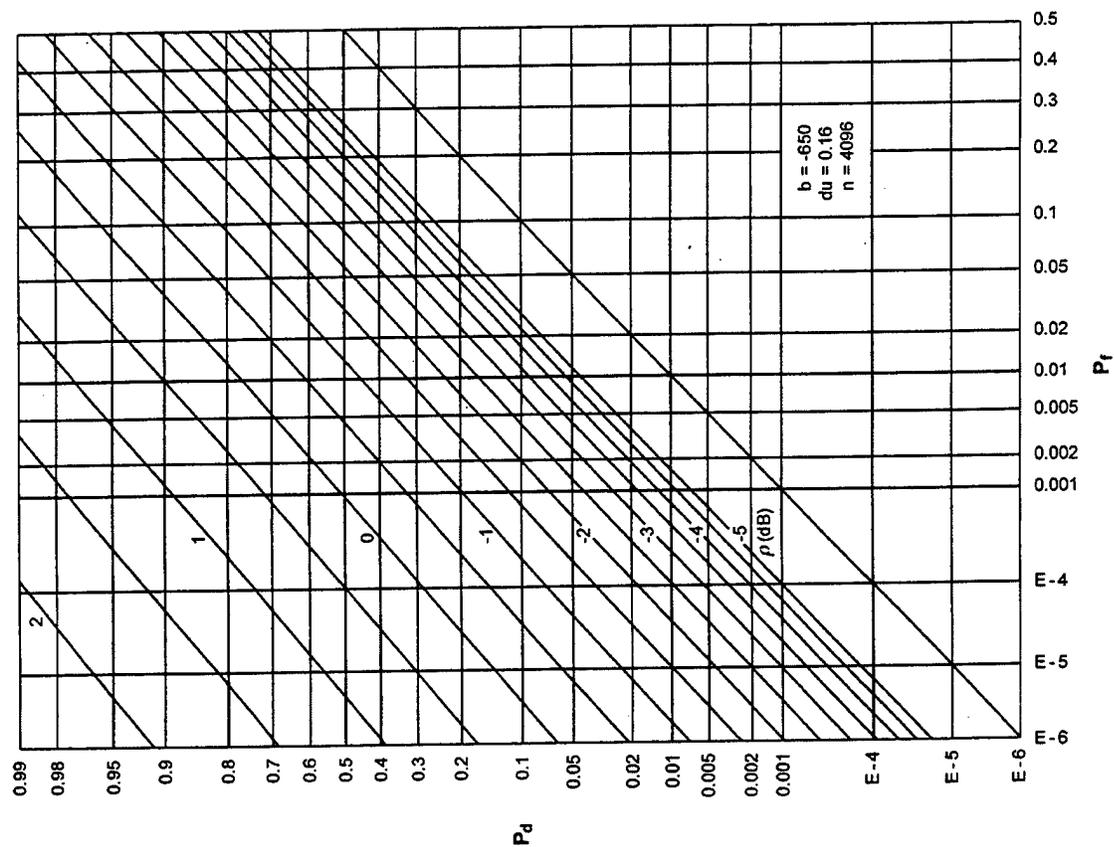
Figure F-41. ROCs for K = 2, N = 32, M = 128
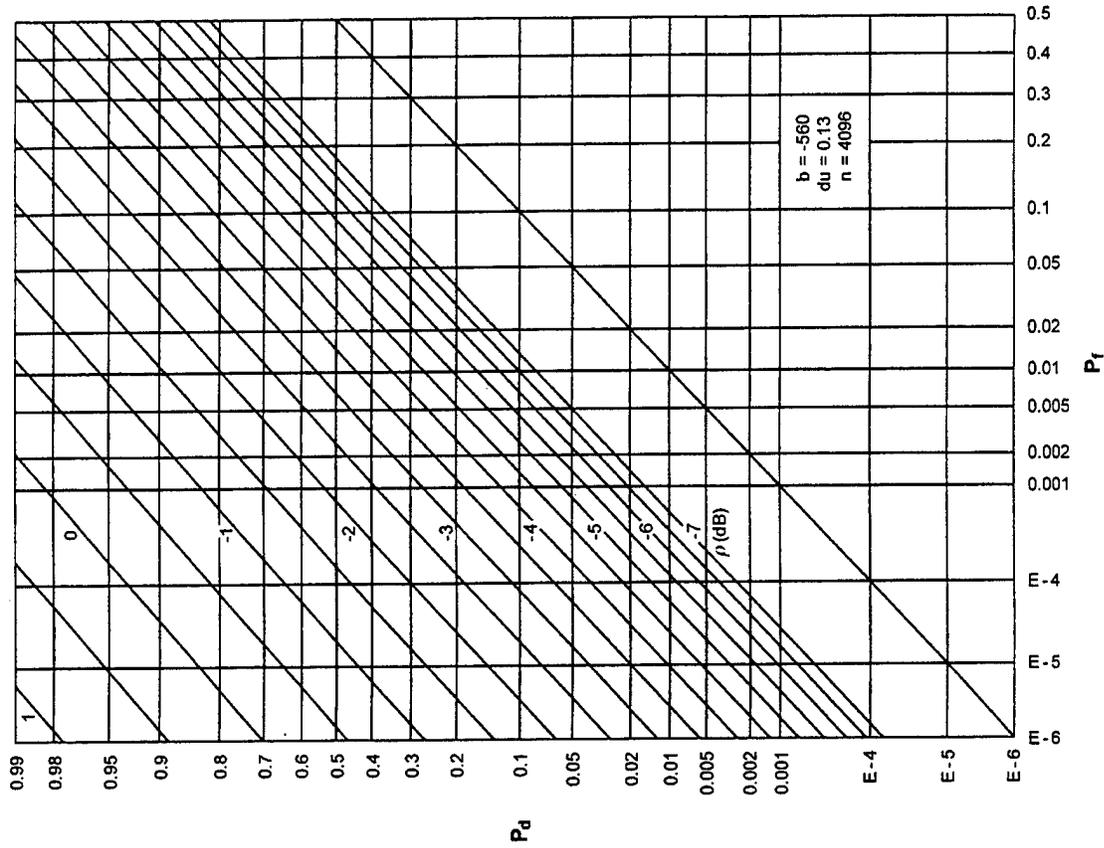
Figure F-44. ROCs for K = 1, N = 8, M = 256

b = -560
du = 0.13
n = 4096

P_f

P_d

ρ (dB)
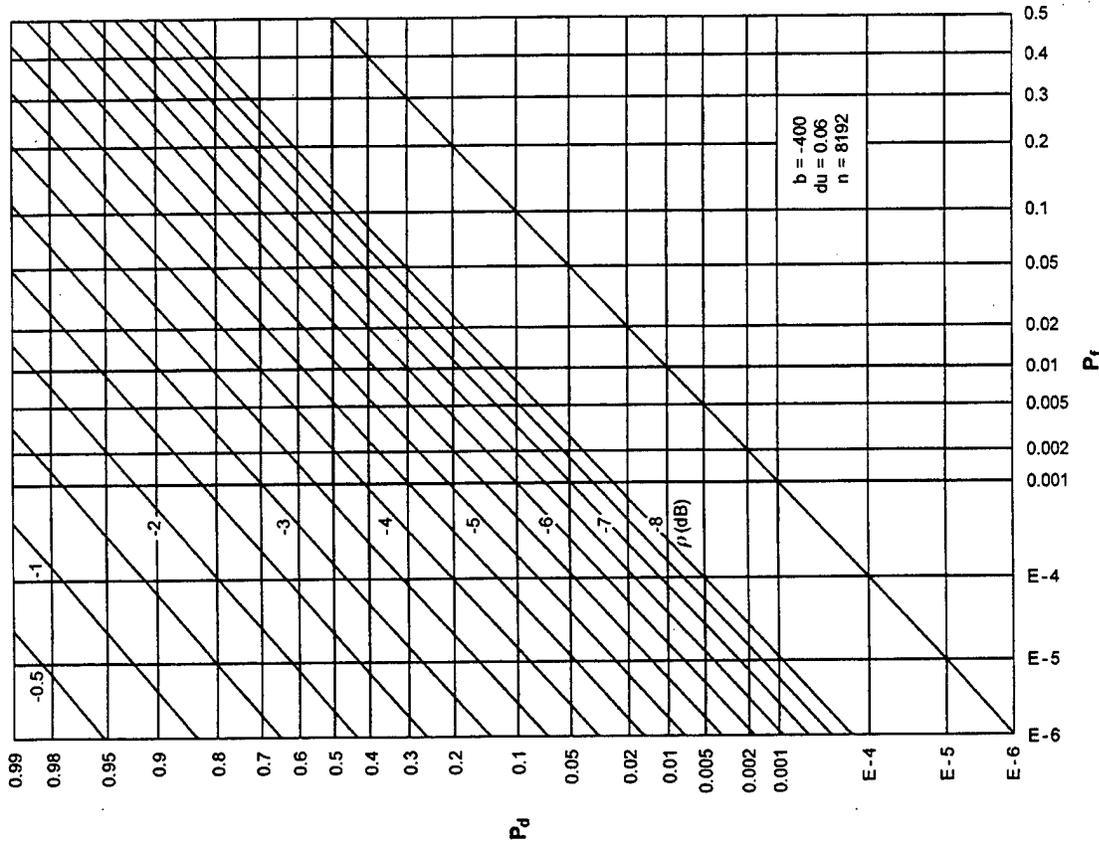
Figure F-43. ROCs for K = 1, N = 4, M = 256

b = -400
du = 0.06
n = 8192

P_f

P_d

ρ (dB)
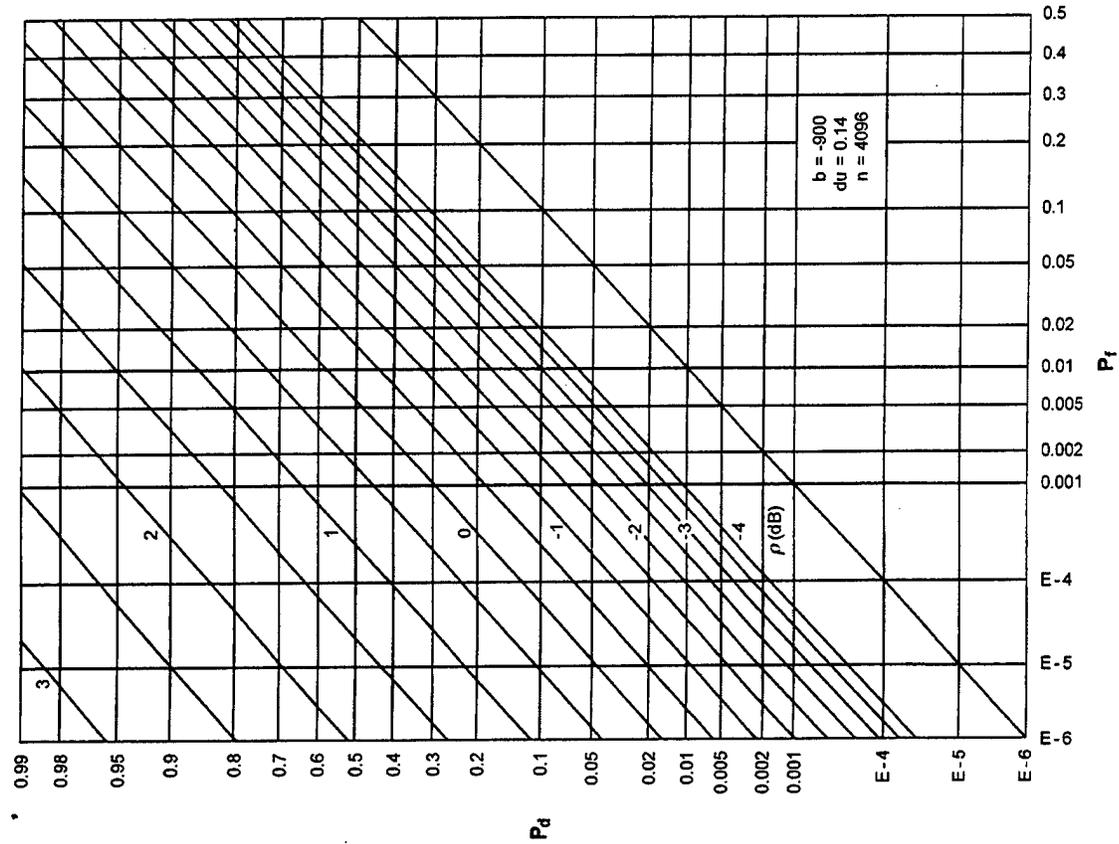
Figure F-46. ROCs for K = 1, N = 32, M = 256
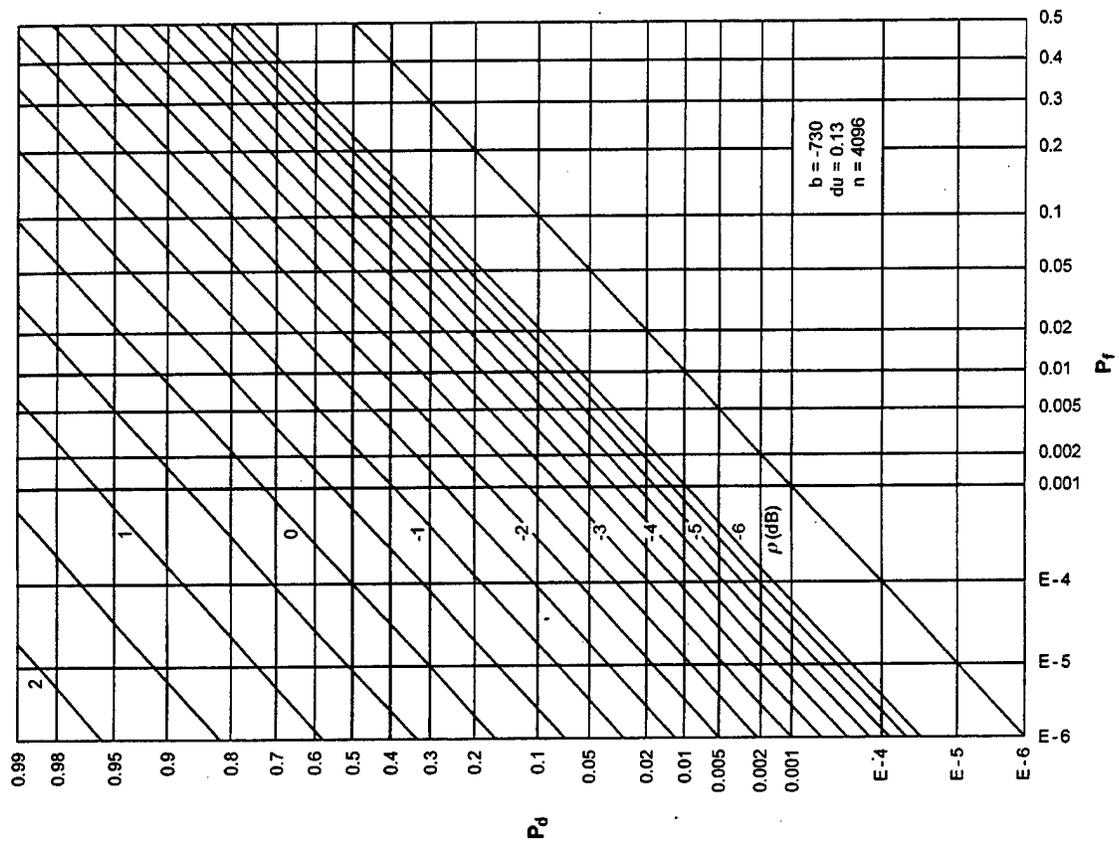
Figure F-45. ROCs for K = 1, N = 16, M = 256

F-24

APPENDIX G — ACCURATE EVALUATION OF A CHARACTERISTIC FUNCTION DIRECTLY FROM SAMPLES OF A CUMULATIVE DISTRIBUTION FUNCTION

Let (real) RV x have (complex) CF $f(\xi)$ and (real) CDF $c(u) = \text{Prob}(x < u)$. The only quantities available are samples $c(n\Delta)$ for all n, which are presumed to be exact. (The PDF $p(u)$ of x, or samples of the PDF $p(u)$, are not available. Also, sample values $\{c(n\Delta)\}$ are not taken close enough to yield a decent approximation to the PDF by taking differences.)

Before trying to relate CF $f(\xi)$ directly to the available samples of CDF $c(u)$, construct a model CDF $c_o(u)$ that is a reasonably good fit to $c(u)$ and that has a corresponding <u>closed form</u> CF $f_o(\xi)$; in addition, CF $f_o(\xi)$ should decay rapidly to zero as $\xi \to \pm\infty$. Then, the desired CF at real argument ξ is given by

$$f(\xi) = \int du \, \exp(i\xi u) \, p(u) = \int du \, \exp(i\xi u) \, \frac{d}{du} c(u) =$$

$$= \int du \, \exp(i\xi u) \, \frac{d}{du}[c_o(u) + c(u) - c_o(u)] =$$

$$= f_o(\xi) - i\xi \int du \, \exp(i\xi u) \, [c(u) - c_o(u)] \, , \qquad (G-1)$$

using integration by parts and the fact that the difference of CDFs tends to zero as $u \to \pm\infty$. For later use, define the auxiliary function

$$g(\xi) \equiv \frac{f(\xi) - f_o(\xi)}{i\xi} = - \int du \, \exp(i\xi u) \, [c(u) - c_o(u)] \, . \quad (G-2)$$

At the origin, $g(\xi)$ is finite, namely, $g(0) = \mu - \mu_o$, which is the difference of the means of the respective CFs $f(\xi)$ and $f_o(\xi)$.

SAMPLING AND ALIASING

Define an approximation to the desired CF $f(\xi)$ by sampling the integral in equation (G-1) at increment Δ in u and by using the trapezoidal rule (compare equations (B-14) and (B-17)):

$$\tilde{f}(\xi) \equiv f_o(\xi) - i\xi\Delta\sum_n \exp(i\xi n\Delta) \, [c(n\Delta) - c_o(n\Delta)] \,, \qquad (G-3)$$

where the sum on n runs over $\pm\infty$. (In practice, the summation on n is conducted until $|c(n\Delta) - c_o(n\Delta)|$ is small enough that the truncation errors on both tails are negligible.) Expression (G-3) can be manipulated as follows:

$$\tilde{f}(\xi) = f_o(\xi) - i\xi \int du \, \exp(i\xi u) \, [c(u) - c_o(u)] \, \Delta \, \delta_\Delta(u) =$$

$$= f_o(\xi) + i\xi \sum_n g\left(\xi - n\frac{2\pi}{\Delta}\right) \,, \qquad (G-4)$$

where $\delta_\Delta(u)$ is an infinite train of delta functions at spacing Δ. This equation utilizes the fact that a Fourier transform of a product is the convolution of the corresponding Fourier transforms. Also, use of the Fourier transform pair (G-2) was made.

When the explicit representation of $g(\xi)$ in equation (G-2) is used for the n = 0 term in equation (G-4), there follows

$$\tilde{f}(\xi) = f(\xi) + i\xi \sum_{n\neq 0} g\left(\xi - n\frac{2\pi}{\Delta}\right) \,. \qquad (G-5)$$

All the manipulations of the approximate CF $\tilde{f}(\xi)$, from its definition (G-3) through equation (G-5), are exact. It can be

immediately seen from equation (G-5) that the summation of aliasing lobes of $g(\xi)$ for $n \neq 0$ constitutes the (complex) error in approximation $\tilde{f}(\xi)$ relative to its desired value $f(\xi)$. To minimize the error, function $g(\xi)$ should have rapidly decaying skirts, so that the aliasing lobes in equation (G-5) do not significantly overlap the $(-\pi/\Delta, \pi/\Delta)$ region of ξ where $f(\xi)$ is substantial. Recall that $|f(\xi)|$ attains its maximum value of unity at the origin.

Function $f_o(\xi)$ can be selected as desired. As a starter, it could be taken as a Gaussian CF, with its mean and variance fairly close to those of the original RV **x**. The rates of decay of $|g(\xi)|$ in equation (G-2) and of $|c(u) - c_o(u)|$ for large arguments, in their respective domains, would then probably be dominated by the specified functions in this problem, namely, $|f(\xi)|/\xi$ and $c(u)$.

COMPUTATION OF APPROXIMATE CHARACTERISTIC FUNCTION VIA A FAST FOURIER TRANSFORM

Approximation $\tilde{f}(\xi)$, defined by equation (G-3), can be calculated at whatever ξ values are desired. However, since only the interval $(-\pi/\Delta, \pi/\Delta)$ in ξ is of interest or can be used, equation (G-3) is evaluated at increment $\Delta_\xi = 2\pi/(N_1\Delta)$ according to

$$\tilde{f}\left(\frac{m2\pi}{N_1\Delta}\right) = f_o\left(\frac{m2\pi}{N_1\Delta}\right) - i\frac{m2\pi}{N_1} \sum_n \exp(i2\pi mn/N_1) \left[c(n\Delta) - c_o(n\Delta)\right] , \quad (G-6)$$

where integer N_1 controls the spacing of the samples in ξ. Only the values for $|m| < N_1/2$ are of interest; in fact, the range $0 \leq m \leq N_1/2$ suffices because of the conjugate symmetry of all the functions of ξ involved in equation (G-3). The values of the summation in equation (G-6), for this m range, are easily realized by means of an N_1-point FFT of the prealiased differences of CDFs $c(u)$ and $c_o(u)$; this prealiasing feature is incorporated to minimize or eliminate truncation errors. Then, combination of the FFT values with the sampled $f_o(\xi)$ function yields the approximation $\tilde{f}(\xi)$ to the desired CF $f(\xi)$ at the values $\xi = m\Delta_\xi$. Since the FFT in equation (G-6) will yield summation values for $0 \leq m \leq N_1-1$, it is recommended that this entire range of equation (G-6) be plotted, so that the left skirt of the first aliasing lobe, namely, $n = 1$ of equation (G-5), can be observed and monitored.

EXAMPLE

An example with a Gaussian CF and a model Gaussian CF with mismatched parameter values was used as a test case; it is

$$f(\xi) = \exp(i\mu\xi - \sigma^2\xi^2/2) \ , \quad c(u) = \Phi\left(\frac{u - \mu}{\sigma}\right) \ ,$$

$$f_o(\xi) = \exp(i\mu_o\xi - \sigma_o^2\xi^2/2) \ , \quad c_o(u) = \Phi\left(\frac{u - \mu_o}{\sigma_o}\right) \ . \qquad \text{(G-7)}$$

The plot in figure G-1 reveals the desired mainlobe of the magnitude of the CF, centered at the origin, with magnitude errors of the order of E-15 when $0 < \xi < \pi/\Delta$. For larger ξ, the first aliasing lobe of $g(\xi)$ dominates, giving useless values for the approximation $\tilde{f}(\xi)$, as expected.

To support the claim that samples $\{c(n\Delta)\}$ of the CDF may not have been taken fine enough to achieve a decent approximation to the PDF $p(u)$ by taking differences, the CF was evaluated (using the trapezoidal rule for integration) for the PDF estimate obtained according to the differences

$$p((n-\tfrac{1}{2})\Delta) \cong \frac{c(n\Delta) - c((n-1)\Delta)}{\Delta} \,. \tag{G-8}$$

The results, displayed in figure G-2, indicate a very significant error between the approximate CF obtained by use of equation (G-8) and the exact CF $f(\xi)$. The maximum magnitude error has increased from 1E-15 to 3E-3, which is more than 10 orders of magnitude. The utility of equations (G-3) and (G-6) is made apparent by this numerical example.

An alternative method (to that in this appendix) of obtaining the CF directly from CDF samples is afforded by the modification in equation (B-20) et seq. When applied to example (G-7) here, excellent results, comparable to figure G-1, were obtained.
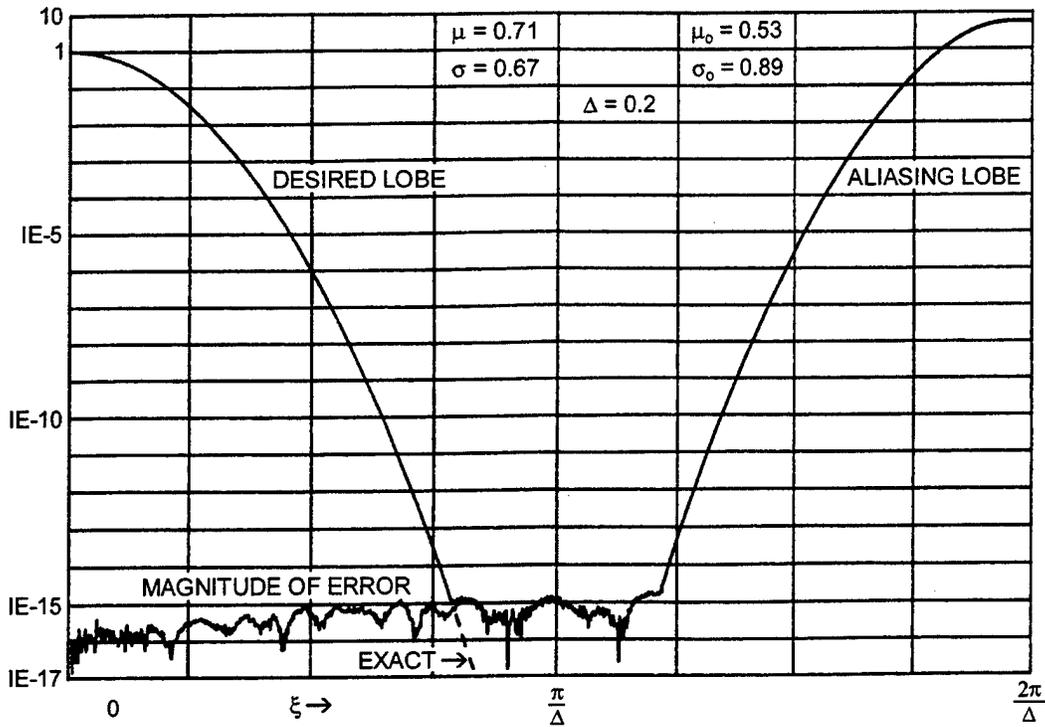
Figure G-1. Magnitude of Approximate CF $\tilde{f}(\xi)$
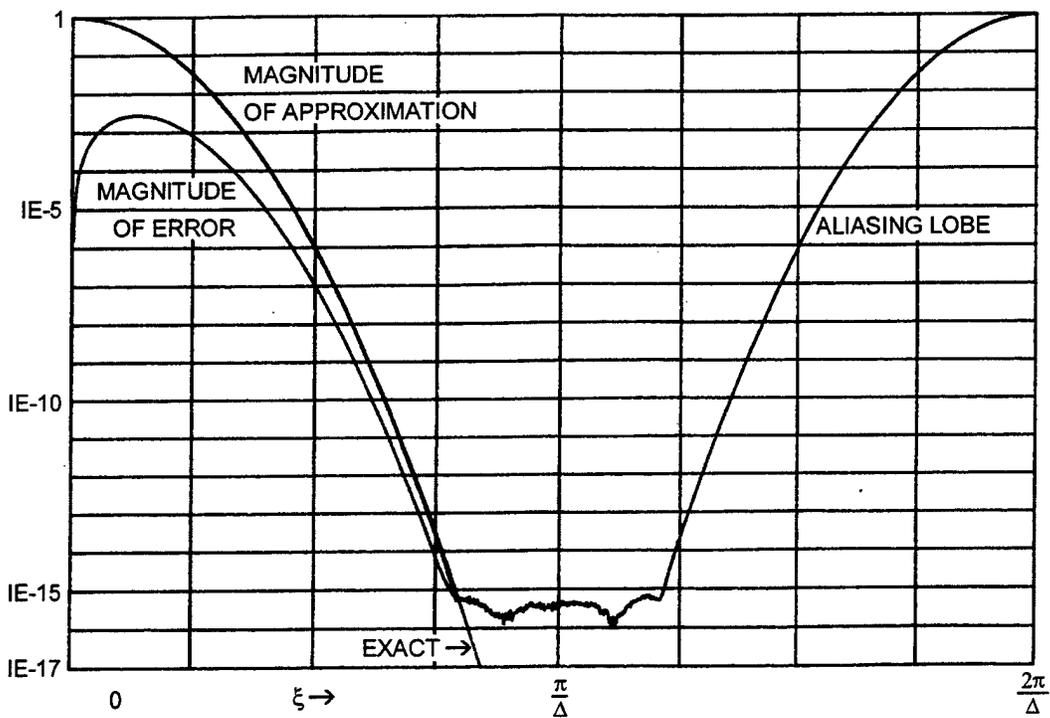
Figure G-2. Alternative CF by Use of Equation (G-8)

APPENDIX H — MATLAB PROGRAM FOR EVALUATION OF
RECEIVER OPERATING CHARACTERISTICS

The numerical procedure utilized is based upon the alias-suppression technique presented in appendix B. In particular, smoothing function $b_1(u)$ in figure B-1, along with the corresponding CF relations (B-14) through (B-17), was used to evaluate the ROCs in appendixes C through F.

Every figure in each set of ROCs has three parameter values listed on it, which were used to generate those specific curves. They are the bias b, sampling increment du, and FFT size n. Because an additive constant to the decision variable in figure 1 does not change the ROC (reference 1), bias b was added to $w(t)$ and chosen so as to make the sum variable as small as possible, but never negative (within roundoff error). This procedure maximizes the unaliased region when the final FFT is conducted from the CF domain, equation (36), to the EDF domain for system output $w(t)$, as well as eases the requirements on du and n.

Sampling increment du is applied in the u domain to equations (26) and (27); it must be taken <u>small</u> enough that the approximation to CF $f_v(\xi)$ in equation (17) is not aliased significantly in the ξ domain. Finally, FFT size n must be taken <u>large</u> enough so that the u-domain span, n du, in the final FFT of equation (36) from the CF to the EDF guarantees insignificant aliasing. Complete details on this cascade procedure are

presented in appendix B of reference 1.

All three parameter values have been chosen by a trial and error procedure, in which intermediate CF $f_v(\xi)$ is observed in the ξ domain, and output EDF $e_w(u)$ is observed in the u domain. Repeated trials led to the tight parameter values listed on each set of ROCs. These values can serve as starting or reference points for evaluation of additional ROCs with different values of K, N, M, and ρ that are of interest to a user. The following listing of the MATLAB program corresponds to figure E-36.

```
clear, clf                  % NUWC TR 11,166
b=-190;         % Additive bias to w
du=0.2;         % Sampling increment in u
n=2^11;         % FFT size
kc=1;           % K, amount of pre-averaging
nc=32;          % N, amount of or-ing
mc=64;          % M, amount of post-averaging
rmin=-2;        % Minimum SNR (dB)
rinc=.5;        % Increment in SNR (dB)
num=16;         % Number of ROCs
disp('b du n; kc nc mc:')
disp([b du n; kc nc mc])
xg=[1e-6 1e-5 1e-4 .001 .002 .005 .01 .02...
.05 .1 .2 .3 .4 .5];
yg=[1e-6 1e-5 1e-4 .001 .002 .005 .01 .02...
.05 .1 .2 .3 .4 .5 .6 .7 .8 .9 .95 .98 .99];
xg=phiinv(xg);
yg=phiinv(yg);
[Xg,Yg]=meshgrid(xg,yg);
Magcf=zeros(n,1);
EDF=zeros(n,1);
Pd=zeros(n,num+1);
n1=n-1; n2=n/2; kc1=kc-1; nc1=nc-1; n3=n2+1;
pn=pi/n; d2=du/2;
arg=pn.*[1:n2]';
sinc=sin(arg)./arg;
disp('         isnr  edf0 - 1')
for isnr=0:num
    rhodb=rmin+rinc*(isnr-1);
    rho=10^(.1*rhodb);
    if(isnr==0) rho=0; end
    aa=sqrt(2*kc*rho);
    X=zeros(n,1)+i*zeros(n,1);
    meanv=0; cdfk=0; k=-1;
    while(cdfk<.5 | area>1e-20)
        k=k+1; uk=du*k; u2=uk+d2;
        sq=sqrt(2*u2); p0=exp(-u2); e0=p0;
        for j=1:kc1
            p0=p0*u2/j;
            e0=e0+p0;
        end
        c0=max(1-e0,0);
        if(aa==0) c1=c0;
```

```
                else [q bes]=Qm(kc,aa,sq);
                c1=max(1-q,0);
                end
                cdfo=cdfk; cdfk=c1*c0^nc1;
                area=cdfk-cdfo;
                j=mod(k,n);
                X(j+1)=X(j+1)+area;
                meanv=meanv+area*uk; % uk, not u2
            end
            X=fftgreen(X);
            Magcf=log10(X.*conj(X)+1e-50)*.5;
            plot(Magcf)
            axis([1 n+1 -16 0]); grid on
            pause(1)
            dxi=2*pi/(n*du);
            X(2:n3)=conj(X(2:n3))./sinc(1:n2);
            X(n3+1:n)=0;
            X=X.^mc;
            X(1:n3)=X(1:n3).*exp(i*b*dxi*[0:n2]');
            meanw=meanv*mc+b;
            X(1)=0;
            X(2:n3)=X(2:n3)./[1:n2]';
            X=fftgreen(X);
            a=.5+meanw/(n*du);
            edf0=a+imag(X(1))/pi;
            disp([isnr edf0-1])
            k=[1:n]';
            edf=a-(k-1)./n+imag(X(k))./pi;
            X=edf;
            EDF=log10(abs(edf)+1e-30);
            plot(EDF)
            axis([1 n+1 -18 0]); grid on
            pause(1)
            edf=real(X(k));
            edf=min(edf,1-1e-12);
            edf=max(edf,1e-12);
            Pd(:,isnr+1)=phiinv(edf);
        end
    beep
    pause
    clf
    hold on
    set(gcf,'PaperPosition',[.25 .25 8 10.5])
```

```
plot(xg,Yg,'k')
plot(Xg,yg,'k')
plot(xg,xg,'k')  % zero SNR ROC
plot(Pd(:,1),Pd(:,[2:num+1]),'k')
axis([xg(1) xg(14) yg(1) yg(21)])
axis off
while 1
    T=input('pf pd isnr: ');
    if T(1)==0 break; end
    pft=phiinv(T(1));
    pdt=phiinv(T(2));
    isnr=T(3);
    for j=0:n1
        if(Pd(j+1,1)<pft) break; end
    end
    x1=Pd(j+1,1);
    x2=Pd(j,1);
    as=Pd(j+1,isnr+1);
    bs=Pd(j+1,isnr+2);
    cs=Pd(j,isnr+1);
    ss=(cs-as)/(x2-x1);
    a1=pdt-ss*pft;
    fs=(a1+ss*x1-as)/(bs-as);
    rc=rmin+rinc*(isnr-1+fs);
    disp([T fs rc])
end

%   function y=phiinv(x)  for  0 < x < 1
%   y=1.414213562373095*erfinv(2*x-1);
```

```
function [q,bes] = Qm(m,a,b)
start=1e-100; num=2000;
a2=.5*a*a; b2=.5*b*b;
q2=start; q3=start;
m1=m-1;
for j=1:m1
    q3=q3*b2/j;
    q2=q2+q3;
end
q1=1; q=q2; bes=q3;
for j=1:num
    q1=q1*a2/j;
    q3=q3*b2/(j+m1);
    q2=q2+q3;
    q4=q1*q2;
    q5=q1*q3;
    q=q+q4;
    bes=bes+q5;
    if(q4<=eps*q & q5<=eps*bes) break; end
end
q2=a2+b2;
if(q2<708)
    e1=exp(-q2)/start;
    q=q*e1;
    bes=bes*e1;
else
    q1=q2+log(start/q);
    if(q1>708) q=0; bes=0; return; end
    q=exp(-q1);
    q1=q2+log(start/bes);
    bes=exp(-q1);
end
```

REFERENCES

1. A. H. Nuttall, "Detection Performance of Or-ing Device with Pre- and Post-Averaging: Part I — Random Signal," NUWC-NPT Technical Report 11,150, Naval Undersea Warfare Center Division, Newport, RI, 26 July 1999.

2. A. H. Nuttall, "Accurate Efficient Evaluation of Cumulative or Exceedance Probability Distributions Directly From Characteristic Functions," NUSC Technical Report 7023, Naval Underwater Systems Center, New London, CT, 1 October 1983.

3. **Handbook of Mathematical Functions**, U.S. Department of Commerce, National Bureau of Standards, Applied Mathematics Series, no. 55, U.S. Government Printing Office, Washington, DC, June 1964.

4. I. S. Gradshteyn and I. M. Ryzhik, **Table of Integrals, Series, and Products**, Academic Press, Inc., New York, NY, 1980.

5. A. H. Nuttall, "Some Integrals Involving the Q_M-Function," NUSC Technical Report 4755, Naval Underwater Systems Center, New London, CT, 15 May 1974.

INITIAL DISTRIBUTION LIST

Addressee	No. of Copies
Center for Naval Analyses, VA	1
Coast Guard Academy, CT	
J. Wolcin	1
Commander Submarine Force, U.S. Pacific Fleet, HI	
W. Mosa, CSP N72	1
Defense Technical Information Center	2
Griffiss Air Force Base, NY	
Documents Library	1
J. Michels	1
Hanscom Air Force Base, MA	
M. Rangaswamy	1
National Radio Astronomy Observatory, VA	
F. Schwab	1
National Security Agency, MD	
J. Maar	1
National Technical Information Service, VA	10
Naval Air Warfare Center, PA	
L. Allen	1
Naval Command Control and Ocean Surveillance Center, CA	
J. Alsup	1
W. Marsh	1
Naval Environmental Prediction Research Facility, CA	1
Naval Intelligence Command, DC	1
Naval Oceanographic and Atmospheric Research Laboratory, CA	
M. Pastore	1
Naval Oceanographic and Atmospheric Research Laboratory, MS	
B. Adams	1
R. Fiddler	1
E. Franchi	1
R. Wagstaff	1
Naval Oceanographic Office, MS	1
Naval Personnel Research and Development Center, CA	1
Naval Postgraduate School, CA	
Superintendent	1
C. Therrien	1
Naval Research Laboratory, DC	
W. Gabriel	1
D. Steiger	1
E. Wald	1
N. Yen	1
Naval Surface Warfare Center, FL	
E. Linsenmeyer	1
D. Skinner	1
Naval Surface Warfare Center, MD	
P. Prendergast	1
Naval Surface Warfare Center, VA	
J. Gray	1
Naval Technical Intelligence Center, DC	
Commanding Officer	1
D. Rothenberger	1
Naval Undersea Warfare Center, FL	
Officer in Charge	1

INITIAL DISTRIBUTION LIST (Cont'd)

Addressee	No. of Copies
Naval Weapons Center, CA	1
Office of the Chief of Naval Research, VA	
ONR 321 (D. Johnson)	1
ONR 321US (N. Harned)	1
ONR 322 (R. Tipper)	1
ONR 334 (P. Abraham)	1
Office of Naval Research	
ONR 31 (R. R. Junker)	1
ONR 311 (A. M. van Tilborg)	1
ONR 312 (M. N. Yoder)	1
ONR 313 (N. L. Gerr)	1
ONR 32 (S. E. Ramberg	1
ONR 321 (F. Herr)	1
ONR 322 (M. Briscoe)	1
ONR 33 (S. G. Lekoudis)	1
ONR 334 (A. J. Tucker)	1
ONR 342 (W. S. Vaughan)	1
ONR 343 (R. Cole)	1
ONR 362 (M. Sponder)	1
Program Executive Office, Undersea Warfare (ASTO), VA	
J. Thompson, A. Hommel, R. Zarnich	3
Space and Naval Warfare Systems Command, DC	
LCDR R. Holland	1
U.S. Air Force, Maxwell Air Force Base, AL	
Air University Library	1
U.S. Department of Commerce, CO	
A. Spaulding	1
Vandenberg Air Force Base, CA	
CAPT R. Leonard	1
Brown University, RI	
Documents Library	1
Catholic University of America, DC	
J. McCoy	1
Drexel University, PA	
S. Kesler	1
Duke University, NC	
J. Krolik	1
Harvard University, MA	
Gordon McKay Library	1
Johns Hopkins University, Applied Physics Laboratory, MD	
H. M. South	1
T. N. Stewart	1
Lawrence Livermore National Laboratory, CA	
L. Ng	1
Los Alamos National Laboratory, NM	1
Marine Biological Laboratory, MA	
Library	1
Massachusetts Institute of Technology, MA	
Barker Engineering Library	1
Massachusetts Institute of Technology, Lincoln Laboratory, MA	
V. Premus	1
J. Ward	1

INITIAL DISTRIBUTION LIST (Cont'd)

Addressee	No. of Copies
Northeastern University, MA	
C. Nikias	1
Pennsylvania State University, Applied Research Laboratory, PA	
R. Hettche	1
E. Liszka	1
F. Symons	1
Princeton University, NJ	
S. Schwartz	1
Rutgers University, NJ	
S. Orfanidis	1
San Diego State University, CA	
F. Harris	1
Sandia National Laboratory, NM	
J. Claasen	1
Scripps Institution of Oceanography, Marine Physical Laboratory, CA	
Director	1
Syracuse University, NY	
D. Weiner	1
United Engineering Center, NY	
Engineering Societies Library	1
University of Colorado, CO	
L. Scharf	1
University of Connecticut, CT	
Wilbur Cross Library	1
C. Knapp	1
P. Willett	1
University of Florida, FL	
D. Childers	1
University of Hartford	
Science and Engineering Library	1
University of Illinois, IL	
D. Jones	1
University of Illinois at Chicago, IL	
A. Nehorai	1
University of Massachusetts, MA	
C. Chen	1
University of Michigan, MI	
Communications and Signal Processing Laboratory	1
W. Williams	1
University of Minnesota, MN	
M. Kaveh	1
University of Rhode Island, RI	
Library	1
G. Boudreaux-Bartels	1
S. Kay	1
D. Tufts	1
University of Rochester, NY	
E. Titlebaum	1
University of Southern California, CA	
W. Lindsey	1
A. Polydoros	1

INITIAL DISTRIBUTION LIST (Cont'd)

Addressee	No. of Copies
University of Texas, TX	
Applied Research Laboratory	1
C. Penrod	1
University of Washington, WA	
Applied Physics Laboratory	1
D. Lytle	1
J. Ritcey	1
R. Spindel	1
Villanova University, PA	
M. Amin	1
Woods Hole Oceanographic Institution, MA	
Director	1
T. Stanton	1
Yale University, CT	
Kline Science Library	1
P. Schultheiss	1
Analysis and Technology, CT	
Library	1
Analysis and Technology, VA	
D. Clark	1
Atlantic Aerospace Electronics Corp.	
R. Stahl	1
Bell Communications Research, NJ	
D. Sunday	1
Berkeley Research, CA	
S. McDonald	1
Bolt, Beranek, and Newman, CT	
P. Cable	1
Bolt, Beranek, and Newman, MA	
H. Gish	1
DSR, Inc., VA	
M. Bozek-Kuzmicki	1
EDO Corporation, NY	
M. Blanchard	1
EG&G, VA	
D. Frohman	1
EG&G Services, CT	
J. Pratt	1
Engineering Technology Center	
D. Lerro	1
General Electric, MA	
R. Race	1
General Electric, NJ	
H. Urkowitz	1
Harris Scientific Services, NY	
B. Harris	1
Hughes Defense Communications, IN	
R. Kenefic	1
Hughes Aircraft, CA	
T. Posch	1
Kildare Corporation, CT	
R. Mellen	1

INITIAL DISTRIBUTION LIST (Cont'd)

Addressee	No. of Copies
Lincom Corporation, MA	
T. Schonhoff	1
Lockheed Martin, Undersea Systems, VA	
M. Flicker	1
Lockheed Martin, Ocean Sensor Systems, NY	
R. Schumacher	1
Marconi Aerospace Defense Systems, TX	
R. D. Wallace	1
MITRE Corporation, VA	
S. Pawlukiewicz	1
R. Bethel	1
Neural Technology, Inc., SC	
E. A. Tagliarini	1
Orincon Corporation, CA	
J. Young	1
Orincon Corporation, VA	
H. Cox	1
Philips Research Laboratory, Netherlands	
A. J. E. M. Janssen	1
Planning Systems, Inc., CA	
W. Marsh	1
Prometheus, RI	
M. Barrett	1
J. Byrnes	1
Raytheon, RI	
R. Conner	1
S. Reese	1
Schlumberger-Doll Research, CT	
R. Shenoy	1
Science Applications International Corporation, CA	
C. Katz	1
Science Applications International Corporation, VA	
P. Mikhalevsky	1
Toyon Research, CA	
M. Van Blaricum	1
Tracor, TX	
T. Leih	1
B. Jones	1
K. Scarbrough	1
TRW, VA	
R. Prager	1
G. Maher	1
Westinghouse Electric, MA	
R. Kennedy	1
Westinghouse Electric, Annapolis, MD	
H. Newman	1
Westinghouse Electric, Baltimore, MD	
R. Park	1
K. Harvel, Austin, TX	1